RIGA TECHNICAL UNIVERSITY

D. Merkulovs

Cylindrical cell based refractometer and its applications methodology

THESIS

2015

RIGA TECHNICAL UNIVERSITY
Faculty of Transport and Mechanical Engineering
Biomedical Engineering and Nanotechnology Institute

Dmitrijs MERKULOVS
Dr. sc. eng. study program "Engineering Technology, Mechanics and Mechanical Engineering (RMDM8)"
The direction "Medical engineering and medical physics"

CYLINDRICAL CELL BASED REFRACTOMETER AND ITS APPLICATIONS METHODOLOGY

Dr. sc. eng. Thesis

Supervisors
Dr. habil. phys.
Y. DEKHTYAR
Dr. habil. sc. eng.
P. SHIPKOVS

Riga - 2015

European Social Fund **European Union**

Development and design of the promotion work
is co-financed by the EU Social Foundation
#2009/0144/1DP/1.1.2.1.2/09/IPIA/VIAA/005

ABSTRACT

The present work is devoted to the new cylindrical cell based refractometer and its application methodology.

In recent years chemistry, physics, medicine, human environment safety and protection and other areas have an increasing demand for accurate measurement of the concentration of the solution components, and the refractive index (RI) obtains the sensitive indication for this purpose.

For the cylindrical cell based refractometer a new physical RI measuring method has been developed.

The developed methodology employs a new criterion for determining the reading point of the refractometer, improving the unambiguity of the measurements results reading.

The technique and calibration methodology to use the refractometers are developed to measure the composition of liquid.

For the first time in the world resolution has been reached for the cylindrical cell based refractometer up to 10^{-5} RI, and mathematically proved possibility to measure RI with a resolution up to 10^{-7}

The thesis consists of an introduction, 4 chapters and resume. It is written on 118 pages, contains 52 figures, 9 tables, 116 references and 10 appendixes. The work is written in English.

ANOTĀCIJA

Šis darbs veltīts jauna veida refraktometra izstrādei un tā praktiskās pielietošanas metodoloģijai.

Pēdējos gados pieaug pieprasījums pēc precīzas un operatīvas dažādu šķīdumu komponenšu koncentrācijas noteikšanas, pielietojot refrakcijas indeksa (RI) mērījumus ķīmiskos un fizikālos pētījumos, pārtikas ražošanas tehnoloģijā, materiālu apstrādē, medicīniskajā diagnostikā, apkārtējās vides piesārņojumu mērīšanā, sabiedrības drošības nodrošināšanā un daudzās citās sfērās.

Cilindriskās šūnas refraktometriem tika izstrādāts jauns fizikāls RI mērījumu paņēmiens.

Darbā piedāvāta jauna pieeja refraktometra atskaites punkta noteikšanai, tādējādi uzlabojot mērījumu rezultātu nolasīšanas viennozīmīgumu.

Izstrādāta jaunā refraktometra kalibrēšanas metodika un metodoloģija šķīdumu sastāva mērīšanai.

Pirmo reizi cilindriskās šūnas refraktometriem tika ievērojami uzlabota mērījumu izšķirtspēja, sasniedzot 10^{-5} RI un teorētiski pierādīta iespēja panākt mērījumu izšķirtspēju līdz 10^{-7} RI .

Disertācija sastāv no ievada, 4 nodaļām, secinājumiem un tā ir uzrakstīta uz 118 lapām, satur 52 zīmējumus, 9 tabulas, 116 atsauces un 10 papildinājumus. Darbs ir uzrakstīts angļu valodā.

АННОТАЦИЯ

Эта работа посвящена новому рефрактометру на базе цилиндрической ячейки и методологии его применения.

В последние годы в химии, в физике, в защите экологической безопасности человека и в других областях есть растущий спрос на точное измерение концентрации компонентов растворов, а коэффициент преломления (RI) является чувствительным индикатором для этой цели.

Для рефрактометров на базе цилиндрической ячейки был разработан новый физический способ измерения RI.

Разработанная методика использует новый критерий для определения точки чтения рефрактометра, улучшая однозначность считывание результатов измерния.

Разработана методика и методология калибровки рефрактометра для измерения состава жидкости.

Впервые в мире для рефрактометров на базе цилиндрической ячейки было получено разрешение рефрактометрических измерений до 10^{-5} RI, и математически доказана возможность измерения RI с разрешением до 10^{-7}.

Диссертация состоит из введения, 4 частей и заключения. Она написана на 118 страницах, содержит 52 рисунка, 9 таблиц, 116 ссылок и 10 приложений. Работа написана на английском языке.

CONTENTS

EXPLORATION OF THE TERMS AND ABBREVIATIONS USED IN THIS WORK

a optical element cylinder axis distance range exceeded the mid-point of the linear scale measuring element;

c speed of light in vacuum;

C concentration;

d density;

k optical element cylinder radius ratio r_1 / r_2;

L cylinder axis of the optical element of the linear distance measured in the plane of the element and the optical input-output center edge angle of intersection of the beginning;

m optical element beam output sequence number;

M mass, kg;

n refractive index;

n_1 ambient refractive index;

n_2 optical element material cell refractive index;

n_3 the liquid refractive index;

r_1 optical element cylinder outer radius;

r_2 an optical element inside radius of the cylinder;

t the temperature;

Q optical element beam exit point;

α angles;

β angles;

υ the velocity of light in the respective medium;

η an optical element in the optical input-output center angle;

λ the wavelength of that light;

Ψ an optical element in the optical input-output center angle of the start edge angle relative to the plane of the linear measuring element;

ADC analog-to-digital converter;

CCD charge-coupled device;

CCR the cylindrical cell based refractometer;

CMOS complementary metal-oxide semiconductor;

MCU microprocessor control unit;

MR the RI measurement resolution;

RI the refractive index.

INTRODUCTION

The refractive index (RI) of a liquid carries important information about its physical properties, including concentration and density, thus making it possible to determine and monitor the composition of the solution.

Purpose of the thesis was to create a refractometer and methodology to reach a higher as compared to present devices resolution of RI measurements. For this purpose the RI is measured as the deviation of a laser beam passed several times through a cylindrical cell containing the tested liquid.

The magnitude of the deviation, which depends on the RI, is measured as the displacement of the transmitted beam's projection on a linear measuring element, such as a linear CMOS or CCD image sensor. In order to significantly improve the resolution and stability of RI measurements, an efficient solution has been developed, based on repeated reflection and refraction of the light beam travelling through the cylindrical cell with liquid. A new method for detecting the position of the projected laser beam on a linear optical sensor was developed, too.

The new refractometer provides more than ten times higher measurement resolution as compared to the existing instruments, and has more than ten times smaller sizes and weight, and does not depend on the stability of the structural elements of the device.

The set of refractometers has been manufactured in the framework of the project "Methanol fuel cell sensor adaptation and other control and measurement systems" TOP 06-14 [Appendix 1] and ERAF project "Innovative bio-ethanol dehydration technology and design parameters of the measuring device" 2010/0281/2DP/2.1.1.1.0/10/APIA/VIAA/003 [Appendix 2].

Refractometer has been demonstrated at the exhibition BIOTECHNICA2013, 08.10.2013-10.10.2013 in Hanover (Germany) and a great interest arose [Appendix 3].

Portable high precision cylindrical cell's refractometer has been shown at the Pittsburgh Conference (Pittcon) in Chicago, IL, USA on March 2 2014 and at the American Association for Clinical Chemistry (AACC) in Chicago, IL, USA on July 27 2014, where a great interest aroused [Appendix 4].

The main results of the research were published in 20 publications: 7 papers (4 published in the SCOPUS DATABASE), 4 patents and 9 scientific conference theses (3 international, 6 Latvia).

The list of the main publications

Papers

1. Kozlov V., Merkulov D., Vilitis O., New method for measuring refractive index of liquids Proc. SPIE 4318, Smart Optical Inorganic Structures and Devices, 89 (March 8, 2001), pp. 89-92. ISSN: 0091-3286, e-ISSN: 1560-2303 doi:10.1117/12.417582. (SCOPUS bibliographic database).
2. Vilitis O., Merkulovs D., Optical cell for measuring refractive index and concentration of liquids, Latvian Journal of Physics and Technical Sciences, Riga, 2004, 4 p.58–66. ISSN 0868 - 8257.
3. Vilitis O., Šipkovs P., Merkulovs D., Refrakcijas indeksa noteikšana šķidrumiem cilindriskā ķivetē, Latvian Journal of Physics and Technical Sciences, Riga, 2008, vol.45, no., pp.50–62. ISSN 0868-8257.
4. Vilitis O., Shipkovs P., Merkulovs D., Determining the liquids refractive index by using a cylindrical cuvette, Measurements science and technology, 2009, no. 20, 117001 (8pp), ISSN 1361-6501, eISSN 1361-6501, doi:10.1088/0957-0233/20/11/117001. (SCOPUS bibliographic database).
5. Vilitis O., Shipkovs P., Merkulovs D., Determination of two-liquid mixture composition by assessing dielectric parameters 1. Precise measuring system, Latvian Journal of Physics and Technical Sciences, Riga, 2013, no.4, pp.62–73. ISSN 0868 - 8257. DOI: 10.2478/ipts-2013-0027. (SCOPUS bibliographic database).
6. Vilitis O., Shipkovs P., Merkulovs D., Rucins A., Zihmane-Ritina K., Bremers G. Determination of two-liquid mixture composition by assessing its dielectric parameters 2. Modified measuring system for monitoring the dehydration process of bioethanol production, Latvian Journal of Physics and Technical Sciences, Riga, 2014, no.1, pp.54–61. ISSN 0868 - 8257. DOI: 10.2478/ipts-2014-0006. (SCOPUS bibliographic database).
7. Merkulovs D., Dekhtyar Y., Vilitis O., Shipkovs P., Merkulova V., Cylindrical Cuvette Light Refraction Measurements Technology to Analyses Biomedical Liquids, International Federation for Medical and Biological Engineering (IFMBE), Volume 45, 2015, pp 298-301, DOI:10.1007/978-3-319-11128-5_74, Online ISBN:978-3-319-11128-5, ISSN:1680-0737 (Springerlink).

Patents

1. Vilitis O., Kozlovs V., Merkulovs D., Mironovs I., Divstaru refraktometers, Patents LV12549, International Publication Date 20.12.2000.
2. Vilitis O., Kozlovs V., Merkulovs D., Plaša diapazona šķidrumu laušanas koeficienta mērīšanas paņēmiens un refraktometers tā īstenošanai, Patents LV13294, International Publication Date 20.05.2005.
3. Vilitis O., Merkulovs D., Refraktometra gaismas staru kūļa optiskā attēla detektēšanas paņēmiens, Patents LV13598, International Publication Date 20.09.2007.
4. Vilitis O., Šipkovs P., Merkulovs D., Šķīdumu koncentrācijas mērīšanas paņēmiens un sensors tā īstenošanai, Patents LV13728, International Publication Date 20.07.2008.

Conference theses

1. Merkulovs D., Kozlovs V., Vilitis O. A new method for measuring refractive index of liquids, 2-nd International Conference «Advanced Optical Materials and Devices», Vilnius, 16-19 August, 2000, Semiconductor Physics Institute, Lithuania 2000 p. 33, ISSN 1392-0952.
2. Merkulovs D., Vilitis O., Kozlovs V. Refractometer DBR-11, New Method for Measuring Refractive Index of Transparent liquids, Hightechbaltic2001, Exhibition Research Technologies Innovation 2001, International Exhibition Centre, Riga, September 14-15.
3. Merkulovs D., Vilitis O., Kozlovs V. Refractometer, 23-th International Award for Technology and Quality. New Millenium Award, (Trade Leader's Club), December 21, 2001, Madrid, Spain; January 10-12, 2002, Geneva, Switzerland.
4. Merkulovs D., Vilitis O., Kozlovs V. Double beam detector of refractive index – main features, 3rd International Conference on Advanced Optical Materials and Devices AOMD-3, Riga, August 19-22, 2002.
5. Merkulovs D., Vilitis O., Kozlovs V. Pocket Refractometer, Baltic Industry 2003, November 5-8, 2003.
6. Merkulovs D., Vilitis O., Shipkovs P. Determining the liquids refractive index by using a cylindrical cuvette, 54th International Scientific Conference, Riga, Latvia, October14-16, 2013.
7. Merkulovs D., Vilitis O., Shipkovs P. Determination of two-liquids mixture composition by assessing dielectric parameters, 54th International Scientific Conference, Riga, Latvia, October 14-16, 2013.
8. Merkulovs D., Dekhtyar Y., Vilitis O., Shipkovs P. and Merkulova V. Cylindrical cuvette

light refraction measurements technology to analyze biomedical liquids, Medical and Biological Engineering (MBEC 2014), Dubrovnik, Croatia 7.-11. sept., 2014.

9. Merkulovs D., Dekhtyar Y., Vilitis O., Shipkovs P. and Merkulova V. Precision cylindrical cell's refractometer to analyze biomedical liquids, 55th International Scientific Conference, Riga, Latvia, October 16-18, 2014.

Exhibitions and seminars

1. Refractometers were demonstrated at the exhibition BIOTECHNICA 2013, 08.10.2013-10.10.2013 in Hanover, Germany.
2. Seminar in RTU Biomedical Engineering and Nanotechnology Institute 22.01.2015, Riga, Latvia [Appendix 5].
3. Seminar in Latvian National Mechanics Committee (LNMK) and RTU Institute of Mechanics (MI) 17.02.2015, Riga, Latvia [Appendix 6].

Theses to defend

1. The new refractometer has been designed and developed. It is equipped with the original optical and control system, and these systems allow many times to increase the MR.

2. The mathematical model of the new CCR is created, that confirms the possibility of increasing the resolution of the RI measurement by 3 powers as compared with the conventional refractometers (from 10^{-4} to 10^{-7}).

3. The new RI measurement algorithm has been developed. This algorithm employs the detectable beam interference pattern of the first minimum space, in such a way increasing the RI measurement resolution (MR) up to 10^{-5}.

4. The new CCR provides the improved resolution (by one power) of the concentration measurements of the calibrated solutions (sugar, sodium chloride, ethanol-water solutions).

5. The new CCR has been created and calibrated, and the testing process of this device has been provided.

Scientific novelty

For the first time:

1. The basic operating principles of the refractometers were developed, where an optical beam refraction and multiple reflections in a cylindrical cell has been used, in such a way increasing the RI measurement resolution by one power and achieving MR = 10^{-5}.
2. The mathematical model has been developed and analyzed, which takes into account the temperature effect on the detection of resolution, the possibility to achieve the resolution up to 10^{-7} has been demonstrated. It has been shown; that the multiple light beam passage through cylindrical cell with test liquid increases the RI measurement resolution in line with the number of the passage cycles.
3. The RI measurement algorithm and measurement method have been developed, where a minimum place of the detectable beam interference pattern has been used, that allows to achieve the RI measurement resolution $2 \cdot 10^{-5}$.

Practical application implementation

- CCR with a new physical principle of RI measurement and concentrations of the solution has been used in the following projects:

  - Project "Methanol fuel cell sensor adaptation and other control and measurement systems" TOP 06-14. Institute of Physical Energetic, Riga, Latvia.

  - ERAF project "Innovative bio-ethanol dehydration technology and design parameters of the measuring device" 010/0281/2DP/2.1.1.1.0/10/APIA/VIAA/003. Institute of Physical Energetic, Riga, Latvia.

- Company ELMI Ltd (Riga, Latvia) has commenced the manufacturing process of 6 CCR prototypes for commercial use and market research. These prototypes were demonstrated at the Pittsburg Conference (Pittcon) in Chicago, IL, USA on July 27 2014. Currently, these devices operate in the United States and Germany.

Chapter 1. REFRACTION INDEX AND CONTENTS OF LIQUIDS

1.1. Refractive index measurement principle

Refractive index (RI) relates to of the speed of light in a medium. The refractive index (n) of a medium is defined as the ratio of the speed of light in vacuum (c=299 792 458 m/s) in to that in the medium (υ):

$$n = \frac{c}{\upsilon} \tag{1.1}$$

As the speed of light is highest in vacuum $c > \upsilon$, n is always greater than 1.

The speed of light in a medium depends on the temperature and wavelength. Due to the wavelength dependency, the refractive index is measured with monochromatic light. The common practice is to use the yellow sodium D-line wavelength 589.3 nm. The refractive index measured at this wavelength is usually denoted by n_D. The standard temperature is +20ºC or +25ºC [102]. Refractometry should be considered as the oldest of the used optical research methods [113].

Detection of liquid concentrations by optical means was already known in antiquity [104]. The law of refraction was mathematically formulated first by Ibn Sahl in 984 [93, 70].

His discovery was not known in Europe, and usually the discovery is attributed to Dutch astronomer and mathematician Willebrord Snellius (Snell), who rediscovered the law and published it in 1621 [93, 70].

Snell's law states that the ratio of the sines of the angles of incidence and refraction is equivalent to the ratio of phase velocities of light in the two media, or equivalent to the reciprocal of the ratio of the indices of refraction:

$$\frac{\sin \alpha_1}{\sin \beta_1} = \frac{\upsilon_1}{\upsilon_2} = \frac{n_2}{n_1}, \tag{1.2}$$

with each α_1, β_1 as the angle measured from the normal of the boundary, υ as the velocity of light in the respective medium (SI units are meters per second, or m/s) and n as the refractive index (which is unitless) of the respective medium (Fig.1.1) [93].

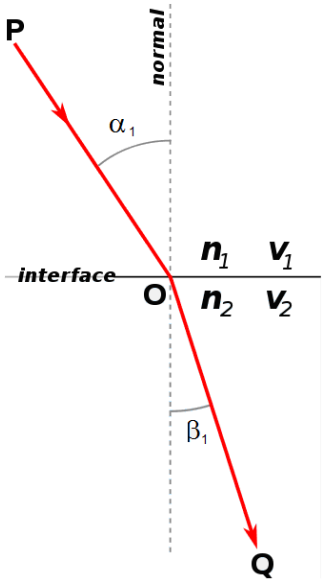

Fig. 1.1. Refraction of light at the interface between two medias of different refractive indices, with $n_2 > n_1$. Since the velocity is lower in the second medium $(v_2 < v_1)$, the angle of refraction β_1 is less than the angle of incidence α_1 [93]

Already in Newton's "Optics" interpretation we can find some data for "refractive power" of a number of substances in terms of the existing notions about their chemical nature at that time [104]. Based on the values of the refractive index and density Newton made some interesting conclusions about the composition of salts, ethyl alcohol and diamond affinity with organic substances which he guessed long before, than it has been proved by chemical means [104].

Extensive program of Lomonosov physicochemical research also included "experiments of refraction in liquids" (1756 et seq.). Among the tools with which Lomonosov "began the difficult business connections chemistry, physics and geometry", was applied quadrant they invented for determining the refractive index in chemical substances. On the design and improvement of this device - one of the first refractometers - Lomonosov worked from 1752 to 1762 years [113].

1.2. Concentration of the components of the liquids, its density and refractive index

Refractive index (RI) is an important characteristic of liquid substances for analyzing, monitoring, and identification of liquids in several industries nowdays. Accurate determination of the concentration of the solution by measuring the RI is widely used in chemical and physical studies, food technology, materials processing, medical diagnostics, monitoring systems, fuel cells directly measuring pollution, and many other fields.

In general, the measured refractive index of a multicomponent mixture is a function of its temperature *T*, concentration *C*, and the wavelength of the incident light λ [49]:

$$n = n(T, C, \lambda) \tag{1.3}$$

In sections 1.3 and 1.4 the dependence of temperature and wavelength of light on RI will be considered in detail.

From Eq.(1.3), the change of RI Δn of a multicomponent mixture is:

$$\Delta n \approx \frac{\partial n}{\partial T}\Delta T + \frac{\partial n}{\partial C}\Delta C + \frac{\partial n}{\partial \lambda}\Delta\lambda\,, \tag{1.4}$$

for small changes of the temperature, concentration, and wavelength. Since laser light is highly monochromatic and wavelength-stable, $\Delta\lambda \approx 0$ and wave length effects can be neglected. In this work, the concentration is defined on a mass basis for liquids A and B,

$$C_A = \frac{M_A}{M_A + M_B}, \tag{1.5a}$$

$$C_B = \frac{M_B}{M_A + M_B}, \tag{1.5a}$$

were *M* - mass, kg.

Thus, by measuring the change in refractive index and the liquid temperature, the concentration change can be expressed using Eq. (1.4) as follows:

$$\Delta C \approx (\Delta n - \frac{\partial n}{\partial T}\Delta T)(\frac{\partial n}{\partial C})^{-1} \tag{1.6}$$

Changes in the density of matter are always accompanied by some change of RI.

Usually RI increases with increasing density. Theoretical study of the relationship between the density of matter and its RI, as well as the experimental data shows that there is a direct proportion between some RI function $f(n)$ and density d :

$$f(n) = rd \tag{1.7}$$

The constant factor r that is specific for this substance is called as specific refraction. As

distinct from n and d the specific refraction does not depend on external conditions (temperature, pressure) and very slightly depends on the state of aggregation of matter [102].

There are many attempts to derive a general formula for the function of all substances $f(n)$, but a universal function that is independent of the properties of matter does not exist [102].

The most widely used theoretical method for predicting the refractive index n_L of binary mixtures of liquids is the Lorentz–Lorenz relation [19]:

$$\frac{n_L^2-1}{n_L^2+2}=\Phi_1\frac{n_{D1}^2-1}{n_{D1}^2+2}+\Phi_2\frac{n_{D2}^2-1}{n_{D2}^2+2}, \tag{1.8}$$

where n_L is the refractive index of the mixture according to the Lorentz–Lorenz formula; Φ_1 and Φ_2 are the volume fractions of alcohol and water, calculated from volume determinations based on the mass and density measurements, and n_{D1} and n_{D2} are the refractive indices of the alcohol and water, respectively.

Empirical equations have also been developed to determine refractive indices of binary systems of liquids, including that proposed by Gladstone-Dale [25]:

$$\frac{n_G-1}{\rho}=\omega_1\left(\frac{n_{D1}-1}{\rho_1}\right)+\omega_2\left(\frac{n_{D2}-1}{\rho_2}\right), \tag{1.9}$$

where n_G is the refractive index of the mixture according to the Gladstone–Dale formula; ρ is the experimental density of the mixture; ω_1 and ω_2 are the mass fractions of alcohol and water; and n_{D1} and n_{D12} are the refractive indices of the alcohol and water, respectively.

The validity of the Lorentz–Lorenz and Gladstone–Dale relations in application to different types of mixtures has been confirmed by a number of investigators.

The concentration can be calculated from the refractive index and temperature when these nonlinear functions are known. There are several possible temperature compensation algorithms. In practical use, a simple 3rd degree polynomial is typically used.

By applying data analysis program, the experimental data were subjected to curve fitting and the temperature coefficient of refractive index of water was found to be equal to -1.853×10^{-4} C°. For measurements with high resolution, the optical constants of the glass

container should also be taken in account because the light will pass through both the solution and the container. According to the literature [102], the temperature coefficient of refractive index of glass is of the order of 10^{-4} C°. It is evident that very small error can occur if the temperature dependence of the refractive index of glass is not taken into account while measuring the temperature coefficient of refractive index of liquids.

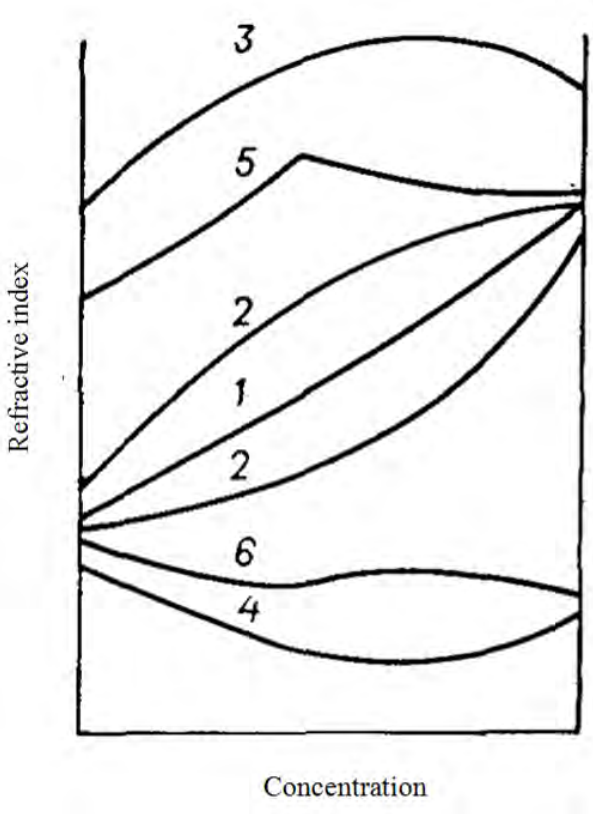

Fig. 1.2. Types of curves characterizing refractive index - concentration (composition):
1 - with a small curvature; 2 - with a big curvature; 3 - with the maximum; 4 - with a minimum;
5 - with the singular point; 6 - to the point of inflection [102]

Chart of the refractive index – this structure for dual systems can have very different shapes (Fig.1.2). They can be curved with a slight curvature or can be almost straight, but may have a significant bulge of a curve to the composition axis or RI axis. Sometimes it is possible to see some minimums and maximums on these curves, where *n* is a value equal to two solutions of different concentrations. Less common on these curves are *n* – parts of breakages (singular points) and some points of inflection. The form of these considered curves depends on two factors: the nature of the components and their interactions in the formation of the solution and on the method of expression of solution's components.

Many oils (such as olive oil) and ethyl alcohol are examples of liquids which are more refractive, but less dense, than water, contrary to the general correlation between density and refractive index [102].

1.3. The influence of temperature of liquids on the refractive index

The first created refractometers in the world were not equipped with any temperature compensation. Therefore, they almost did not find any wide application in practice. And only then, when it was possible to manufacture refractometers with thermal stabilization, and it happened in the late 19th century, refractometers have been widely used in practice [6, 15, 16, 102].

The influence of temperature and pressure on the RI is determined by the following two factors:

1) changing the number of particles per unit of volume when we have heating or pressure (i.e., expansion coefficient and compressibility coefficient), and

2) dependence on the polarizability of the molecules according to the temperature and pressure.

The second of these factors usually becomes significant only at very high pressures and a wide range of temperatures.

The general expression for the temperature coefficients of the RI can describe it:

$$\frac{\partial n}{\partial t} = \left(\frac{\partial f(n)}{\partial n}\right)^{-1} \left(r\frac{\partial d}{\partial t} + d\frac{\partial r}{\partial t}\right), \tag{1.10}$$

where r - refraction d -dispersion, t - temperature [102].

For the vast majority of liquids, the value $\delta n / \delta t$ is in a narrow range from -0.0004 to -0.0006 deg^{-1}, on the average it is 0.0005 deg^{-1}. Some important exceptions are water and diluted aqueous solutions ($\partial n / \partial t = -0.0001$), glycerin (-0.0002) glycol (-0.00026) as well as some high refractive liquids, such as carbon disulfide (-0.0008). The relation (1.69) shows that $\partial n / \partial t$, as well as n are wavelength dependent. These values increase with decreasing of λ. However, this increase in the visible range is negligible. The following formula can describe it:

$$(n_\lambda - 1)^{-1} \frac{\partial n_\lambda}{\partial t} = (n_\infty - 1)\frac{\partial n_\infty}{\partial t} + \frac{n}{\lambda^2} \tag{1.11}$$

A linear extrapolation of the variables n is permissible for some small temperature difference (10-20˚C). Already in the temperature range of 40-60˚C for organic liquids a clearly expressed (and not strictly linear) dependence $\partial n / \partial t$ on the temperature is found. Accurate calculations n for a wide temperature range are made from the empirical formulas as follows:

$$n_t = n + a \cdot t + b \cdot t^2 \ldots, \tag{1.12}$$

where a, b - coefficients.

As an example we can use the empirical formula expressing the temperature dependence of the benzol RI up to the boiling point:

$$n_t = 1.51431 - 6.44 \cdot 10^{-4} t + 0.033 \cdot 10^{-6} t^2 - 2.391 \cdot 10^{-9} t^3 \tag{1.13}$$

In liquids and solids, the compressibility is very small; the increase in pressure of 1 atm is generally increasing n by several units of 10^{-5}.

For example, for water $\partial n / \partial p = 1.48 \cdot 10^{-5}$ for alcohol - $3.95 \cdot 10^{-5}$, and for benzene $4.8 \cdot 10^{-5}$. The growth of the temperature leads to an increase of the coefficient $\partial n / \partial p$, which is about 1% (when the temperature is 1˚C). Consequently, some fluctuations in atmospheric pressure so slightly affect the refraction of solids and liquids that this usually is not taken into account. For gases, on the other hand, the influence of pressure so as great as the influence of the temperature, and is always taken into consideration when measuring RI [102].

1.4. Refractive index in dependence on the wavelength

The refractive index can be seen as the factor by which the speed and the wavelength of the radiation are reduced with respect to their vacuum values: the speed of light in a medium is Eq.(1.1), and similarly the wavelength in that medium is:

$$\lambda = \frac{\lambda_0}{n}, \tag{1.14}$$

where λ_0 is the wavelength of that light in vacuum.

The refractive index varies with the wavelength of light.

In the reference literature for the media materials the data *n* are mainly referred. These data correspond to the standard wavelength. In these developed refractometers a laser with a non-standard wavelength is employed and for mathematical calculations empirically obtained approximation formulas are used. The resolution of the RI measurements obtained in this manner can reach to 10^{-5}. There is an extensive database of RI depending on the wavelength of the laser [71].

Below are some graphs, showing dependence of λ on the RI and the formula for the materials mentioned in the paper:

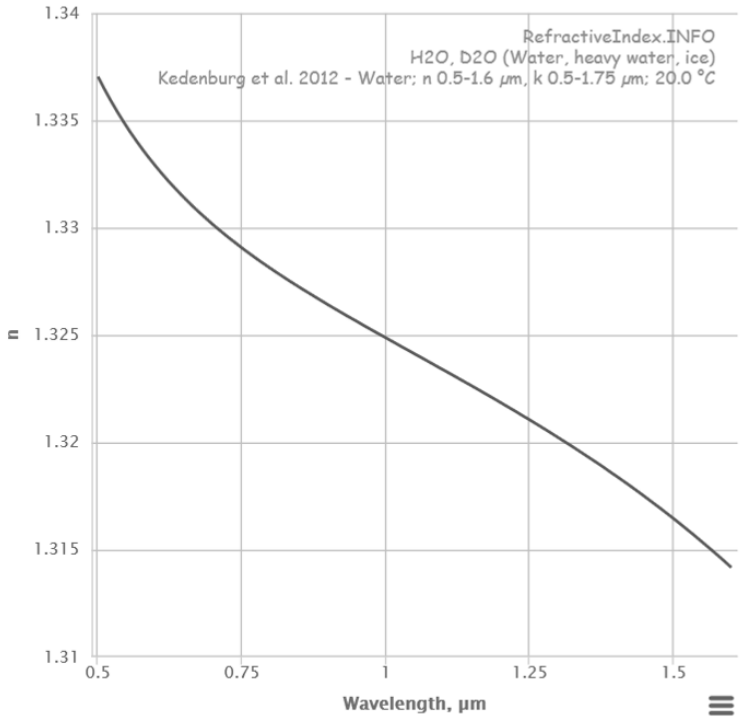

$$n^2 - 1 = \frac{0.75831\lambda^2}{\lambda^2 - 0.01007} + \frac{0.08495\lambda^2}{\lambda^2 - 8.91377}$$

Fig. 1.3. Influence of wavelength of the laser on water's refractive index [71]

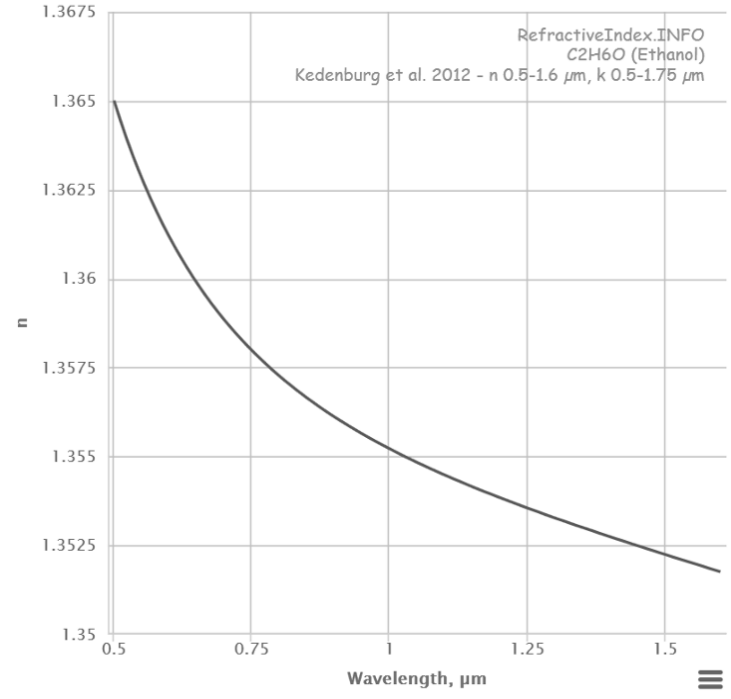

$$n^2 - 1 = \frac{0.83189\lambda^2}{\lambda^2 - 0.00930} + \frac{-0.15582\lambda^2}{\lambda^2 + 49.45200}$$

Fig. 1.4. Influence of wavelength of the laser on the refractive index for ethanol [71]

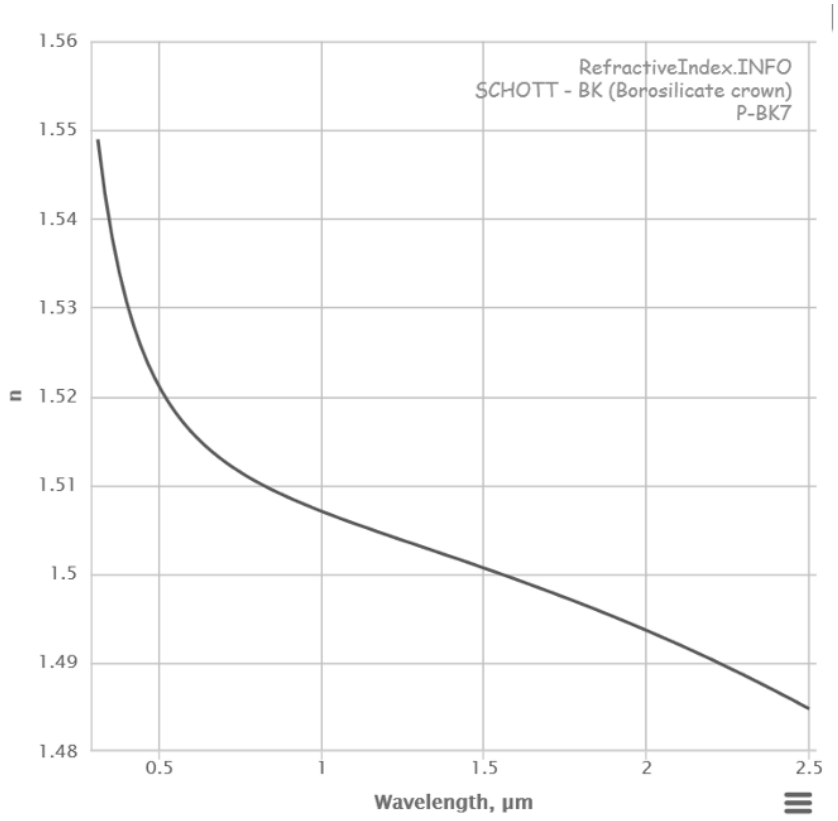

$$n^2 - 1 = \frac{1.18318503\lambda^2}{\lambda^2 - 0.00722141956} + \frac{0.0871756426\lambda^2}{\lambda^2 - 0.0268216805} + \frac{1.03133701\lambda^2}{\lambda^2 - 101.702362}$$

Fig. 1.5. Influence of wavelength of the laser on the refractive index for borosilicate crown BK [71]

1.5. Conclusion

Refractive index (RI) is an important characteristic of liquid substances for analyzing, monitoring, and identification of liquids in several industries nowadays.

Refractive index (RI) has a very complex, non-linear dependence on many factors: concentration, density, temperature and pressure of the measuring liquid. The RI of the measuring liquid also depends on the optical material, air and wavelength of the light source.

High sensitivity of the RI measurements in aqueous solutions depending on concentrations and density makes these refractometers as highly sensitive and accurate devices.

But a great influence of the temperature on the resolution of the RI measurements requires taking into account the temperature change already from 10^{-4} RI [102].

All this must be considered carefully when designing.

Chapter 2. REFRACTOMETERS. STATE OF THE ART

2.1. Abbe refractometer

Intensive development of refractometry began in the second half of the XIX century, when one of the main problems was finding the dependence of properties of substances on their composition and structure, and growing industry required the development of convenient and simple methods of analysis. Important role in spreading refractometric analysis methods played by professors Ernst Abbe (1840-1905) and Carl Pulfrich (1858-1927) from Jena, who created the design of refractometers, that are widely used now days [102, 79].

The Fig.2.1 shows a schematic diagram of its optical system. The sample is contained as a layer (~0.1mm) between two prisms. The upper prism is firmly mounted on a bearing that allows its rotation by means of the side arm shown in dotted lines. The lower prism is hinged to the upper to permit separation for cleaning and for the introduction of the sample. The lower prism face is rough-ground: when light is reflected into the prism, this surface effectively becomes the source for an infinite number of rays that pass through the sample at all angels. The radiation is refracted at the interface of the sample and the smooth-ground face of the upper prism. After this it passes into the fixed telescope. Two Amici prisms that can be rotated with respect to another serve to collect the divergent critical angle rays of different colors into a single white beam that corresponds in path to that of the sodium D ray. The eyepiece of the telescope is provided with crosshairs: in making a measurement, the prism angle is changed until the light-dark interface just coincides with the crosshairs. The position of the prism is then established from the fixed scale (which is normally graduates in units of n_D). Thermosetting is accomplished by the circulation of water through the jackets surrounding the prism.

The Abbe refractometer is very popular and owes its popularity to its convenience, its wide range (n_D=1.3 to 1.75), and to the minimal sample is needed. The resolution of the instrument is about ±0.0002; its precision is half this figure. The most serious error in the Abbe instrument is caused by the fact that the nearly glazing rays are cut off by the arrangement of to prisms; the boundary is thus less sharp than is desirable.

A precision Abbe refractometer, that diminishes the uncertainties of the ordinary instrument by a factor of about three, is also available; the improvement in resolution is obtained by replacing the compensator with a monochromatic source and by using larger and more

precise prism mounts. The former provides a much sharper critical boundary, and the latter allows a more accurate determination of the prism position [39].

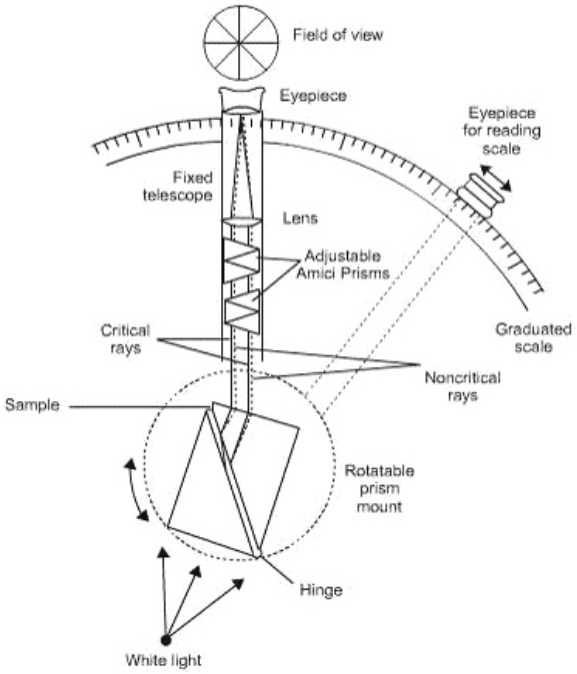

Fig. 2.1. Abbe refractometer [39]

2.2. Pulfrich refractometer

Pulfrich refractometer is the second design (after Abbe refractometer) that became commercially available in 19th century. It is another type of the critical angle refractometer. Unfortunately, probably because it is rarely used and much less common in labs, people tend to call every refractometer that is different from Abbé design "Pulfrich refractometer" - in effect you will commonly see many types of refractometers named "Pulfrich", in most cases without any reason [34].

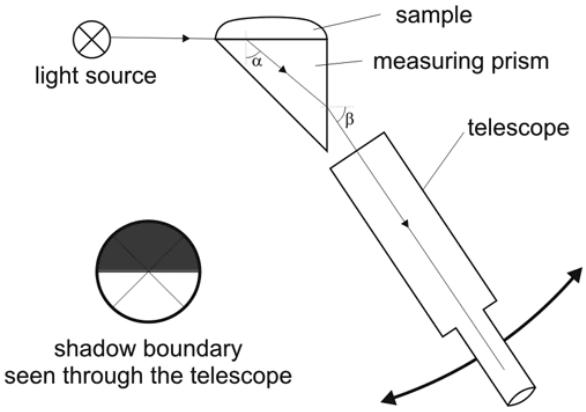

Fig. 2.2. Pulfrich refractometer [34]

This description of the instrument was published in the early 20th century in the Arthur H. Thomas Company catalogue. A glass prism of high refractive index has two plane polished faces, which are perpendicular to one another, and is so placed that one of these is vertical and the other horizontal. The substance whose refractive index is required to place on the horizontal surface, and in the case of a liquid is contained in a glass cell cemented to the prism so as to contain that face. A beam of monochromatic light is directed almost horizontally through the substance so that it meets the prism face at grazing incidence. The emergent beam is bounded sharply by the ray which actually grazes the prism surface, and the sharp boundary is observed with a telescope attached to a divided circle. On this circle, whose axis of rotation is horizontal, the angle of emergence of the beam from the vertical prism face can be read to one minute, with the aid of a vernier. For making measurements of dispersion a clam and a micrometer are provided, the smallest division on the drumhead of the micrometer screw corresponding to 6 seconds of arc. A condensing lens and supporting rod for vacuum tube form part of the apparatus. A small reflecting prism us also provided so that another source of light, e.g., a sodium flame, is easily interchangeable with the vacuum tube.

A special feature of the instrument is the increased effectiveness in the temperature control as compared with that to be found in previous designs. The hollow metal water jacket surrounding the prism is provided with a top cover with is itself of hollow metal. These two are connected in train with the thermometer jacket which dips into the cell for liquids. The prism and the substance experimented upon are thus completely jacketed with the exception of the vertical prism face from which the light emerges, and a small rectangular aperture by which the light enters the prism. The temperature can thus be maintained very constant by pumping a stream of water at a constant temperature through the system described.

Although the two main refractometers - Abbé and Pulfrich - were able to meet needs of the majority of analytical laboratories, work on better devices never stopped. New designs included devices suitable for use outside the laboratory (such as immersion refractometers, offered by Zeiss since around 1900) and devices providing better precision than the typical value of 0.0001 attainable with Abbé refractometers [34].

2.3. Cell based refractometers

Various methods and devices are used conventionally to measure the refractive index. The diversity of methods is largely due to differences in applications, test objects and the required measurement resolution. A separate class of devices for measuring the refractive index

of transparent liquids consists of systems designed for examining liquids in cells made of glass, quartz or other transparent materials.

A light beam, usually a laser beam, is directed through the cell, whose walls serve as an optical element that, together with liquid, determines the beam's path through the optical system depending on the RI of the liquid. Intensive evolution of photo-electrical linear measuring element technologies in recent years makes it possible to determine the deviation of the beam exiting the cell accurately, conveniently and quickly. Devices of this kind can be used for measuring RI of stationary liquids contained in the cell and they are also interesting for easy incorporation of the cell directly in the liquid production/utilization circuit and measuring the RI's of continuous liquid flows (including aggressive liquids) in real time.

During the last decade, numerous practical devices based on the principle described above using various cells have been constructed for determining the refractive index. In a device for measuring sugar concentration under stationary conditions, designed in 1997 [61], a laser light source and a cell of triangular cross section were used. In a similar device [42], the triangular cell was adapted to measure the RI of various liquids flowing through it.

The refractometer is shown in Fig.2.3(a) diode laser with a nominal wavelength of 635 nm serves as the light source. A single-mode optical fiber terminated with an aspheric lens delivers a 0.5 mm diameter collimated beam to the test cell. The cell is a triangular custom made cell, with interior dimensions of 14.8x15.1x21.1 mm, as shown in Fig.2.3(b). The laser beam is incident normal to the first cell wall and exits the adjacent wall at an angle that depends on the refractive index of the test liquid in the cell, n_l. After exiting the cell, the beam strikes a semiconductor position sensor. A mechanical pump drives the test liquid through the optical cell at a flow rate of ≈ 38 g/min.

A concentration change in the cell results in changes in n_l and a corresponding movement of the beam position on the sensor. A linear position sensor monitors the beam position change over a 5 mm range and is capable of detecting beam displacements as small as 2 μm . The sensor output current is sent to a position-to-voltage converter, which produces an output voltage linearly proportional to the beam position that is measured using a 6.5 digit digital multimeter (DDM). The measured position sensor sensitivity was 3.0/ mV/ μm . The DMM is connected to an IBM computer using a general purpose interface bus for data acquisition. In this measurement, the sampling rate is 2 samples/s.

To validate the technique, two aqueous salt solutions, NaCl–H_2O and $MgCl_2$–H_2O, are measured. Experiments are performed for both large (0%–25%) and small (0%–2) and (0%–

0.2%) concentration variations. These particular solutions were chosen because of their linear relationship between n and C, which simplifies the analysis and aids in determining the smallest resolution of the system. An additional advantage of aqueous salt solutions is that very small concentration changes can be accurately and easily prepared. Solutions of known concentrations were prepared by measuring the mass of the salt and water on an Ohaus digital balance with a resolution of 0.01g. The resolution to measure RI is no more than 10^{-4}.

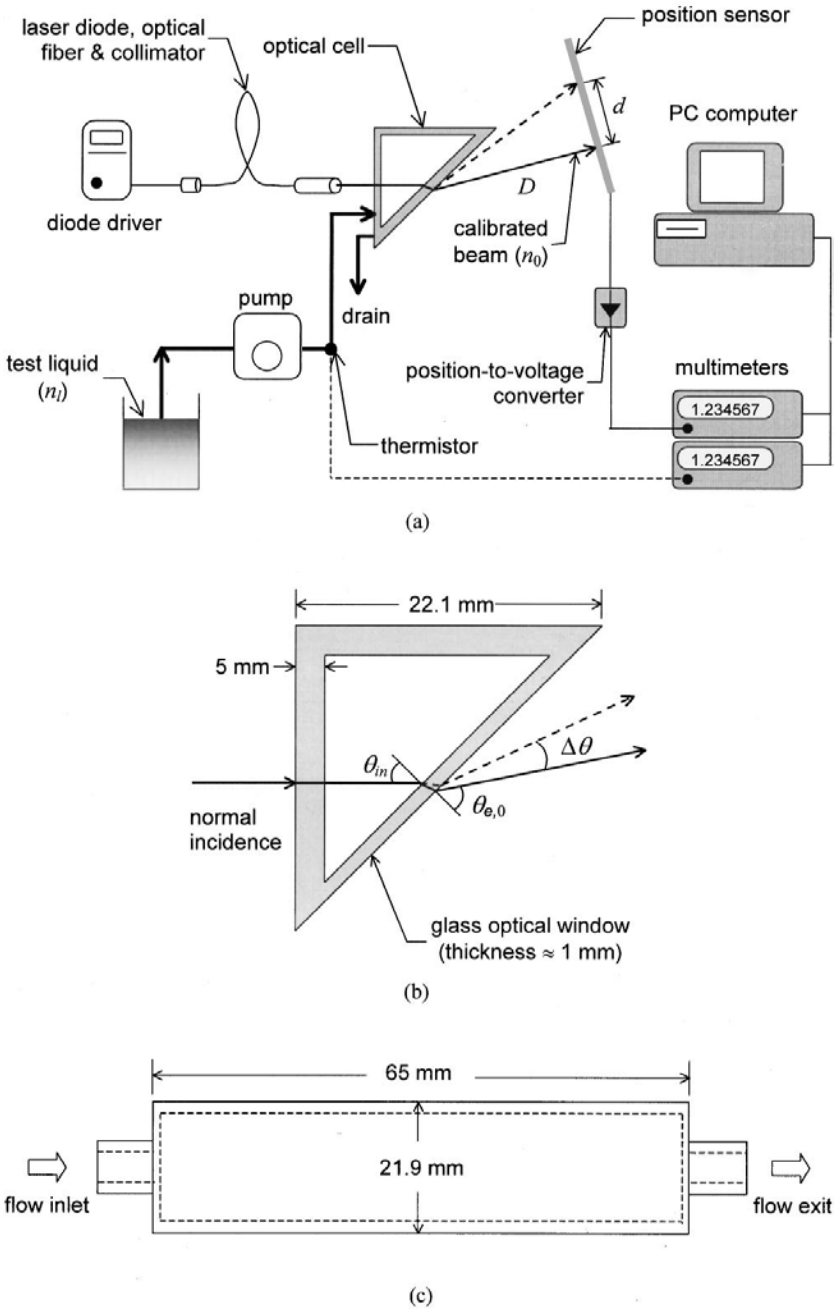

Fig. 2.3. Schematic of the experimental setup [42]
(a) Experimental setup for concentration measurement of flowing liquids;
(b) Geometry of beam path through optical cell;
(c) Side view of the optical flow cell

and is modulated with a look-in amplifier. The lock-in amplifier provides a sinusoidal signal to modulate the diode laser output at a unique frequency that is detected at the photodiode amplifier output. The laser diode has an integrated photodiode to provide feedback to the diode driver, resulting in very stable laser intensity; the intensity from this configuration is stable to $\pm 0.02\%$.

A high-quality circular optical fused silica window 25.4 mm in diameter and 9.625 mm thick covers the test liquid Fig.2.4(b). For the experiment, the window provides high transmittance through the visible spectrum and a smooth, flat surface for the solid-liquid interface. Note that the optical window is not necessary for the measurement. If a high optical quality glass container is used, then the glass wall of this container can replace the optical window as a view port. The liquid under the window can either be flowing or stationary with comparable results in both cases.

The resolution to measure RI is no more than 10^{-4}.

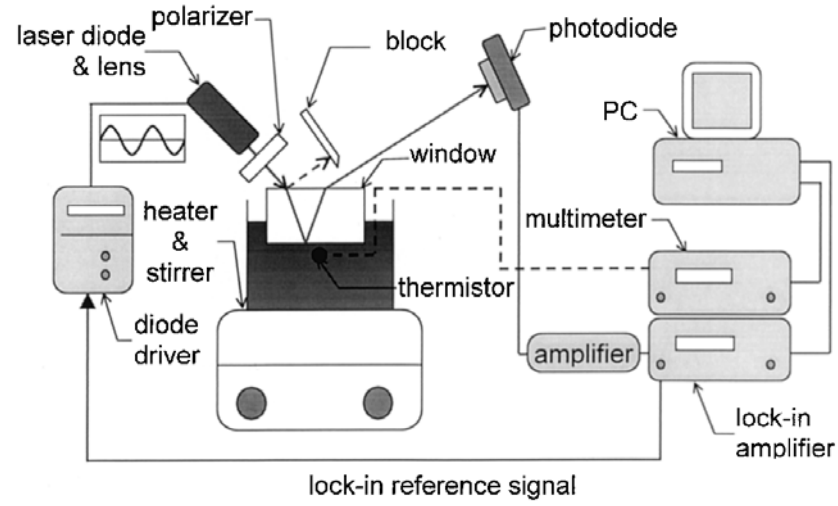

(a)

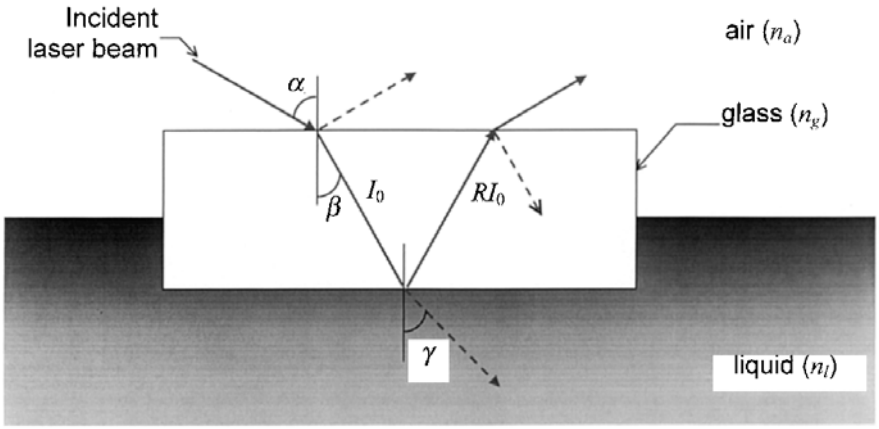

(b)

Fig. 2.4. Schematic of the experimental setup [49]

The same kind of cell was used in another optical system [49], where the plane containing the path of the laser beam was parallel to opposite walls of the rectangular cell.

The refractometer is shown in Fig.2.5. A 1-mW linearly polarized HeNe laser with a wave length of 632.8 nm serves as the light source. A precision square glass cell, with interior dimensions of 10x10x35 mm, is used as the liquid container and optical cell. The lengths of each cell side were measured and found to be within 0.25 μm , and the edges were square to within ± 3.0 mrad. The laser beam is directed onto the cell wall at a specified incident angle ranging from 70 to 80º using a rotation stage. The beam exits the adjacent cell wall at an angle that depends on the index of fraction of the liquid in the cell, n, and strikes on a semiconductor position sensors Fig.2.5(a).

The resolution to measure RI is no more than 10^{-4}.

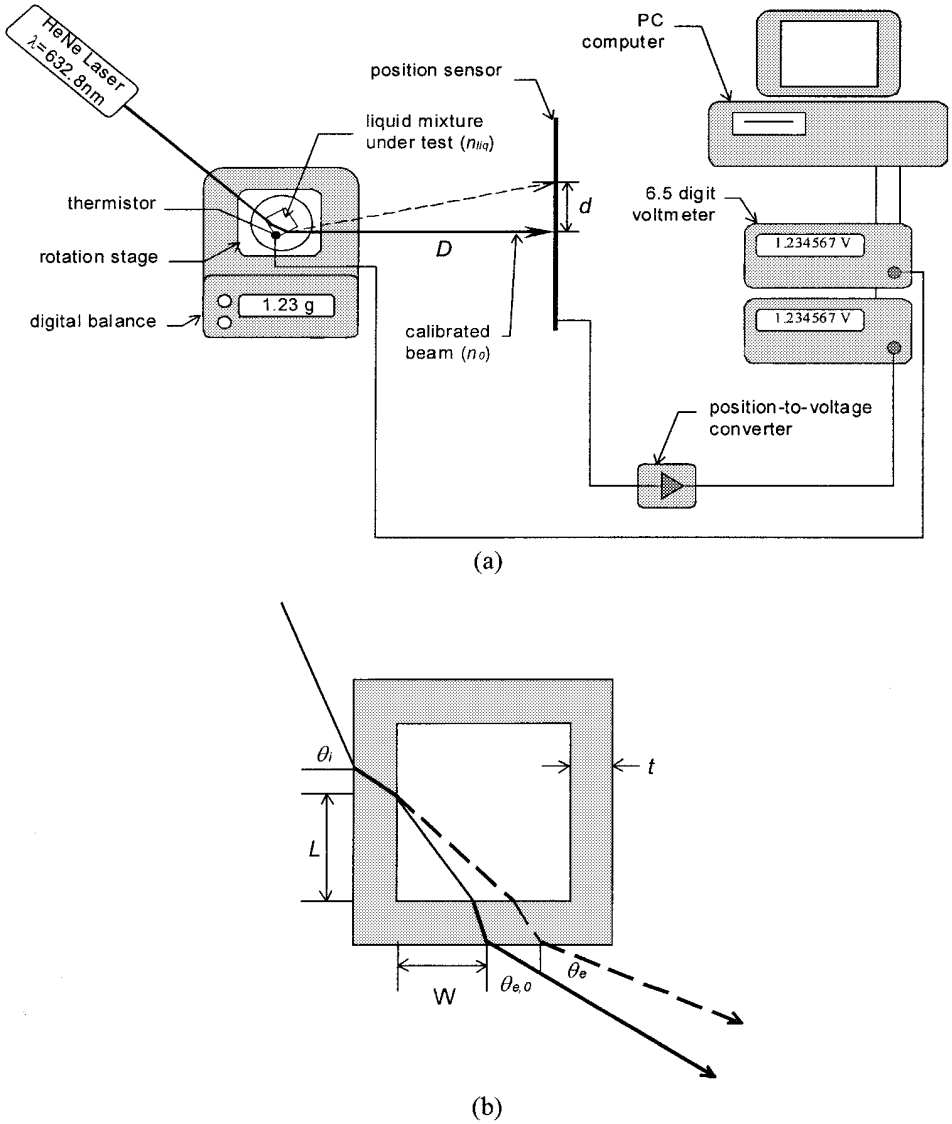

Fig. 2.5. Schematic of the experimental setup
(a) Experimental setup for laser-based concentration measurement;
(b) Geometry of the beam path through the cell

Despite the advantages gained by using a cell whose walls operate as an optical element, the magnitude of the deviation of the beam in such systems is relatively small— both when using a cell of polygonal and of cylindrical cross section [40]. This imposes strong requirements on the devices determining the deviation of the beam and restricts their compactness.

The optical measuring element of such a detector consists of plane-parallel glass or sapphire ground and polished faced plate pos.1, which forms the part of the measuring cell pos.2., for instance, its bottom, as sown on Fig. 2.6.

A parallel beam of light from the laser diode pos.3 is directed through the transparent entry window pos.4 into the cell with the liquid under study pos.5. This beam is refracted at the dividing surface between the plate and the liquid.

Fig 2.7 shows the distribution I_R light intensity, expressed in relative units for one light beam, with distilled water as the liquid under investigation.

The changes in light intensity along the cross section of the beam reveal a pronouncedly steeply linear rising front which may be observed also in measurements on other liquid solutions.

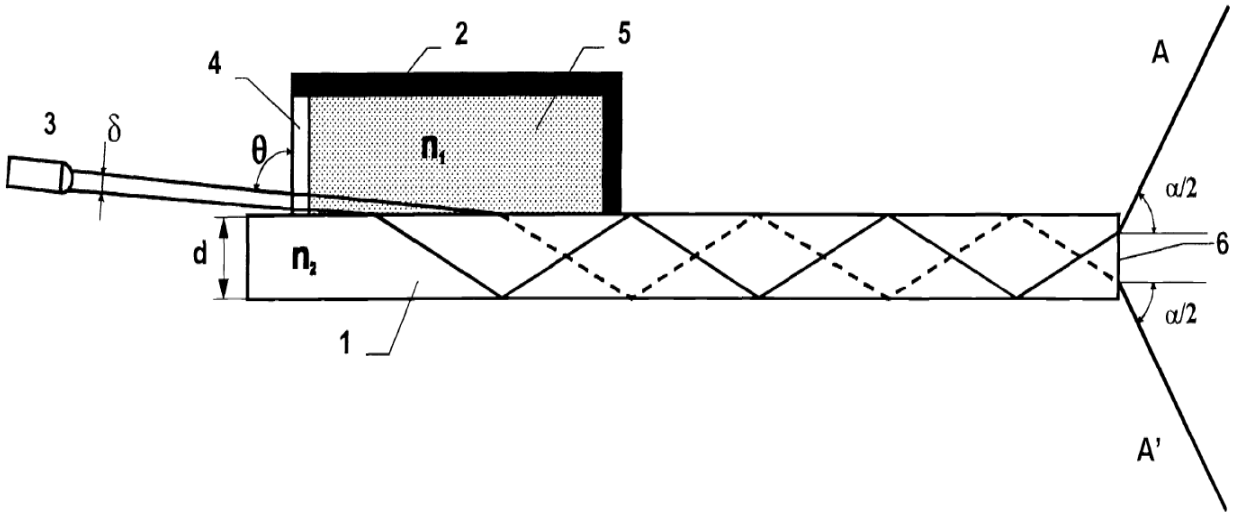

Fig. 2.6. Optical set-up of the double-beam detector [40]

The resolution to measure RI is no more than 10^{-5}, at a considerable distance from the circuit board pos.1 to a linear optical element (180 mm). Such large sizes required a special rigid mounting of all the main components of the refractometer: the laser diode pos.3, measuring the cell pos.2 and the linear optical element.

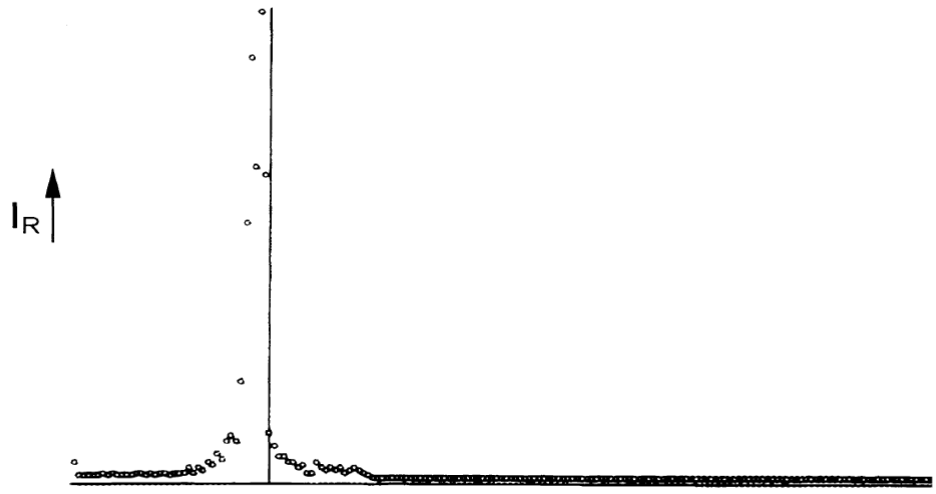

Fig. 2.7. Light intensity I_R distribution (arbitrary units) along the cross section of one of the deflected beams pos. A, registered at 120 μm intervals [40]

Method for measuring the refractive index of liquids using a cylindrical cell shown in Fig.2.8, [17] where it shows an incident laser beam of diameter d upon the cylindrical cell, where the principal ray of the laser beam emerges from the cell with a deviation angle θ with respect to the axis x. Fig.2.8 also shows the angles ϕ1 and ϕ2 which are the angles of the upper and lower marginal rays, respectively, of the divergent laser beam emerging from the cylindrical cell. The resolution to measure RI is no more than 10^{-4}.

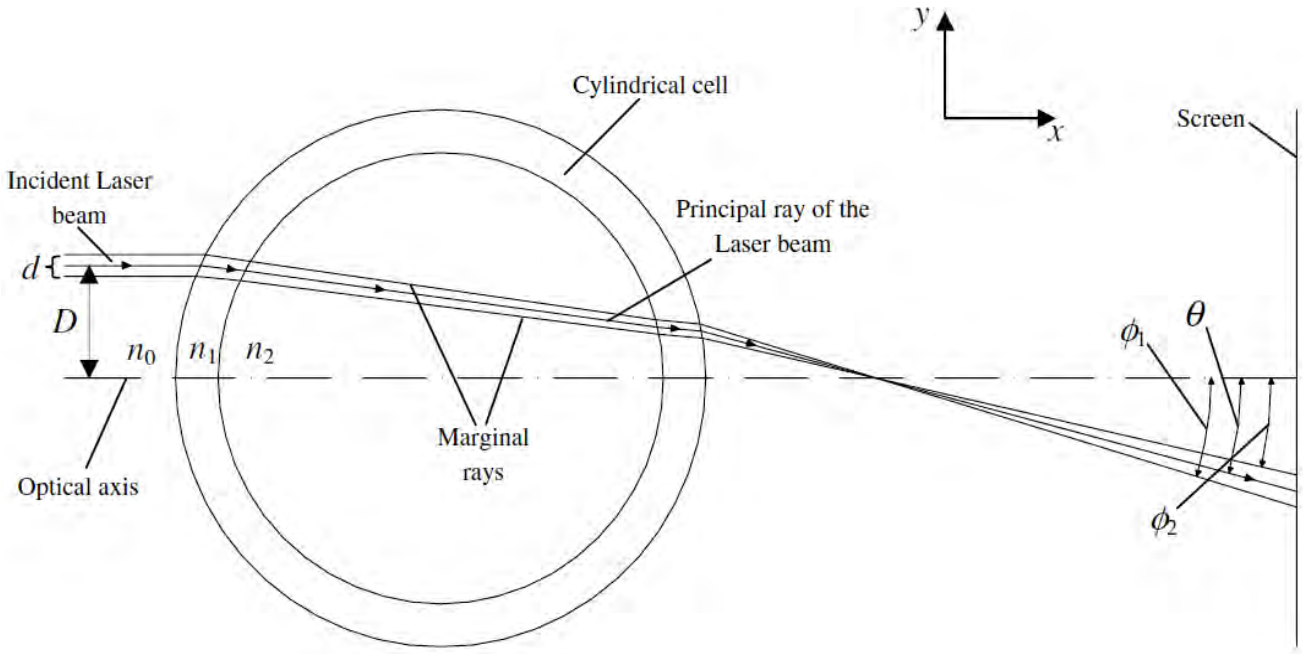

Fig. 2.8. Angles of the principal and marginal rays emerging from the cylindrical cell [17]

2.4. Modern refractometers

These days, a modern digital refractometer is part of the standard equipment of practically all laboratories. The reason for this is obvious: refractive index determination is usually the simplest and fastest method to characterize liquid samples.

With the development of CCD the increasing development has refractometers without telescopes or where telescopes are used as additions to the refractometer (Fig 2.9).

Fig. 2.9. Abbe refractometer today DR-A1 [1]

The K-Patents inline refractometer sensor determines the refractive index (R.I.) of the process solution by measuring the critical angle of refraction. Light from a light source ((L) in Fig. 2.10) in the sensor is directed to this interface. Two of the prism surfaces (M) are total-reflecting mirrors bending the light rays that thus meet the interface at different angles [31, 41, 68].

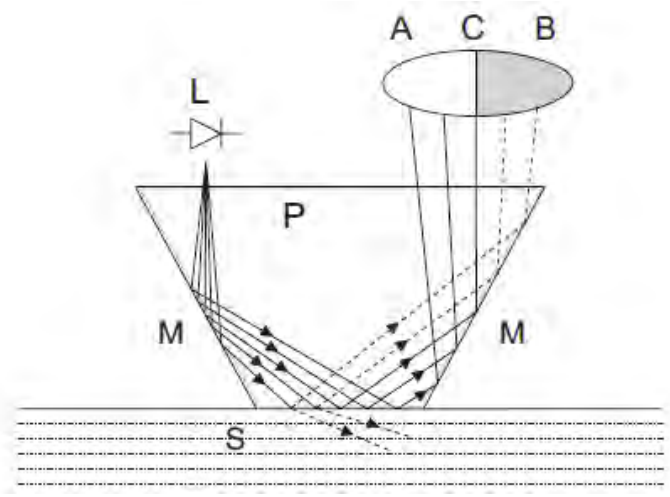

Fig. 2.10. Optical system of the K-Patents refractometer [31]

The reflected rays of light form an image (ACB), where (C) is the position of the critical angle ray. The rays at (A) are totally reflected at the process interface, the rays at (B) are partially reflected and partially refracted into the process solution. In this way the optical image is divided into a light area (A) and a dark area (B). The position of the borderline (C) between the areas shows the value of the critical angle and thus of the refractive index (R.I.) of the process solution.

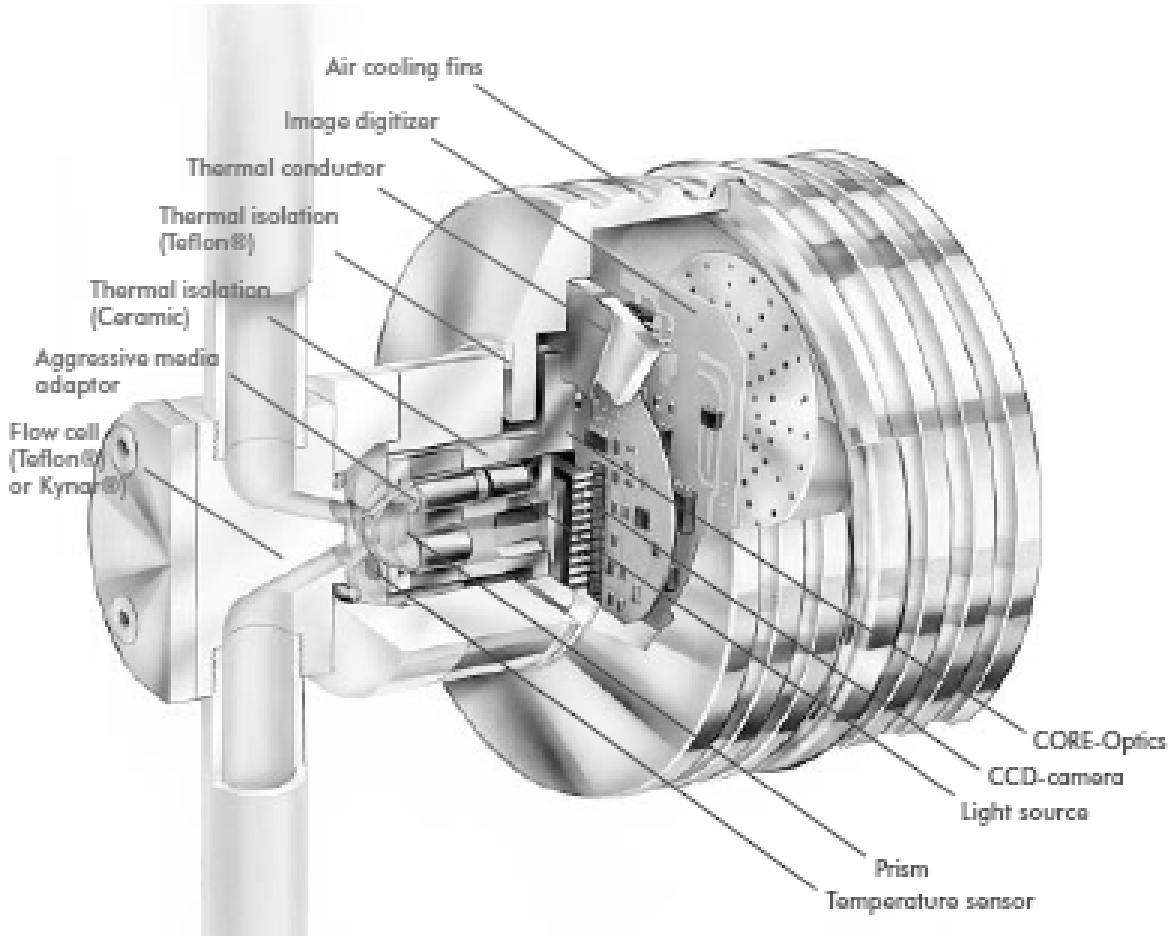

Fig. 2.11. The K-Patents refractometer [31, 36, 38, 41, 68, 75]

There is a large group of electronic hand refractometers, which are not equipped with thermal stabilization. These refractometers have an integrated temperature sensor (usually made from platinum), which measures the temperature of the entire optical system consisting of prisms and special measuring chamber (volume), where the sample is placed. In these refractometers the final readings are calculated by the microcontroller, which is built into this device. This microcontroller by special mathematical calculations calculates the coefficient of refraction or immediately determines the concentration and density of the study sample, and outputted these results as the final output to the display device or a remote computer.

These refractometers are small and not heavy. They can easily hold in your hand. But they have an average measurements resolution due to their limited size. On Fig.2.12 it is possible to see an example of this kind of refractometers [4]. Below is the table that shows the current state of refractometry (see Table 2.1).

Fig. 2.12. AR200 Automatic Digital Refractometer **[4]**

Table 2.1.

Refractometers. State of the art

Type of refractometers	Measurement resolution, ± RI	Dimensions	Weight
Handheld	10^{-3} ... 10^{-4}	small	small
Laboratory desk-mounted	10^{-3} ... 10^{-5}	medium	medium
Scientific	10^{-5} ... 10^{-7}	big	big
Cell's refractometers	10^{-3} ... 10^{-4}	medium	medium
Refractometers to provide extreme resolution - goniometry [102]	10^{-10}	big	big

2.5. Conclusion

Despite the fact that the refractometry research methods are used already a very long period of time, all the time there are new publications describing some innovative approaches in refractometry, because the old classical refractometers are not available to cope with the growing demands of modern technologies. Therefore, there is a demand of constant search for new design ideas and technologies in a refractometry.

In the modern world, there is a great need for accurate refractometers with small dimensions and weight, because sensors very often must be build into a variety of technological systems for chemical and biological industries, where placement of sensors with large dimensions and weight is a big problem. Refractometers made by the classical scheme can not always be used here.

For medical practices, it is necessary to have more and more accurate refractometers to provide a remote analysis of the patients' conditions. In addition to the traditional use of refractometry as a method of analyzing the content of sugar in the blood and urine of patients, serological blood tests, determination of protein in urine, measurement the density of urine, analysis of the brain fluid, density determination of the intraocular liquid, etc, constantly there are new ways of the possible use of the refractometer, requiring simpler operating principles and more suitable construction for mass production.

Additionally there is a great need for small sensors for quality control in the bio-fuel industry.

Portable and precise refractometers are necessary to ensure the safety and protection of the environment and for use in household.

Very important is the price of a refractometer and a power consumption of this device.

GOALS AND TASKS OF THE RESEARCH

The goals:

To develop a new physical fundamentals and approach to create and use a portable refractometer with high RI resolution (~ 10^{-5}).

To reach the goals the following activities should be performed the task.

The tasks:

1. To develop of the physical fundamentals of the cylindrical cell based refractometer (CCR).

2. To develop the mathematical model of CCR to determine the properties of the refractometers.

3. To develop of the CCR prototype, including optical, electronic, computing and mechanical systems.

4. To develop the CCR calibrate methodology, its algorithm for measurements of the RI and concentrations of the solutions.

5. To explore RI measurement resolution available from the CCR.

6. To verify of CCR practical applicability.

Chapter 3. MULTIPLE LIGHT BEAM REFRACTION AND REFLECTION IN THE CYLINDRICAL CELL WITH THE TEST SOLUTION

3.1. The physical approach of the cylindrical cell based refractometers

One of the ways to increase the sensitivity of the refractometer can be multiple passages of the light beam through the sample when the light beam passes each time through the following system: [wall] - [the sample for investigation] - [wall] - [the sample for investigation] - and so on. It greatly increases the exiting angle of the beam at the end from the cell.

The more are these reflections; the bigger is the angle of the outgoing light beam, going from the cylindrical cell. Below it will be shown **that the deflection angle of the light beam coming from the cylindrical cell increases as many times as the number of reflections of the beam inside the cell**.

All classical type Abbe or Pulfrich refractometers employ only one pass of the light beam through the sample, because multiple passages through the sample are impossible because of the design features of these refractometers.

Turning back the light beam and passing it again through the sample is an unsolvable and complex problem. In order to increase the sensitivity of the refractometer it is possible to use special lenses, which makes the construction of the refractometer very complicated and expensive. Moreover, it will increase the resolution of measurements.

But it is very easy to redirect the light beam in a cell with a cylindrical cell, where the cylinder works as the measuring element and the element that redirects the light beam back into the cell. It is possible many times to repeat measurements and redirect the light beam back to the cylindrical cell.

Refractometer with the testing sample area in the form of a cylinder has a lot of advantages as compared to the refractometers with straight walls (for example, triangle, rectangle, and so on). Besides technical simplicity of the cylinder in a cylindrical cell is much easier to remove the sample after measurements are complete, as compared to the refractometers with straight walls, because it is very difficult to remove the sample from the corners.

The corners of the refractometers are typically gas bubble formation zones, which are usually dissolved in the test samples, and by changing the pressure in the sample liquid; gas bubbles begin to form immediately in the corners of the cell.

Big volume of air bubbles can completely block the work of the refractometer. Even fast pumping of the testing liquid does not always help, as tearing the gas bubble from the corner of the cell is even impossible sometimes. The cylindrical cell's refractometers do not have these problems.

If the outer side of the cylindrical cell is coated by the reflective coating of the light, then the light beams, repeatedly passing through the walls will completely come back in the testing sample [89].

3.2. Influence of the refractive index on the light deviation in the exit of the refractometer

Fig.3.1 shows a simplified ray-tracing diagram in which the final deflected ray exit the cell at reference points $\mathbf{Q}_4$ ($m = 4$) along the tangent of the outer surface and is projected on a linear scale at the point **a**. The plane of the scale intersects at point **P** the straight line drawn through point **O** (on the cell axis) and point **1** (see Fig.3.1). Angle ψ between the two straight lines and distance L=OP determine the position of the point **a** depending on the RI value of the liquid. Together with optical parameters of the cylindrical cell, ψ and **L** determine the sensitivity of refractometer and linearity of the scale. A set of standard samples, e.g. liquids solutions of known refractive indices, is usually used to graduate a refractometer.

The laser beam is directed onto the wall of the cylindrical optical cell in such a way that the beam axis is lined up with the outer wall tangent and perpendicular to the axis of the cylinder **O**.

The cell is filled with either immobile or flowing liquid. The position **a** of the beam is identified using a linear CMOS image sensor, the graduated screen with readable divisions being in use for the simplest device design.

Let us consider the part of parallel rays of monochromatic laser beam through the optical cell from the point of incidence 1 on the outer wall of the cylindrical cell. In case shown in Fig.3.1: is the RI of the medium outside the cell, that is air; - RI of the cell material; - RI of the liquid inside the cell; - the inside radius of the cell, and - the outside radius of the cell wall.

Points **1**, **2**, **3**,. . . , **Q** are reference points in which the beam is refracted at the interface between two transparent media with different RI.

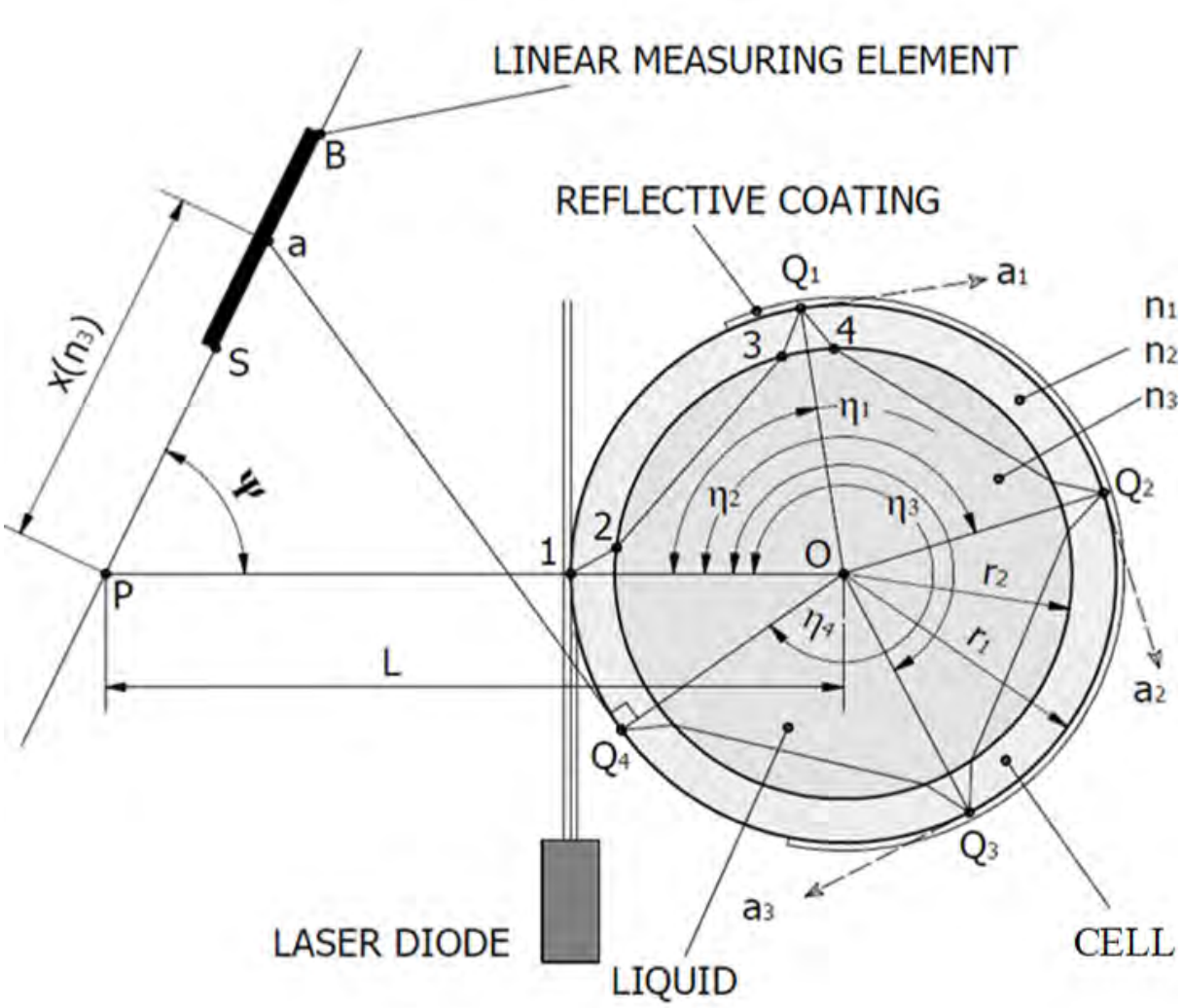

Fig. 3.1. Schematic cross section of the cylindrical cell illustrating a simplified path of the laser beam in the measuring system

Cylindrical optical element calculation expressions indicators used (Fig.3.1.):

n_1 ambient refractive index;

n_2 optical element material cell refractive index;

n_3 the liquid refractive index;

r_1 optical element cylinder outer radius;

r_2 an optical element inside radius of the cylinder;

k optical element cylinder radius ratio r_1 / r_2;

m optical element beam output sequence number;

Q optical element beam exit point;

η an optical element in the optical input-output center angle;

a optical element cylinder axis distance range exceeded the mid-point of the linear scale measuring element;

Ψ an optical element in the optical input-output center angle of the start edge angle relative to the plane of the linear measuring element;

L cylinder axis of the optical element of the linear distance measured in the plane of the element and the optical input-output center edge angle of intersection of the beginning.

3.3. Cylindrical cell based refractometers and fundamentals of the theory

According to Snell's law Eq. (1.2) (Fig.1.1), we can write for the angles of incident refracted rays at point **1** - α_1 and β_1, respectively (not shown in Fig.3.1):

$$n_1 \sin\alpha_1 = n_2 \sin\beta_1 . \tag{3.1}$$

From here we find

$$\sin\beta_1 = \frac{n_1}{n_2}\sin\alpha_1 \tag{3.2}$$

Since $\alpha_1 = \pi/2$ and RI of air $n_1 \approx 1$, **[**93**]**

$$\sin\beta_1 = \frac{1}{n_2}. \tag{3.3}$$

Angle β_1 of the completely refracted ray with respect to the normal of the outside wall of the cylindrical drawn at point **1** expressed as

$$\beta_1 = \beta_{cr} = \arcsin(1/n_2). \tag{3.4}$$

No light is passed to the other medium (e.g., cylindrical glass optical cell) at angles larger than the critical angle β_{cr}.

As the angle of the incident ray approaches its limits, $\alpha_1 = \pi/2$, the angle of refracted ray approached its maximum - the critical value β_{cr}.

From Eq. (3.2) it follows that $n_1 = 1$:

$$\beta_1 = \arcsin\left(\frac{\sin\alpha_1}{n_2}\right) \tag{3.5}$$

Derivative of the Eq. (3.5) with respect to α_1 is

$$\frac{\partial\beta_1}{\partial\alpha_1} = \frac{\cos\alpha_1}{n_2\sqrt{1-\frac{\sin\alpha_1{}^2}{n_2^2}}} \tag{3.6}$$

Under the given circumstances it is possible to use the region around the critical ray for accurate identification of the angle of deflection depending on the RI of the liquid as the ray travels through the optical system of the cylindrical cell. As this critical ray arrives at point **2**, we may write a relation between the angle of incidence α_2 and the angle of refraction β_2 similar to that at point **1**:

$$n_2 \sin\alpha_2 = n_3 \sin\beta_2, \tag{3.7}$$

wherefore it follows that

$$\sin\beta_2 = \left(\frac{n_2}{n_3}\right)\sin\alpha_1, \tag{3.8}$$

$$\beta_2 = \arcsin\left(\frac{n_2}{n_3}\sin\alpha_2\right), \tag{3.9}$$

hold for the ray refracted at point **2**. At a certain value of RI n_2 of the optical cell material and sufficiently small inner radius $r_{2\min}$ it is possible that a ray refracted at point **1** does not cross the inner wall of the cylinder.

The critical radius of the inner wall is:

$$r_{2\min} = r_1 / \sin\beta_1. \tag{3.10}$$

With an account for (3.1), $r_{2\min} = r_1 / n_2$, and $r_1 / r_{2\min} = n_2$.

From Eq. (3.5) the ratio

$$k = r_1 / r_2, \tag{3.11}$$

must satisfy the inequality:

$$k < n_2. \tag{3.12}$$

A ray refracted at point **2** passes travels through the liquid and arrives at a point on the inner surface of the cylindrical cell under condition that

$$n_3 < n_2 \tag{3.13}$$

It is very important to take into consideration these formulas (3.10), (3.12) and (3.13) when choosing the size of the projected measuring cell of the refractometer!

This condition puts limits on the smallest measurable value of the RI. A ray is refracted at point **3**, travels through the cell wall and reaches the outer wall at point $\boldsymbol{Q}_1$.

On Fig. 3.2 the increased sector is shown **1**, **2**, **3**, $\mathbf{Q}_1$, **O** from Fig. 3.1.

Simple trigonometric relations and values of angles α_1, α_2, β_1, β_2 (see Fig. 3.2) found above allow one calculate the corresponding incidence angles α_3 and α_{Q1}, refractive angle β_3 and the centric angle η_1 that determines position of point $\boldsymbol{Q}_1$ on the outer circumference of the cell: $\alpha_3 = \beta_2$, $\alpha_{Q1} = \beta_1$, $\beta_3 = \alpha_2$.

$$\eta_1 = \varphi_1 + \varphi_2 + \varphi_3 \tag{3.14}$$

$$\varphi_1 = \varphi_3 \tag{3.15}$$

$$\eta_1 = \varphi_2 + 2\varphi_1 \tag{3.16}$$

From of the triangle **O 2 3** it follows that,

$$\varphi_2 = \pi - \alpha_3 - \beta_2 \tag{3.17}$$

$$\varphi_2 = \pi - 2\alpha_3 \tag{3.18}$$

From Eq. (3.10), Eq. (3.11) the ratio

$$\varphi_2 = \pi - 2\arcsin(k / n_3) \tag{3.19}$$

From of the triangle **O 1 2** it follows that,

$$\varphi_1 = \alpha_2 - \beta_1 = \arcsin(k / n_2) - \arcsin(1 / n_2) \tag{3.20}$$

$$\eta_1 = \pi - 2\left(\arcsin\left(k / n_3\right) + \arcsin\left(k / n_2\right) - \arcsin\left(1 / n_2\right)\right) \tag{3.21}$$

According to Fresnel's law, a part of the ray striking the outer surface of the wall at point $\mathbf{Q}_1$ is reflected back into the wall. Being refracted at point **4** (see Fig. 3.1) it is returned into the liquid. Unless the outer surface of the cell around point $\mathbf{Q}_1$ is coated with a reflecting layer, the other part of the incident ray is refracted at the interface with outer medium and leaves the cell along the tangent of the outer circumference at point $\mathbf{Q}_1$. The incidence and reflection angles of

the internally reflected part of the ray striking the outer wall at point $\mathbf{Q}_1$ are equal to each other. With an account for $\alpha_{Q1} = \beta_1$, a ray reflected at point $\mathbf{Q}_1$ travels to point $\mathbf{Q}_2$ along a path similar to that from point **1** to point $\mathbf{Q}_1$. In a similar way, the ray arrives at point $\mathbf{Q}_3$, $\mathbf{Q}_4$, etc. (see Fig.3.1).

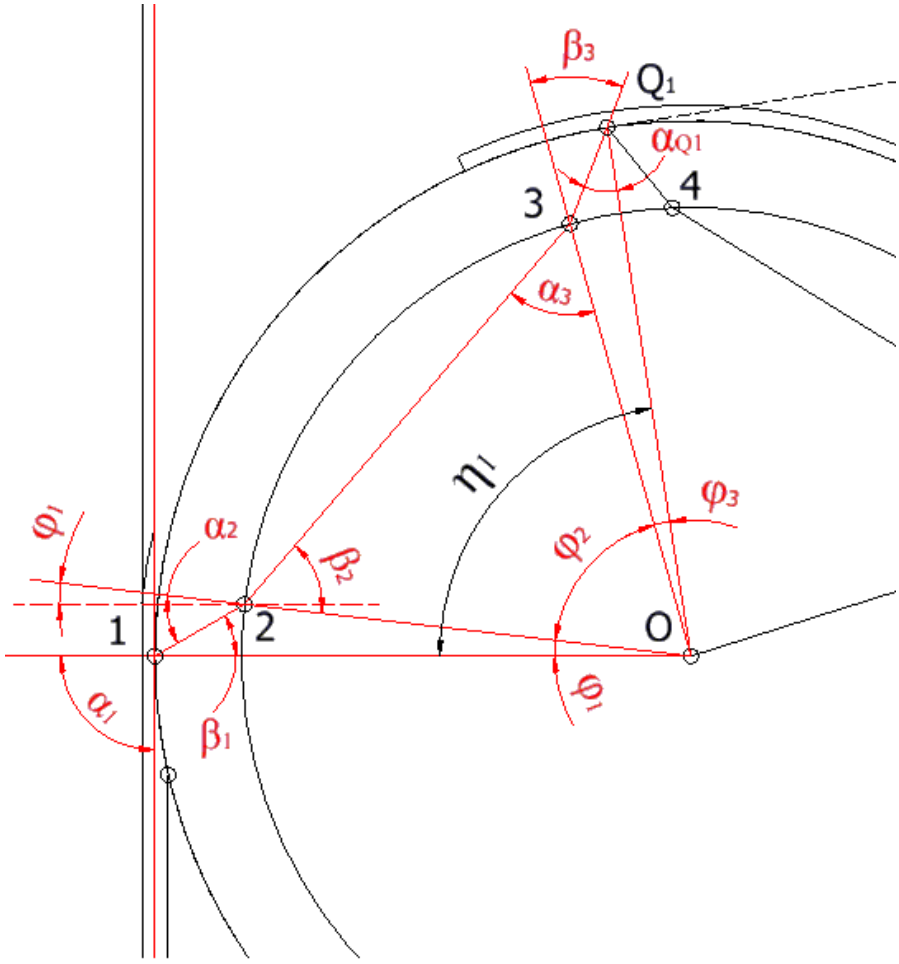

Fig. 3.2. Increased sector **1**, **2**, **3**, $\mathbf{Q}_1$, **O** with Fig. 3.1

With an account for Eq.(3.21), the centric angles η_1, η_2, ... η_m between the radii drawn from points $\mathbf{Q}_1$, $\mathbf{Q}_2$,... $\mathbf{Q}_m$ on the outer surface of the cylindrical cell to its axis can be calculated as

$$\eta_m = 2m\left[\pi/2 - \arcsin\left(k/n_3\right) + \arcsin\left(k/n_2\right) - \arcsin\left(1/n_2\right)\right] \quad \text{(rad)}, \quad (3.22)$$

where m=1,2,... ; $k < n_2$; $n_3 < n_2$.

Eq. (3.22) shows the course of the most intensive central part of the laser beam from a point **1** to the first point of its output from the point **Q**.

The derivative of the function (3.22) with respect to n_3 present the sensitivity of the cylindrical cell:

$$\frac{\partial \eta_m}{\partial n_3} = \frac{2mk}{n_3^2 \sqrt{1 - k^2 / n_3^2}}. \tag{3.23}$$

The measuring sensitivity, as seen from Eq.(3.23), depends on the choice of the exit point, $\mathbf{Q}_1, \mathbf{Q}_2$ ..., of the ray and may be increased by a factor m. Compared to other techniques where part of the light beam crosses the liquid only once [42, 49, 84], the method allows for multiple increases in the sensitivity of measurements. However, according to Fresnel's law, the possible growth in sensitivity is limited due to losing intensity of the exiting ray with the number of reflections m. Difficulties with visual identification of the exiting ray appear at m>3, due to the exit of the part of the light stream at the points $\mathbf{Q}_1, \mathbf{Q}_2$ ... outside from the cylindrical cell.

We offer a way to remove this limitation. This may be achieved by a reflecting layer on the outer surface of the cylindrical cell applied over potential exits of the laser beam prior the chosen exit. For example, in Fig.3.1 the exit is point Q_4, while a reflecting (e.g. aluminium) coating prevents exit of the beam at points $\mathbf{Q}_1$, $\mathbf{Q}_2$, $\mathbf{Q}_3$ providing reflection of the beam over the whole range of RI measurements of the liquid. It has to be noted that the part of the beam reflected from the surface at point **2** is neither described nor shown in Fig.3.1. However, this does not affect realisation of the presented principle of RI measurements of liquids and liquids solutions. If the axis of the laser beam and the axis of the cylindrical cell are not quite orthogonal, the points $\mathbf{Q}_1$, $\mathbf{Q}_2$,... $\mathbf{Q}_m$ will be positioned along a spiral. In this case the points of exit may be conveniently located at larger m values. Since the path of rays through the cylindrical cell with liquids is different in this case, the calculations change as well (see Fig.3.3).

Theoretically, it is possible to increase the sensitivity of the new refractometer endlessly, the limiting factor here will be only loss of laser intensity due to dispersion in the sample; it depends on its transparency and the presence of suspended solids. The loss of the material of the cell is much less due to the small thickness of the wall. Very important will be the reflective coating of the cell.

If you make a window into the evaporated surface of the cell sufficient only to enter the laser beam, then when we have a large number of multipath reflections m inside the cell will be

superimposed on the previous point reflections, and it would be impossible to determine the number of the specified point.

It is possible to solve this problem when we let the ray go spiral, as shown in Fig. 3.3. **Then, the number m theoretically may be infinite, and it is possible to have nearly infinite sensitivity of the refractometer!**

The position and size of the output window that provides exit of the laser beam from the cell to the desired number of the reflections point, as it will be shown later can be easily pre-theoretically calculate in line with the formulas obtained.

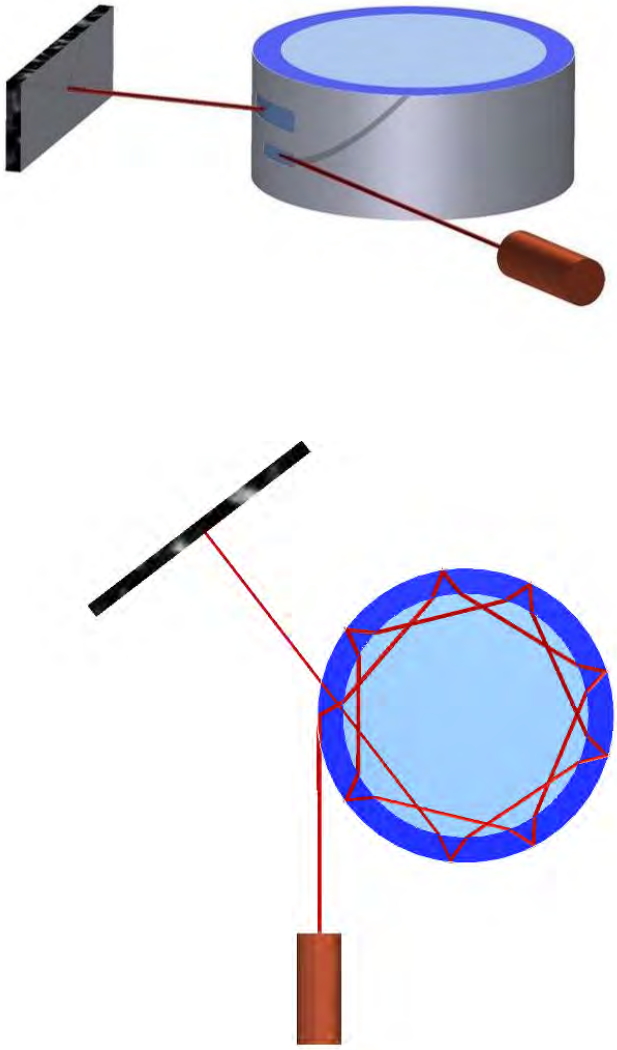

Fig. 3.3. The axis of the laser beam and the axis of the cylindrical cell are the points $\mathbf{Q}_1$, $\mathbf{Q}_2$,... $\mathbf{Q}_m$ will be positioned along a spiral

The described above cylindrical optical cell may be used in refractometric devices for different tasks. A number of considerations should be accounted for in designing such devices. A cylindrical optical cell may be made as a vertical cell with closed bottom or as a flow cell for continuous in-line control of liquids. Geometrical parameters of the cell (e.g. glass cylinder), including wall thickness, smoothness of the surface, and optical homogeneity, should be of sufficient quality.

According to Eq. (3.23), with m-fold increase of the central angle by choosing the exit number, the value of the parameter $\partial\eta/\partial n_3$ characterizing the sensitivity of the cell also increases. The beam of rays from the chosen exit $\mathbf{Q}_4$ (see example in Fig.3.1) is projected on a linear scale of measuring element. In the case of the optical cell depicted in Fig. 3.1, by simple trigonometric relations the point of projection **a(x)** of the ray exiting at Q_4 (m = 4) can be shown to depend on the RI of the liquid, n_3. See Fig. 3.4.

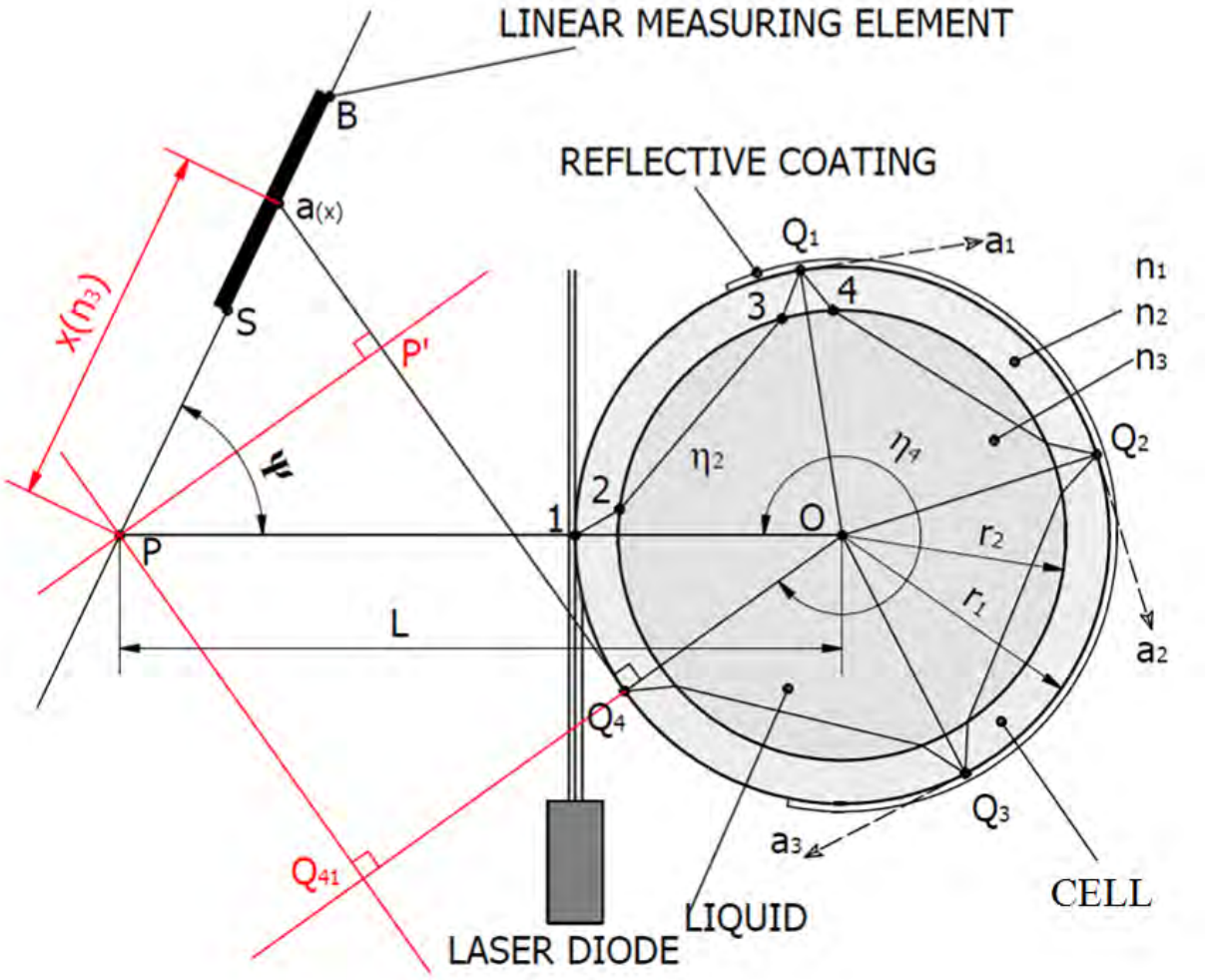

Fig. 3.4**.** Schematic cross section of the cylindrical cell that illustrates a simplified path of the laser beam in the measuring system

Therefore, it is possible to construct the following auxiliary lines:

$$Q_4\ Q_{41}\ ;\quad P\ Q_{41}\ ;\quad P\ P^{'}$$

$$P\ P^{'} \parallel\ \ Q_4\ Q_{41}\ \ ;\ \ P\ Q_{41} \parallel P^{'}\ Q_4\ ;\ Q_4\ Q_{41} \perp\ P\ Q_{41}$$

From of the triangle POQ_{41} it follows that,

$$Q_4Q_{41} = L\cos\eta_4 - r_1$$

From of the triangle $Pa(x)P_1$ it follows that,

$$x(n_3) = \frac{L\cos\eta_m - r_1}{\cos(\eta_m + \psi)}, \tag{3.24}$$

where η_4 is the central angle of the cylinder if m = 4 and the distance x is measured from the point **P** in mm.

When we use the formula Eq. (3.22) in the equation, we will get:

$$x(n_3) = \frac{L\cdot\cos\left\{2\cdot m\left[\frac{\pi}{2} - \arcsin\left(\frac{k}{n_3}\right) + \arcsin\left(\frac{k}{n_2}\right) - \arcsin\left(\frac{1}{n_2}\right)\right]\right\} - r_1}{\cos\left\{\psi + 2\cdot \mathrm{m}\cdot\left[\frac{\pi}{2} - \arcsin\left(\frac{k}{n_3}\right) + \arcsin\left(\frac{k}{n_2}\right) - \arcsin\left(\frac{1}{n_2}\right)\right]\right\}} \tag{3.25}$$

For simplicity of the Fig. 3.1 we will imagine that the angle ψ = 90º. See below Fig. 3.5.

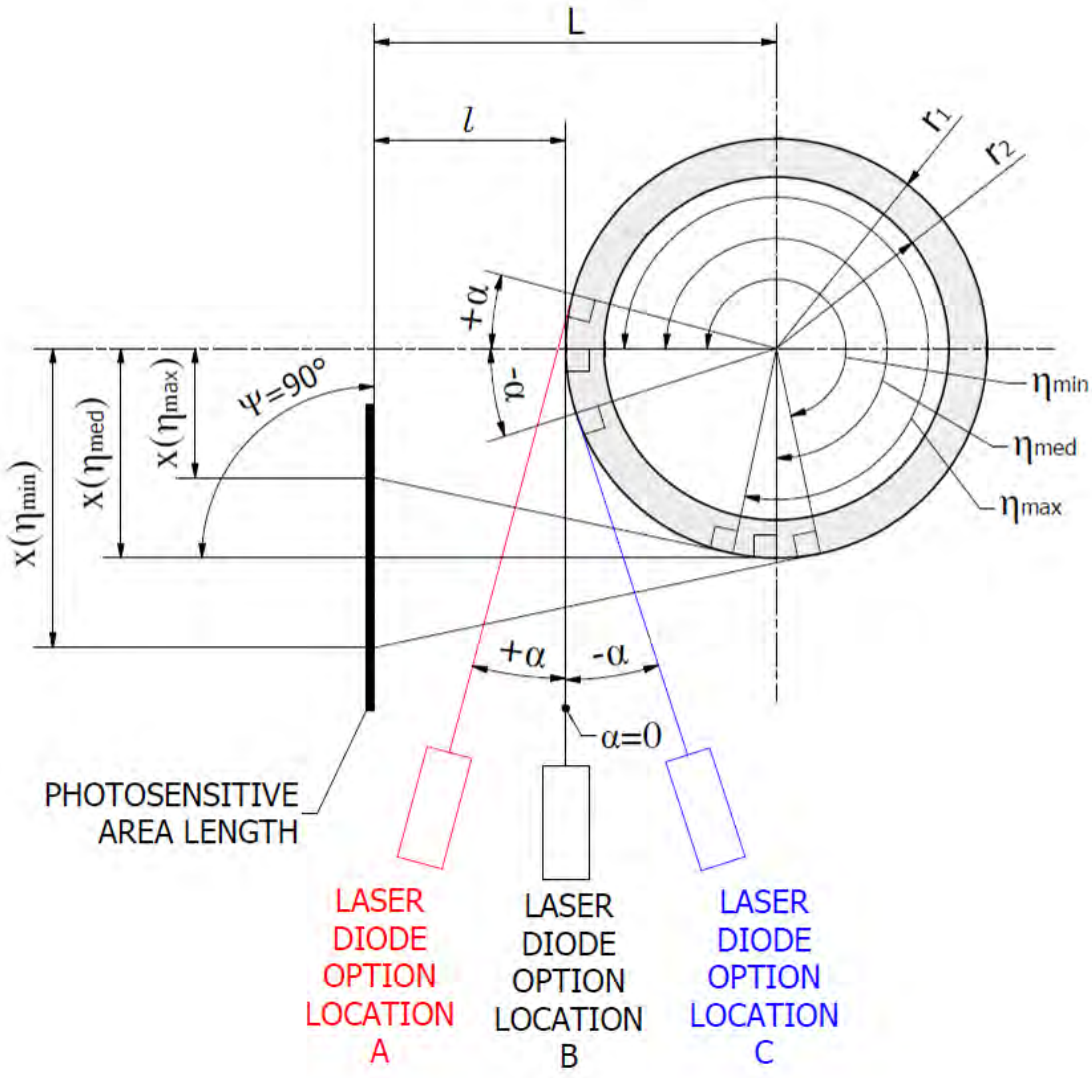

Fig. 3.5. α - central angle of the laser impact position in the tangential line on the lateral surface of the cell

The laser beam coming out of the cell must get perpendicularly to the center of the photosensitive area length of linear measuring element. This center is determined by the angle η_{med} of the limiting possible angles $\eta_{\min}$, $\eta_{\max}$, depending on the limit for the measured RI for the newly developed a refractometer (see Fig. 3.5).

Angle $\eta_{\min}$ - will be equal to the minimum value of the measured refractive index RI, angle $\eta_{\max}$ - the maximum value of RI. Angle η_{med} is calculated as the average of the angles $\eta_{\min}$ and $\eta_{\max}$.

When we determine the locations $\eta_{\min}$, η_{med} and $\eta_{\max}$ the temperature dependence of the measured sample must be taken into account, which makes the displacement of the laser beam exiting from the cell.

With temperature decreasing, the refractive index increases (respectively increases the angles $\eta_{\min}$, η_{med} and $\eta_{\max}$), and when the temperature increases, the refractive index of the sample is reduced, and consequently the angles $\eta_{\max}$, η_{med} and $\eta_{\max}$ are decreased. All values are selected from the reference tables, and intermediate values are usually interpolated.

The number of refraction of the laser beam inside the cell m is determined by calculation. The number of refraction depends on the outer and internal diameter of the cell as well as on the refractive index of the cell and the sample; it also depends on the wavelength of the laser beam. Dimensions and material of the cell are determined by the intended use of the refractometer and the affordable range of materials.

To increase the sensitivity of the refractometer it is necessary to have a big number must of reflections inside the cell. But the determining factor here is the design features of the newly designed refractometer.

On Fig. 3.5 it is possible to see some desirable positions of the laser beam to expose the exact position η_{med}: Laser diode option location A, Laser diode option location B, Laser diode option location C. Laser in a position B is compatible with the case when the angle η_{med} goes exactly into the center of the photosensitive area length of linear measuring element. But this is a rare possibility. In order not to change the determined distances and the location of the cell and the linear measuring element, we can introduce the corrective angles $-\alpha$ and $+\alpha$.

We need the angle $-\alpha$ when it is necessary to change the central angle η_{med} counterclockwise to set the output of the cell (the laser beam) to the center of the photosensitive area length of linear measuring element. We need the angle $+\alpha$ when it is necessary to change the central angle η_{med} clockwise to set the output of the cell (the laser beam) to the center of the photosensitive area length of linear measuring element.

Then the formulas Eq.(3.22), Eq.(3.24), Eq.(3.25) take the final form Eq.(3.26), Eq.(3.27):

$$\eta_m = 2m\left[\pi/2 - \arcsin\left(k/n_3\right) + \arcsin\left(k/n_2\right) - \arcsin\left(1/n_2\right) + \alpha\right] \quad \text{(rad)}, \quad (3.26)$$

$$x(n_3) = \frac{L\cdot\cos\left\{2\cdot m\left[\frac{\pi}{2} - \arcsin\left(\frac{k}{n_3}\right) + \arcsin\left(\frac{k}{n_2}\right) - \arcsin\left(\frac{1}{n_2}\right)\right] + \alpha\right\} - r_1}{\cos\left\{\psi + 2\cdot \mathrm{m}\cdot\left[\frac{\pi}{2} - \arcsin\left(\frac{k}{n_3}\right) + \arcsin\left(\frac{k}{n_2}\right) - \arcsin\left(\frac{1}{n_2}\right)\right] + \alpha\right\}} \quad (3.27)$$

In addition to the notation used previously, we introduce the light beam position parameter Δx, equal to the distance between the point **P** and the start coordinate **S** of the linear

measuring sensor on the line **Pa** (see Fig. 3.1). Therefore, it is possible to assign the sequential number **1** to the initial pixel of the linear image sensor. By using Eq.(3.26) and Eq.(3.27) and maintaining the notation used earlier, for CMOS linear image sensor, if known pixel dimensions Δp , you can determine the number of pixels on the move - $p(n_3)$.

$$p(n_3) = \frac{x(n_3)}{\Delta p} \tag{3.28}$$

$$p(n_3) = \frac{L \cdot \cos\left\{2 \cdot m\left[\frac{\pi}{2} - \arcsin\left(\frac{k}{n_3}\right) + \arcsin\left(\frac{k}{n_2}\right) - \arcsin\left(\frac{1}{n_2}\right)\right] + \alpha\right\} - r_1}{\Delta \mathrm{p} \cos\left\{\psi + 2 \cdot \mathrm{m} \cdot \left[\frac{\pi}{2} - \arcsin\left(\frac{k}{n_3}\right) + \arcsin\left(\frac{k}{n_2}\right) - \arcsin\left(\frac{1}{n_2}\right) + \alpha\right]\right\}} \tag{3.29}$$

Theoretical the resolution of the measurements of the future refractometer can be calculated using the formulas Eq.(3.29).

$$\delta = \frac{n_{3T1} - n_{3T2}}{p(n_{3T1}) - p(n_{3T2})} = \frac{n_{3T1} - n_{3T2}}{\Delta P}, \tag{3.30}$$

where:

n_{3T1} - the refractive index of the liquid where the temperature t_1 is taken from the reference literature,

n_{3T2} - the refractive index of the liquid where the temperature t_2 is taken from the reference literature,

$\Delta P = p(n_{3T1}) - p(n_{3T2})$

$k = r_1 / r_2$ - see Eq.(3.11)

Formulas Eq.(3.26), Eq.(3.27), Eq.(3.29), Eq.(3.30) are basic and sufficient in mathematical modeling and are suitable for all cases of the new design of the cylindrical cell's refractometer.

Let's consider the following options for the output of the laser beam from the cell. See Fig.3.6.

On Fig. 3.6(a) and Fig. 3.6(b) it is possible to see the possibility, when a small number m (close to 1), or m is very high number in case of multiple reflections of the laser beam in a spiral. See Fig.3.3.

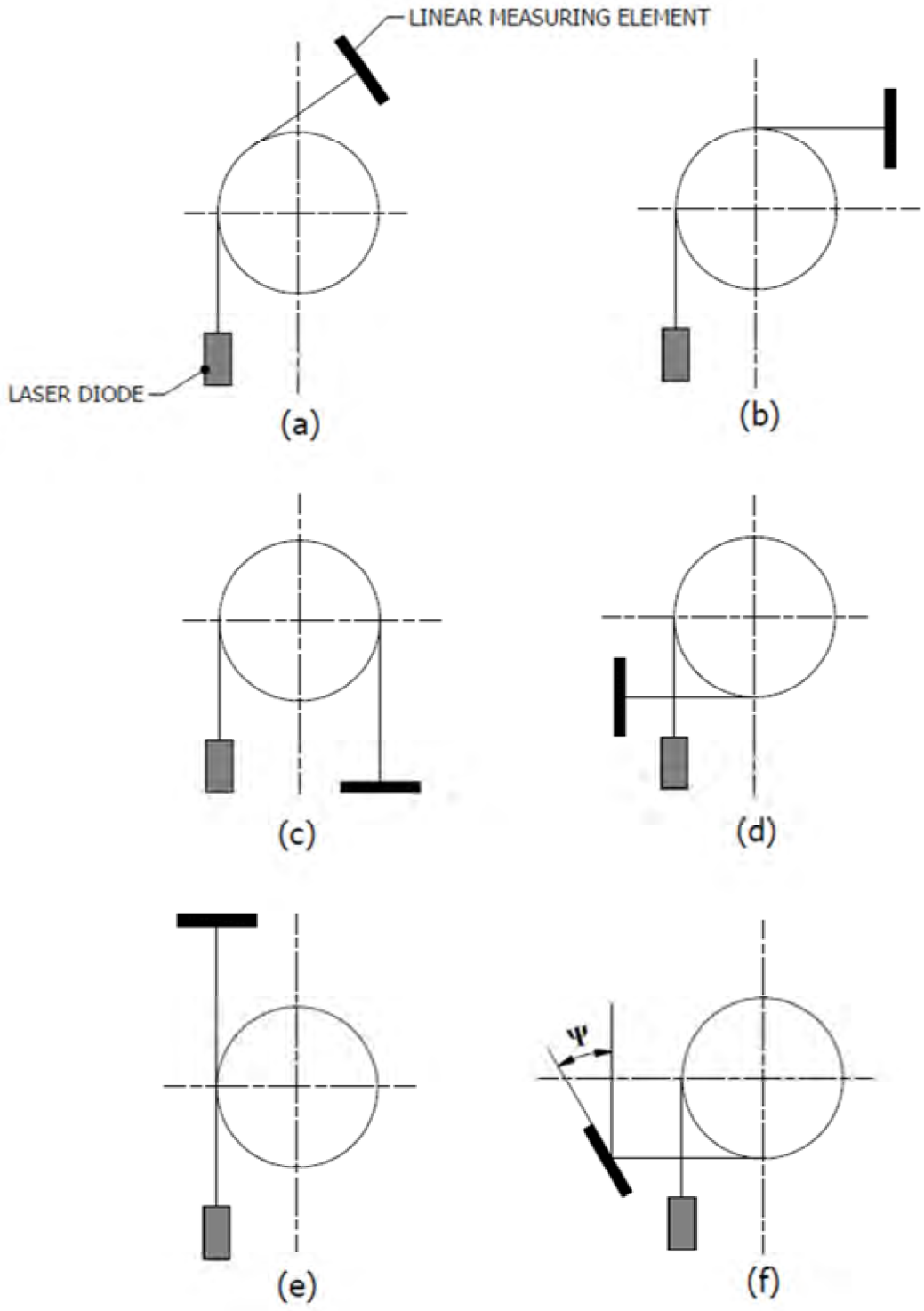

Fig. 3.6. Options for the output of the laser beam from the cell

On Fig.3.6(c) it is possible to see a variant which is real in a practice of a newly designed refractometer. Laser and a linear measuring element are located on one side of the cell so that they can be accommodated on a single printed circuit board. In addition to simplifying the design, this option allows you to remotely mount the laser and linear measuring element from

the cell where the high-temperature sample will be analyzed. The high temperature is unacceptable for the laser and the linear measuring element.

Option on the Fig.3.6(d) is the case of the compromise solutions when solving the problem of the optimal number *m*.

Option on the Fig.3.6(e) is undesirable, as the photosensitive area length of linear measuring element is exposed to the first laser beams, not entered in the cell from the point $\mathbf{Q}_1$ (Fig. 2.1).

Option on the Fig.3.6(f) characterizes the case when the linear measuring element is turned at the angles $\psi \neq$ of 0 º, 90 º, 180 º, 270 º. This option shows how it is possible to increase the passage of the laser beam on the photosensitive area length of linear measuring element in order to increase the sensitivity of the refractometer. The inclination of the angle ψ can be made from any side of the cell.

Analysis of Eq.(3.24) shows that the multiple angular sensitivity of the outlet point $\partial \eta_4 / \partial n_3$ and, consequently, the equal growth in sensitivity of the refractometer can be achieved by optimising the ratio of outer and inner radii $k = r_1 / r_2$, that is, the wall thickness of the cylindrical cell.

An illustration of that at $\eta_m = \eta_4$, (m=4) is shown by $\partial \eta_4 / \partial n_3 (n_3)$ diagrams in Fig. 3.7 .

This graph is crucial because it demonstrates the importance of determining the ratio of the outer and inner radius of the cell. For very thin cell walls (k = 1.15) we have a little gradient, and when the walls are thick (k = 1.30) we have a very big gradient that is not linear. The optimum would be around k = 1.25.

Dependence of angle η_m on the refractive index of the liquids n_3 with respect to the choice of exit points $\mathbf{Q}_1$, $\mathbf{Q}_2$, $\mathbf{Q}_3$, and $\mathbf{Q}_4$, i.e., of the exit number m (m = 1, 2, ... 4), according to Eq. (3. 26) is illustrated in Fig. 3.8.

Here you can see how with each subsequent reflection of the laser beam (inside in the cell) greatly increases the sensitivity of the refractometer. If at the point $\boldsymbol{Q}_1$ we have barely noticeable inclination characterizing the movement of the central angle n_1, than at the point $\boldsymbol{Q}_4$ the central angle n_4 has a very significant slope, that shows how much increases the sensitivity of the refractometer.

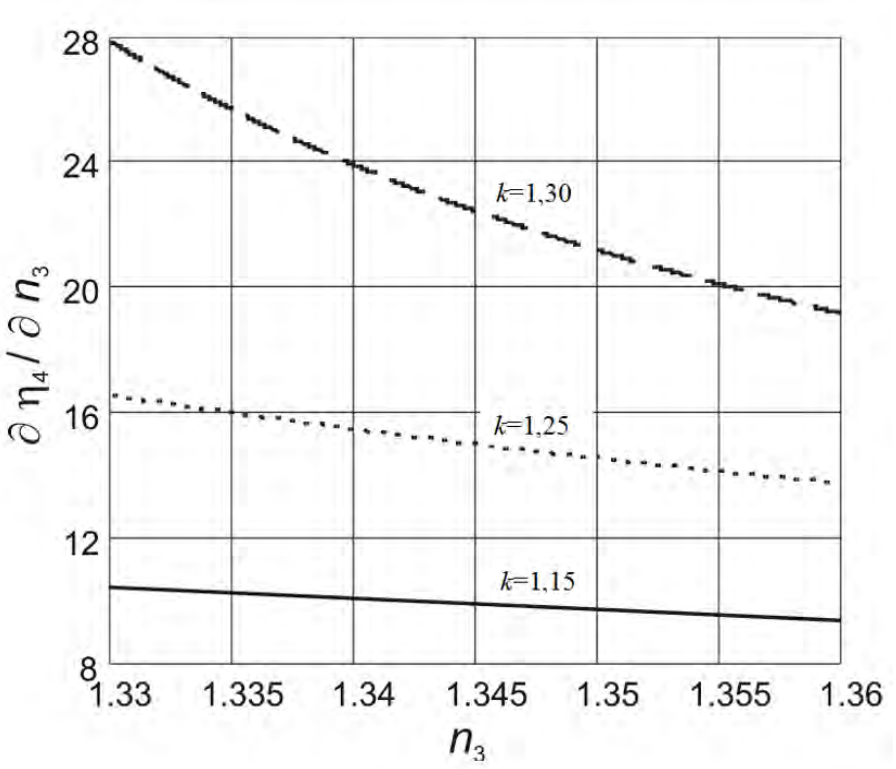

Fig. 3.7. Angular sensitivity $\partial\eta_4/\partial n_3$ of the output beam of the optical cell as a function of refractive index n_3 at different outer-to-inner radius ratios $k = r_1/r_2$

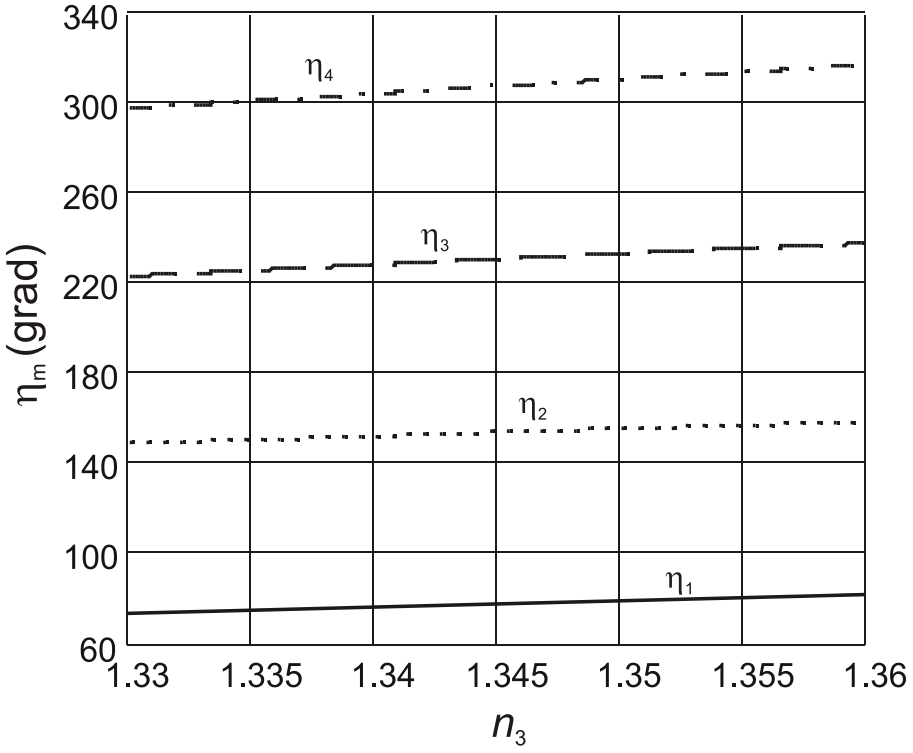

Fig. 3.8. Angular positions η_1, η_2, η_3, and η_4, *of* the respective output points $\mathbf{Q_1}$, $\mathbf{Q_2}$, $\mathbf{Q_3}$, and $\mathbf{Q_4}$ as functions of refractive index n_3

3.4. Mathematical simulation of the refractometers

By using Eq.(3.26), Eq.(3.27), Eq.(3.29), Eq.(2.30) it is possible to completely preliminary calculate all the basic parameters of the newly designed refractometers.

We can mathematically simulate several types of the refractometers, and then in the 4th chapter of this work we will give a comparison of the calculated parameters with the real experimental data (for some of these new types).

3.4.1. The simplest refractometers

Let's have the goal to develop a simple refractometer for measuring the concentration of aqueous solutions of ethanol from 0 to 80% alc/weight within a temperature range from +15°C to +25°C), and the resolution of this refractometer should be $\delta = 2 \cdot 10^{-3}$. This refractometer would not be accurate because it does not have the temperature compensation of the measurement process. This refractometer can work only as an indicator or as a demonstration model for some teaching purposes, when it is worthwhile to explain the operation principles of the new refractometer.

We need to choose a semiconductor laser ADL-63054TL $\lambda = 635nm$ [44]. This refractometer does not have the electronical optical linear sensor. As the information's output device the projection screen coated with the scale (where the laser beam enters the cylindrical cell) is used.

As the optical measuring element of the cell we can use the cylinder with an outer and inner diameter $r_1 = 5.1\,\text{mm}$ and $r_2 = 4.5\,\text{mm}$ respectively, made of borosilicate glass BK (Borosilicate crown), the working length of the laser $\lambda = 635$ nm and the refraction coefficient of the cell's material will be $n_2 = 1.515$ [71].

For aqueous ethanol 0% alc/weight, in this case it is distilled water, $n_3 = 1.3318$, for 80% alc/weight $n_3 = 1.3646$ (20°C and $\lambda = 635$ nm) [47, 71].

The Fig.3.9 schematically shows the option of the spatial distribution of parts of the refractometer with the preliminary sizes. In line with the Fig.3.1 we can assume the following:

$$L = l + r_1 = 112 + 5.1 = 117.1\,\text{mm}$$

$$\psi = 90° = \frac{90 \cdot \pi}{180} = 1.570796\,\text{rad}$$

$$-\alpha = -46.6° = \frac{-46.6 \cdot \pi}{180} = -0.813323 \text{ rad.}$$

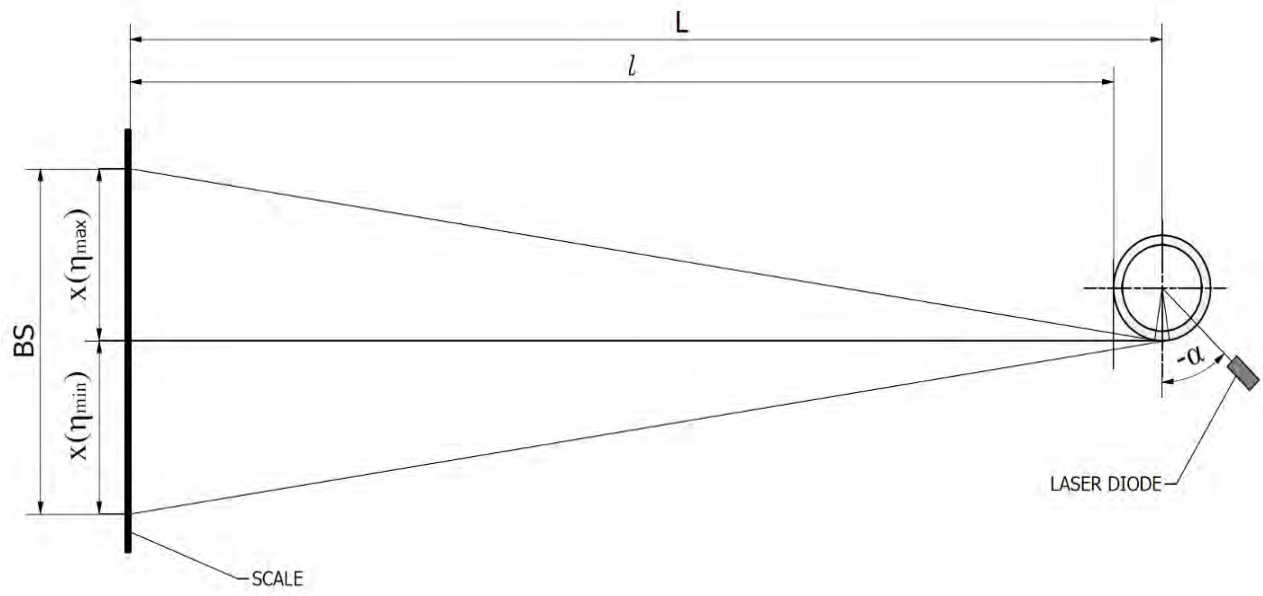

Fig. 3.9. Scheme of the optical system of the simplest refractometer

Number $m = 4$ is not specifically selected. This is the nearest number in this embodiment of the refractometer.

The central angle $\alpha = -46.6°$ and its sign (counterclockwise direction) are obtained by optimizing the mathematical modeling, with the expectation that η_{med} came in the middle of the scale, which is placed in the single line **OP** (Fig. 3.1.).

When we substitute the values of all final geometrical and physical parameters in Eq.(3.27), we will obtain the following:

$$x(\eta \min) =$$

$$= \frac{117.1 \cdot \cos\left\{2 \cdot 4\left[\frac{\pi}{2} - \arcsin\left(\frac{1.133333}{1.3318}\right) + \arcsin\left(\frac{1.133333}{1.515}\right) - \arcsin\left(\frac{1}{1.515}\right)\right] - 0.813323\right\} - 5.1}{\cos\left\{1.570796 + 2 \cdot 4\left[\frac{\pi}{2} - \arcsin\left(\frac{1.133333}{1.3318}\right) + \arcsin\left(\frac{1.133333}{1.515}\right) - \arcsin\left(\frac{1}{1.515}\right)\right] - 0.0.813323\right\}} =$$

$$= -17.839358 \approx -17.8 \text{ mm}, \quad \text{(at 0\% alc/weight)} \quad (3.34)$$

$$x(\eta\max)=$$

$$=\frac{117.1\cdot\cos\left\{2\cdot4\left[\frac{\pi}{2}-\arcsin\left(\frac{1.133333}{1.3646}\right)+\arcsin\left(\frac{1.133333}{1.515}\right)-\arcsin\left(\frac{1}{1.515}\right)\right]-0.0.813323\right\}-5.1}{\cos\left\{1.570796+2\cdot4\left[\frac{\pi}{2}-\arcsin\left(\frac{1.13333333}{1.3646}\right)+\arcsin\left(\frac{1.133333}{1.515}\right)-\arcsin\left(\frac{1}{1.515}\right)\right]-0.0.813323\right\}}=$$

$$=17.841783\approx17.8\,\text{mm},\qquad\text{(at 80\% alc/weight)}\ (3.35)$$

where $k=r_1/r_2$=5.1/4.5=1.133333, see Eq.(3.11).

The negative sign according to Eq.(3.34) and positive sign according to Eq.(3.35) indicates that the position of the projected point on the photosensitive area length of the linear measuring element is below the horizontal line **OP** (see Fig.3.1). As the result, we will obtain the following:

$$|BS|=|x(\eta\max)|+|x(\eta\min)|=35.6\ \ \text{mm},\qquad(3.36)$$

When heated to the temperature of 25° C degrees the refractive index decreases to $n_3=1.3312$. Let's calculate the displacement $x(\eta\min 25)$ now, by taking into account the temperature of the sample being measured.

$$x(\eta\min 25)=$$

$$=\frac{117.1\cdot\cos\left\{2\cdot4\left[\frac{\pi}{2}-\arcsin\left(\frac{1.133333}{1.33113}\right)+\arcsin\left(\frac{1.133333}{1.515}\right)-\arcsin\left(\frac{1}{1.515}\right)\right]-0.0.813323\right\}-5.1}{\cos\left\{1.570796+2\cdot4\left[\frac{\pi}{2}-\arcsin\left(\frac{1.133333}{1.33113}\right)+\arcsin\left(\frac{1.133333}{1.515}\right)-\arcsin\left(\frac{1}{1.515}\right)\right]-0.0.813323\right\}}=$$

$$=-18.617\ \text{mm},\qquad(3.37)$$

When the temperature of 15° C degrees the refractive index increases to $n_3=1.36528$. Let's calculate the displacement $x(\eta\max 15)$ now, by taking into account the temperature of the sample being measured.

$$x(\eta\max 15)=$$

$$=\frac{117.1\cdot\cos\left\{2\cdot4\left[\frac{\pi}{2}-\arcsin\left(\frac{1.133333}{1.36528}\right)+\arcsin\left(\frac{1.133333}{1.515}\right)-\arcsin\left(\frac{1}{1.515}\right)\right]-0.0.813323\right\}-5.1}{\cos\left\{1.570796+2\cdot4\left[\frac{\pi}{2}-\arcsin\left(\frac{1.133333}{1.36528}\right)+\arcsin\left(\frac{1.133333}{1.515}\right)-\arcsin\left(\frac{1}{1.515}\right)\right]-0.0.813323\right\}}=$$

$$=18.559\ \text{mm},\qquad(3.38)$$

From Eq.(3.34), Eq.(3.35), Eq.(3.37) and Eq.(3.38) it can be seen that the thermal displacement of the photosensitive area length will be $\approx \pm 0{,}8$ mm for a variation of 20 ± 5°C degrees, which is almost equal to the half partition of the scale |**BS**|.

In the figure below (Fig.3.10) it is possible to see the mathematically modeled (on Mathcad software) passage of the laser beam on the scale |**BS**|.

In chapter 4 a comparison of the real data and the basic data of the mathematic modeling for the newly designed refractometer is described.

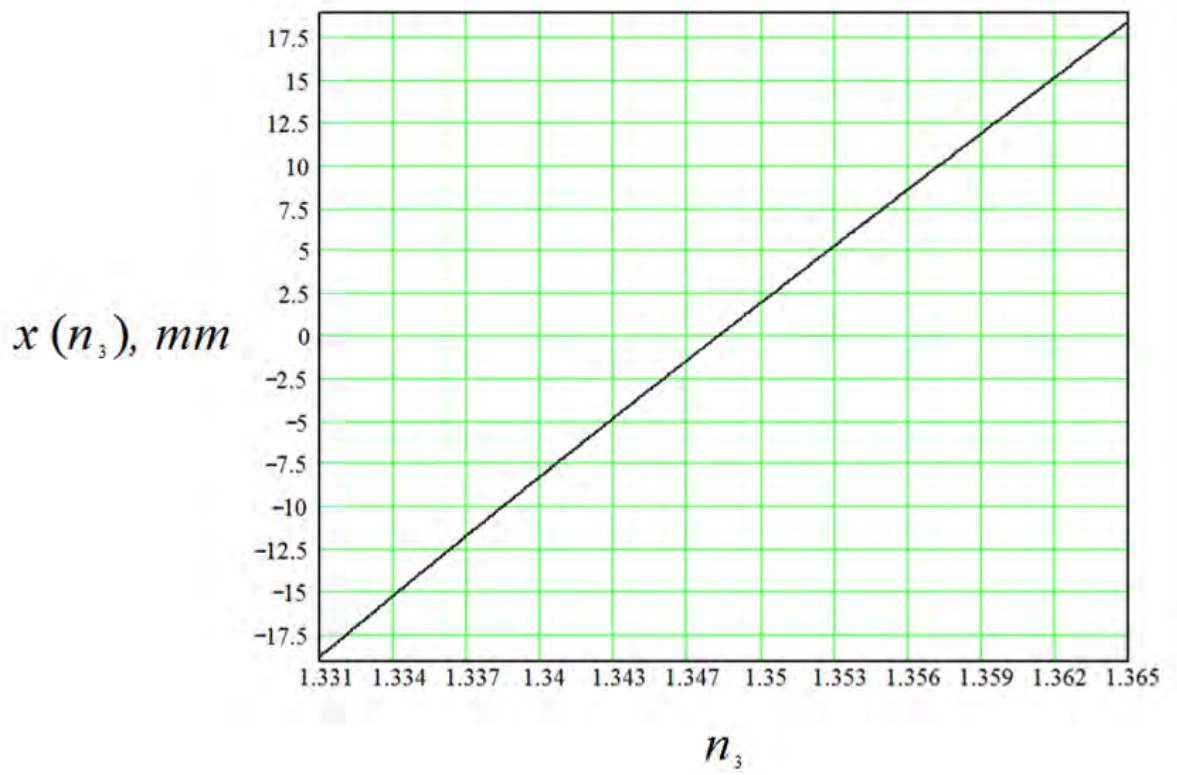

Fig. 3.10. The calculated position x of the exiting laser beam projection on the CMOS linear image sensor, as a function of the refractive index n_3 of the liquid contained in the cell's (the simplest refractometer)

3.4.2. The refractometers with a large RI measuring range

We can mathematically simulate a refractometer for determining the percentage concentrations of aqueous ethanol by weight in the range from 0 to 60% alc/weight within a temperature range from +15°C to +25°C.

We need to choose a semiconductor laser diode ADL-63054TL $\lambda = 635nm$, 5 mW [44] and optical linear sensor S9226 (Hamamatsu), photosensitive pixel pitch $\Delta p = 7.8\,\mu m$, pixel height 125 μm, number of pixels 1024, photosensitive area length 7.9872 mm [13]. The choice

of these elements is determined by the task, and can be changed during the mathematical calculations.

As the optical measuring element of the cell we can use the cylinder with an outer and inner diameter $r_1 = 5.5\,\text{mm}$ and $r_2 = 4.5\,\text{mm}$ respectively, made of borosilicate glass BK (Borosilicate crown), the working length of the laser $\lambda = 635$ nm and the refraction coefficient of the cell's material will be $n_2 = 1.515$ [71].

Temperature changes n_2 and coefficient of thermal expansion of structural elements are neglected.

For aqueous ethanol 0% alc/weight, in this case it is distilled water, $n_3 = 1.3318$, for 70% alc/weight $n_3 = 1.3640$ (20°C and $\lambda = 635$ nm) [47, 71].

The Fig.3.11 schematically shows the option of the spatial distribution of parts of the refractometer with the preliminary sizes. According Fig.3.1 we can assume the following:

$$L = l + r_1 = 5 + 5.5 = 10.5\,\text{mm}$$

$$\psi = 90° = \frac{90 \cdot \pi}{180} = 1.570796\,\text{rad}$$

$$-\alpha = -28.6° = \frac{-28.6 \cdot \pi}{180} = -0.499164\,\text{rad}.$$

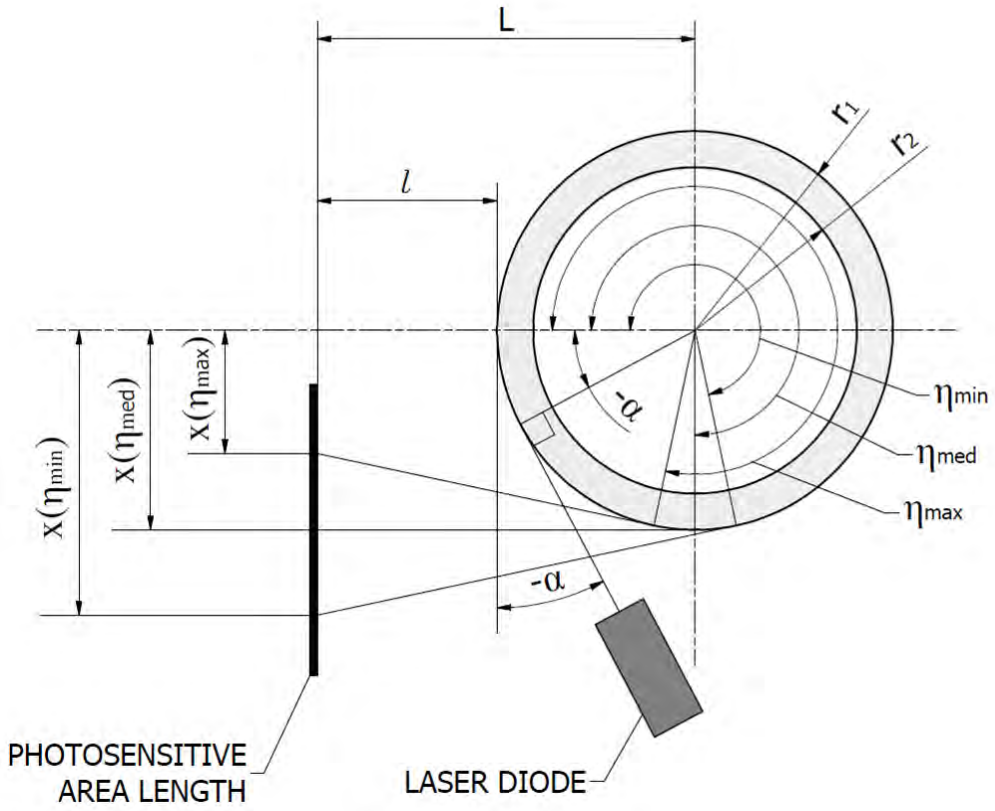

Fig. 3.11. Scheme of the optical system (refractometer, version A)

Number $m = 4$ is not specifically selected. This is the nearest number in this embodiment of the refractometer.

The central angle $\alpha = -28.6°$ and its sign (counterclockwise direction) are obtained by optimizing the mathematical modeling.

To get the laser beam to the center of the photosensitive area length of the linear measuring element by η_{med} the following condition must be obtained:

$$x(\eta_{med}) \approx r_1 = 5.5\,\text{mm}. \tag{3.39}$$

When we substitute the values of all final geometrical and physical parameters in Eq.(3.27), we will obtain:

$$x(\eta\min) =$$

$$= \frac{10.5 \cdot \cos\left\{2 \cdot 4\left[\frac{\pi}{2} - \arcsin\left(\frac{1.222222}{1.3318}\right) + \arcsin\left(\frac{1.222222}{1.515}\right) - \arcsin\left(\frac{1}{1.515}\right)\right] - 0.499164\right\} - 5.5}{\cos\left\{1.570796 + 2 \cdot 4\left[\frac{\pi}{2} - \arcsin\left(\frac{1.222222}{1.3318}\right) + \arcsin\left(\frac{1.222222}{1.515}\right) - \arcsin\left(\frac{1}{1.515}\right)\right] - 0.499164\right\}} =$$

$$= -7.763 \text{ mm}, \tag{3.40}$$

$$x(\eta\max) =$$

$$= \frac{10.5 \cdot \cos\left\{2 \cdot 4\left[\frac{\pi}{2} - \arcsin\left(\frac{1.222222}{1.364}\right) + \arcsin\left(\frac{1.222222}{1.515}\right) - \arcsin\left(\frac{1}{1.515}\right)\right] - 0.499164\right\} - 5.5}{\cos\left\{1.570796 + 2 \cdot 4\left[\frac{\pi}{2} - \arcsin\left(\frac{1.222222}{1.364}\right) + \arcsin\left(\frac{1.222222}{1.515}\right) - \arcsin\left(\frac{1}{1.515}\right)\right] - 0.499164\right\}} =$$

$$= -3.384\,\text{mm}, \tag{3.41}$$

where $k = r_1 / r_2$=5.5/4.5=1.222222.

The negative sign according to Eq.(3.40), Eq.(3.41) indicates that the position of the projected point on the photosensitive area length of the linear measuring element is below the horizontal line **OP** (see Fig.3.1). As the result we get:

$$\eta_{med} = \frac{x(\eta\max) + x(\eta\min)}{2} \approx 5.7 \text{ mm}, \tag{3.42}$$

In photosensitive area the length of the linear measuring element $x(\eta\max) - x(\eta\min) = 4{,}474$ mm is used; that is about $\approx 55\%$ (photosensitive area length 7.9872 mm) [13].

Let's calculate the displacement $x(\eta \min 25)$ now, by taking into account the temperature of the sample being measured. When heated to the temperature of 25° C degrees the refractive index decreases to $n_3 = 1.33113$.

$$x(\eta \min 25) =$$

$$= \frac{10.5 \cdot \cos\left\{2 \cdot 4\left[\frac{\pi}{2} - \arcsin\left(\frac{1.222222}{1.33113}\right) + \arcsin\left(\frac{1.222222}{1.515}\right) - \arcsin\left(\frac{1}{1.515}\right)\right] - 0.499164\right\} - 5.5}{\cos\left\{1.570796 + 2 \cdot 4\left[\frac{\pi}{2} - \arcsin\left(\frac{1.222222}{1.33113}\right) + \arcsin\left(\frac{1.222222}{1.515}\right) - \arcsin\left(\frac{1}{1.515}\right)\right] - 0.499164\right\}} =$$

$$= -7.876 \text{ mm}, \qquad (3.43)$$

Let's calculate the displacement $x(\eta \max 15)$ now, by taking into account the temperature of the sample being measured, for 15° C degrees the refractive index increases to $n_3 = 1.36468$.

$$x(\eta \max 15) =$$

$$= \frac{10.5 \cdot \cos\left\{2 \cdot 4\left[\frac{\pi}{2} - \arcsin\left(\frac{1.222222}{1.36468}\right) + \arcsin\left(\frac{1.222222}{1.515}\right) - \arcsin\left(\frac{1}{1.515}\right)\right] - 0.499164\right\} - 5.5}{\cos\left\{1.570796 + 2 \cdot 4\left[\frac{\pi}{2} - \arcsin\left(\frac{1.222222}{1.36468}\right) + \arcsin\left(\frac{1.222222}{1.515}\right) - \arcsin\left(\frac{1}{1.515}\right)\right] - 0.499164\right\}} =$$

$$= -3.306 \text{ mm}, \qquad (3.44)$$

From Eq. (3.40), Eq. (3.41), Eq. (3.43) and Eq. (3.45) we can see that the thermal displacement in the photosensitive area length will be only max=0,113 mm, that by using the photosensitive area length of 55% the laser beam will not come out beyond the photosensitive area length.

When we have the photosensitive pixel pitch $\Delta p = 7{,}8\ \mu m$, we will obtain the following:

$$\delta = \frac{(n_{\max} - n_{\min})\Delta p}{x(\eta \max) - x(\eta \min)} = 5.7 \cdot 10^{-5} \qquad (3.45)$$

In the figure below Fig.3.12. It is possible to see the mathematically modeled (on Mathcad software) passage of the laser beam on the photosensitive area length of the linear measuring element.

In chapter 4 a comparison of the real data and the basic data of the mathematic modeling for the newly designed refractometer is described.

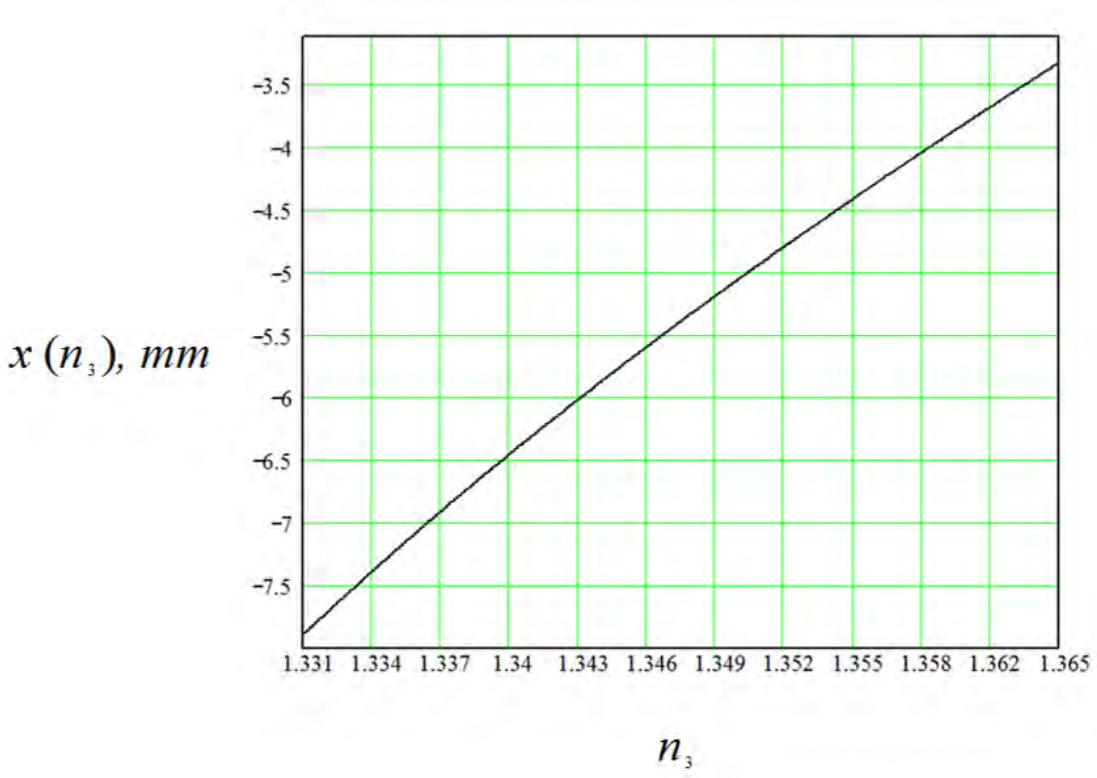

Fig. 3.12. The calculated position x of the exiting laser beam projection on the CMOS linear image sensor, as a function of the refractive index n_3 of the liquid contained in the cell's for the refractometers with a large RI measuring range (refractometer, version A)

3.4.3. The refractometers with a small RI measuring range

We aim to develop a more accurate refractometer for measuring the concentration of ethanol aqueous solutions from 0 to 20% alc/weight. $n_3 = 1.3457$, when the temperature is 20% alc/weight, 20°C and $\lambda = 635$ nm [47, 71]. The temperature range is from +15°C to +25°C). Measurement should be $\delta = 2 \cdot 10^{-5}$.

The Fig.3.13 schematically shows the option of the spatial distribution of parts of the refractometer with the preliminary sizes. In order not to increase very much the size of the refractometers construction we will use the type close to Fig.3.6(f) – we will increase the sensitivity of the refractometer due to a passage of the laser beam at an angle with respect to the photosensitive area length of the linear measuring element.

In line with the Fig.3.1 we will assume the following:

$$L = l + r_1 = 5 + 5.5 = 10.5\,\text{mm}$$

$$\psi = 90° = \frac{90 \cdot \pi}{180} = 1.570796\,\text{rad}$$

$$-\alpha = -68° = \frac{-68 \cdot \pi}{180} = -1.186824 \text{ rad.}$$

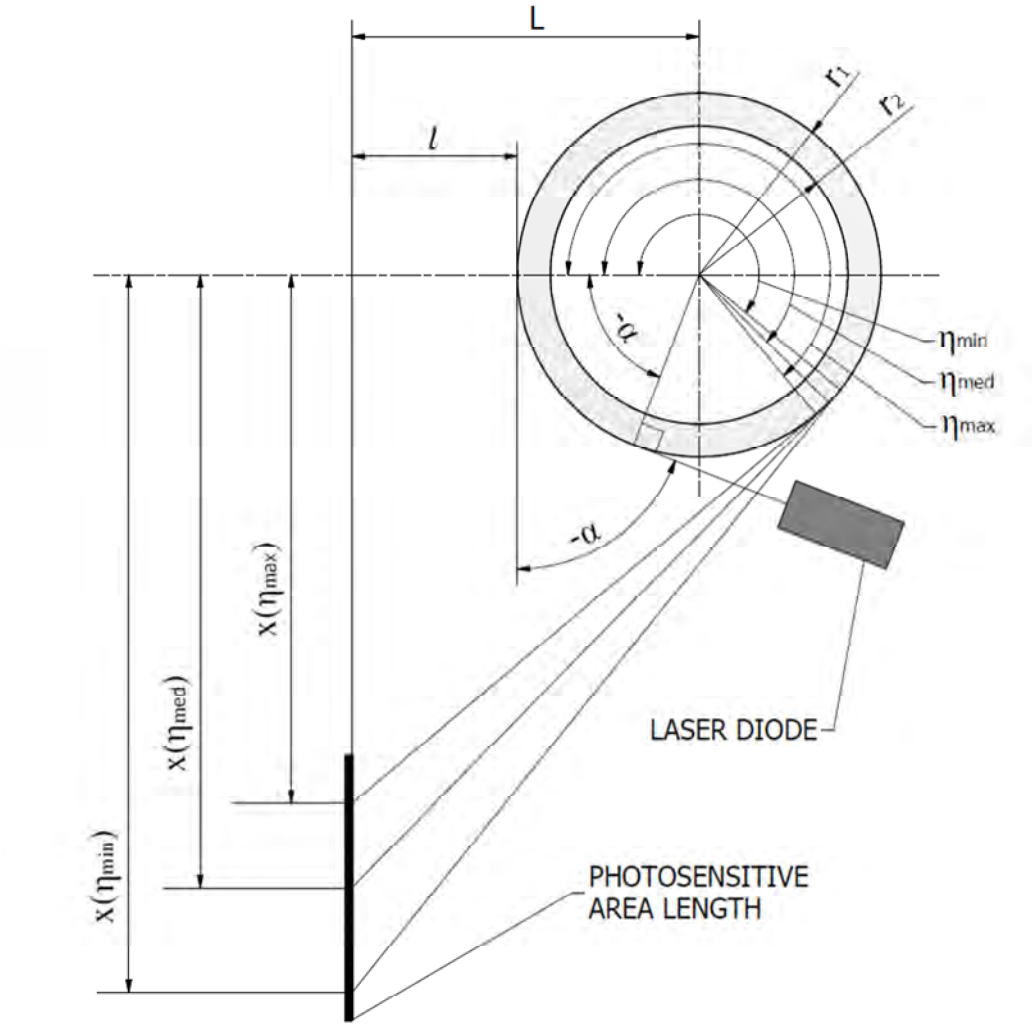

Fig.3.13. Scheme of the optical system (refractometer, version B)

We will not comply with the condition of Eq. (3.39) there, we will determine the angle η_{med} of contact with the center of photosensitive area length of the linear measuring element in line with the Eq. (3.27).

When we put in the values of all final geometrical and physical parameters in Eq. (3.27), we will obtain the following:

$$x(\eta \min) =$$

$$= \frac{10.5 \cdot \cos\left\{2 \cdot 4\left[\frac{\pi}{2} - \arcsin\left(\frac{1.222222}{1.3318}\right) + \arcsin\left(\frac{1.222222}{1.515}\right) - \arcsin\left(\frac{1}{1.515}\right)\right] - 1.186824\right\} - 5.5}{\cos\left\{1.570796 + 2 \cdot 4\left[\frac{\pi}{2} - \arcsin\left(\frac{1.222222}{1.3318}\right) + \arcsin\left(\frac{1.222222}{1.515}\right) - \arcsin\left(\frac{1}{1.515}\right)\right] - 1.186824\right\}} =$$

$$= -21.684 \text{ mm,} \qquad (3.46)$$

$$x(\eta\max)=$$

$$=\frac{10.5\cdot\cos\left\{2\cdot4\left[\frac{\pi}{2}-\arcsin\left(\frac{1.222222}{1.3457}\right)+\arcsin\left(\frac{1.222222}{1.515}\right)-\arcsin\left(\frac{1}{1.515}\right)\right]-1.186824\right\}-5.5}{\cos\left\{1.570796+2\cdot4\left[\frac{\pi}{2}-\arcsin\left(\frac{1.222222}{1.3457}\right)+\arcsin\left(\frac{1.222222}{1.515}\right)-\arcsin\left(\frac{1}{1.515}\right)\right]-1.186824\right\}}=$$

$$=-16.122\ \text{mm}, \qquad (3.47)$$

where $k=r_1/r_2$=5.5/4.5=1.222222 remained the same.

The negative sign according to Eq. (3.46) and Eq. (3.46) indicates that the position of the projected point on the photosensitive area length of the linear measuring element is below the horizontal line **OP** (see Fig. 3.1). As the result we will obtain the following:

$$\eta_{med}=\frac{x(\eta\max)+x(\eta\min)}{2}\approx-18.9\ \text{mm}, \qquad (3.48)$$

In the photosensitive area the length of the linear measuring element is involved as follows: $x(\eta\max)-x(\eta\min)=5.50298$ mm, that is about $\approx 70\%$ (photosensitive area length is 7.9872 mm).

Let's calculate the displacement $x(\eta\min 25)$, by taking into account the temperature of the sample, $n_3=1.33113$.

$$x(\eta\min 25)=$$

$$=\frac{10.5\cdot\cos\left\{2\cdot4\left[\frac{\pi}{2}-\arcsin\left(\frac{1.222222}{1.33113}\right)+\arcsin\left(\frac{1.222222}{1.515}\right)-\arcsin\left(\frac{1}{1.515}\right)\right]-1.186824\right\}-5.5}{\cos\left\{1.570796+2\cdot4\left[\frac{\pi}{2}-\arcsin\left(\frac{1.222222}{1.33113}\right)+\arcsin\left(\frac{1.222222}{1.515}\right)-\arcsin\left(\frac{1}{1.515}\right)\right]-1.186824\right\}}=$$

$$=-22.036\ \text{mm}, \qquad (3.49)$$

Let's calculate the displacement $x(\eta\max 15)$, by taking into account the temperature of the sample.

When heated to the temperature of 15° C degrees the refractive index increases to $n_3 = 1.34637$ (Eq. (1.11)).

$$x(\eta \max 15) =$$

$$= \frac{10.5 \cdot \cos\left\{2 \cdot 4\left[\frac{\pi}{2} - \arcsin\left(\frac{1.222222}{1.34637}\right) + \arcsin\left(\frac{1.222222}{1.515}\right) - \arcsin\left(\frac{1}{1.515}\right)\right] - 1.186824\right\} - 5.5}{\cos\left\{1.570796 + 2 \cdot 4\left[\frac{\pi}{2} - \arcsin\left(\frac{1.222222}{1.34637}\right) + \arcsin\left(\frac{1.222222}{1.515}\right) - \arcsin\left(\frac{1}{1.515}\right)\right] - 1.186824\right\}} =$$

$$= -15.915 \text{ mm}, \qquad (3.50)$$

From Eq. (3.46), Eq. (3.47), Eq. (3.49) and Eq. (3.50) it can be seen that the thermal displacement in the photosensitive area length will be about max=0.352mm, that by using the photosensitive area length on 70% the laser beam will not come out beyond the photosensitive area length.

When we have the photosensitive pixel pitch $\Delta p = 7.8\ \mu m$, we will obtain the following:

$$\delta = \frac{(n_{\max} - n_{\min})\Delta p}{x(\eta \max) - x(\eta \min)} \approx 1.95 \cdot 10^{-5} \approx 2 \cdot 10^{-5} \qquad (3.51)$$

In the figure below (Fig.3.14) it is possible to see the mathematically modeled (on Mathcad software) passage of the laser beam on the photosensitive area length of the linear measuring element.

In chapter 4 a comparison of the real data and the basic data of the mathematic modeling for the newly designed refractometer is described.

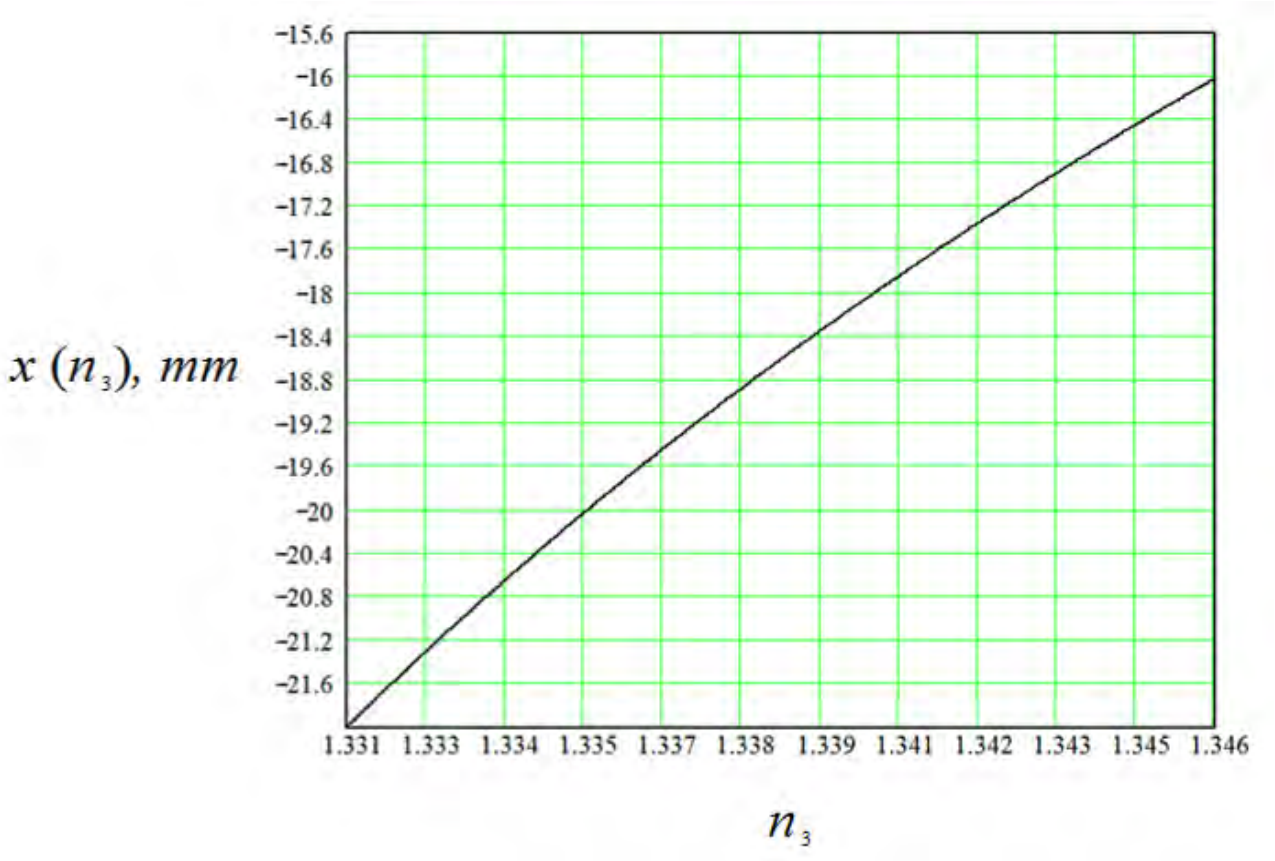

Fig. 3.14. The calculated position x of the exiting laser beam projection on the CMOS linear image sensor, as a function of the refractive index n_3 of the liquid contained in the cell for refractometers with a small RI measuring range (refractometer, version B)

3.4.4. The refractometers with a maximum RI measurement resolution

Let's have a goal to develop the most resolution refractometer to measure $n_3 = 1.3318$ up to $n_3 = 1.3324$, but with the resolution of the $\delta \approx 10^{-7}$. With the previously described resolution alcohol can be measured in the range of from 0 to 1 % alc. / weight. This refractometer for measuring resolution is already comparable to the resolution of the measurement interferometers [102].

Let's use the same laser where $\lambda = 635$nm. Let's have the optical linear sensor photosensitive pixel pitch $\Delta p = 1.12\,\mu m$ (S5K3L2-13-megapixel, 1.12µm pixel image sensor, 4208 × 3120 pixels, Samsung) [77].

As the optical measuring element of the cell we can use the cylinder with an outer and inner diameter r_1 = 5.95mm and r_2 = 4.5 mm respectively, made of optical glass with a big refractive index (n_2 = 2.185, $\lambda = 635$ nm [106]) that will allow for almost the same size of the

cell, which was used in previous calculations, to obtain the increasing number of reflections m. In order to increase the number m we will let the laser beam gyrate (as shown in Fig.3.3).

Number $m = 22$ is not pre-selected here. It is the nearest number in this embodiment of the refractometer.

The Fig.3.11 schematically shows the option of the spatial distribution of parts of the refractometer with the preliminary sizes. For the sake of clarity, the large values increase of the number m we can leave the distance $l = 5\,\text{mm}$ and the position of the cell, as section 3.4.2.

$$L = l + r_1 = 5 + 5.98 = 10.98\,\text{mm}$$

$$\psi = 90° = \frac{90 \cdot \pi}{180} = 1.570796\,\text{rad}$$

$$-\alpha = +6° = \frac{23.66 \cdot \pi}{180} = 0.10472\,\text{rad.}$$

To get the laser beam to the center of the photosensitive area length of the linear measuring element, when we have η_{med} the following condition must be obtained:

$$x(\eta_{med}) \approx r_1 = 5.98\,\text{mm.} \tag{3.52}$$

When we put in the values of all final geometrical and physical parameters in Eq.(3.27), we will obtain the following:

$$x(\eta\,\text{min}) =$$

$$= \frac{10.98 \cdot \cos\left\{2 \cdot 22\left[\frac{\pi}{2} - \arcsin\left(\frac{1.328889}{1.3318}\right) + \arcsin\left(\frac{1.328889}{2.1862}\right) - \arcsin\left(\frac{1}{2.1862}\right)\right] + 0.10472\right\} - 5.98}{\cos\left\{1.570796 + 2 \cdot 22\left[\frac{\pi}{2} - \arcsin\left(\frac{1.328889}{1.3318}\right) + \arcsin\left(\frac{1.328889}{2.1862}\right) - \arcsin\left(\frac{1}{2.1862}\right)\right] + 0.10472\right\}} =$$

$$= -7.481\ \text{mm,} \tag{3.53}$$

$$x(\eta\,\text{max}) =$$

$$= \frac{10.98 \cdot \cos\left\{2 \cdot 22\left[\frac{\pi}{2} - \arcsin\left(\frac{1.328889}{1.3324}\right) + \arcsin\left(\frac{1.328889}{2.1862}\right) - \arcsin\left(\frac{1}{2.1862}\right)\right] + 0.10472\right\} - 5.98}{\cos\left\{1.570796 + 2 \cdot 22\left[\frac{\pi}{2} - \arcsin\left(\frac{1.328889}{1.3324}\right) + \arcsin\left(\frac{1.328889}{2.1862}\right) - \arcsin\left(\frac{1}{2.1862}\right)\right] + 0.10472\right\}} =$$

$$= -4.347\,\text{mm,} \tag{3.54}$$

where $k = r_1 / r_2$=5.98/4.5=1.328889.

The negative sign according to Eq.(3.53) indicates that the position of the projected point on the photosensitive area length of the linear measuring element is below the horizontal line **OP** (see Fig. 3.1). As the result we will have the following:

$$\eta_{med} = \frac{x(\eta \max) + x(\eta \min)}{2} \approx -5.9 \text{ mm}, \tag{3.55}$$

When we have the photosensitive pixel pitch $\Delta p = 1{,}12\ \mu m$, we will obtain the following:

$$\delta = \frac{(n_{\max} - n_{\min})\Delta p}{x(\eta \max) - x(\eta \min)} = 2.14 \cdot 10^{-7} \approx 2 \cdot 10^{-7} \tag{3.56}$$

The figure Fig.3.15. shows a portion of the image of the incident laser beam on the two-dimensional photosensitive area.

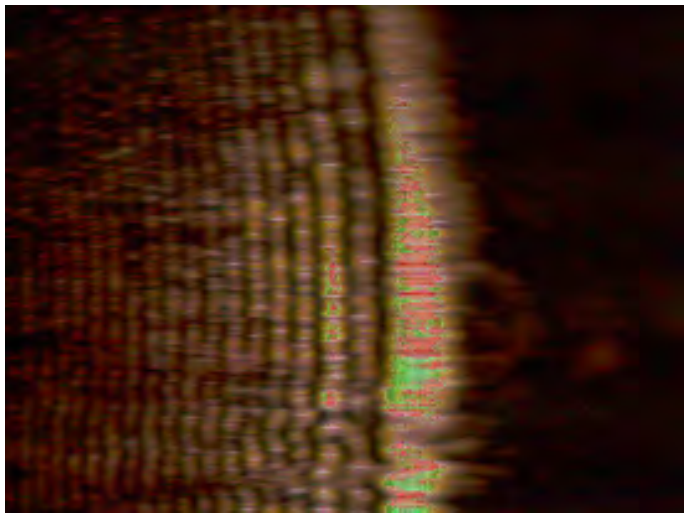

Fig. 3.15. The image of the incident laser beam on the two-dimensional photosensitive area

3.5. Approach to analyze the image by cylindrical cell based refractometer

Projected on a linear measuring element (for example, on a CMOS linear image sensor), the beam forms an image area containing a *front*, namely, a transition region from darkness to light (as shown in Fig.3.16.). The position of the front is determined by the critical angle of the optical system comprising the cell and the liquid being measured. Usually this front is used to define and detect the projection position of the beam passed through the cylindrical cell [31, 75].

Since the transition between the dark and light parts of the image is gradual, it is necessary to define the position of the boundary. This position is usually defined as the point where the light intensity distribution graph is the steepest and is calculated for each RI value, an ordinal number of a pixel (a position) on the image sensor is thus assigned.

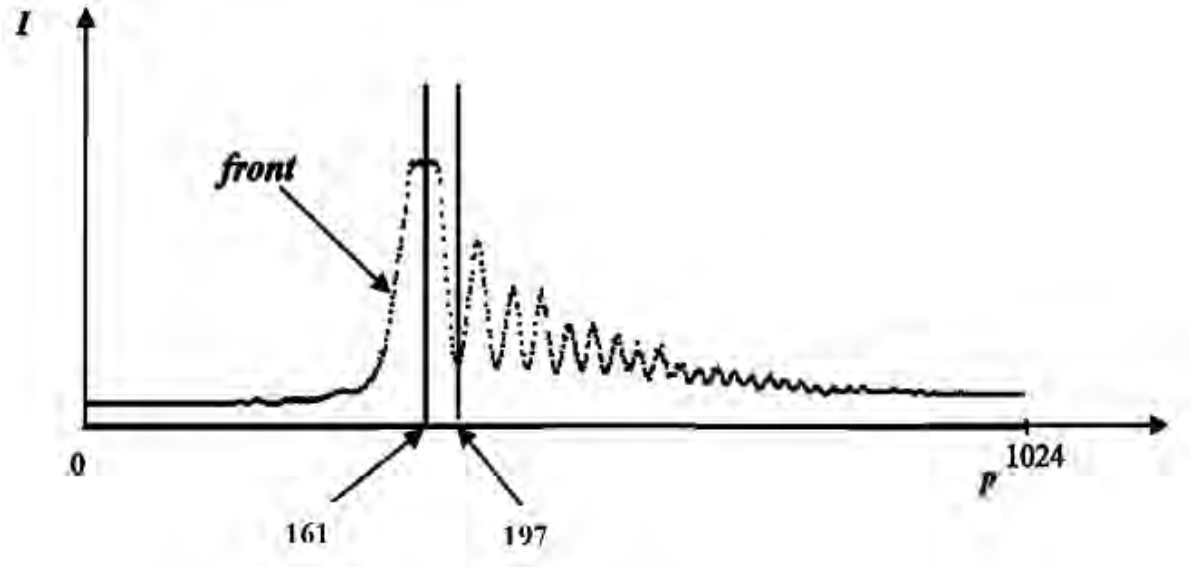

Fig. 3.16. Overall image on a linear optical sensor with *p*-number of pixels (Hamamatsu CMOS monochromatic linear 1024 pixel image sensor S9226), *I*- intensity of the light

Such an approach, however, has some disadvantages. The distribution of the light intensity on the front depends on the slope of the light intensity graph, the intensity and stability of the light source and the presence of some colloidal particles or small gaseous bubbles in the measured liquid. Consequently, the detection of the front position is indeterminate and sometimes even impossible, particularly in the case of flowing liquids.

The Fig.3.17 (only the part of the images Fig. 3.16 is shown) presents diagrams of the beam for image position detection due to the developed [90] and conventional techniques [31, 75], the cell contains the distilled water. The solid vertical lines shown in Fig.3.17 represent the positions detected by the developed technique, while the dashed vertical lines correspond to the positions determined by the conventional technique.

Another method for determining the position of the illuminated area of the light beam projection on the linear image sensor has been developed in [90] to increase the resolution of the measuring device and to practically eliminate the bulk of the effects caused by the varying intensity of the light source and the influence of gas bubbles or admixtures of particles on the quality of measurements. This method is based on detection of the location of the beam projection image, which is fixed by equation (3.27). The whole width of the image is several tenths of a millimeter. A narrow area of each whole image is scanned by the sensor and

characterizes the light intensity distribution of the cross section of projected beam over the area of the sensor. Waveform of the images shows that the interference of laser light after it is reflected from different regions in the cell generates an interference pattern, as described in more detail in [80].

The image position is determined by the position of the first or any subsequent minimum following the position of the maximum intensity of distribution. From the whole image of the beam projected on the linear sensor, the location of the minimum intensity is used as a conveniently and precisely detectable position.

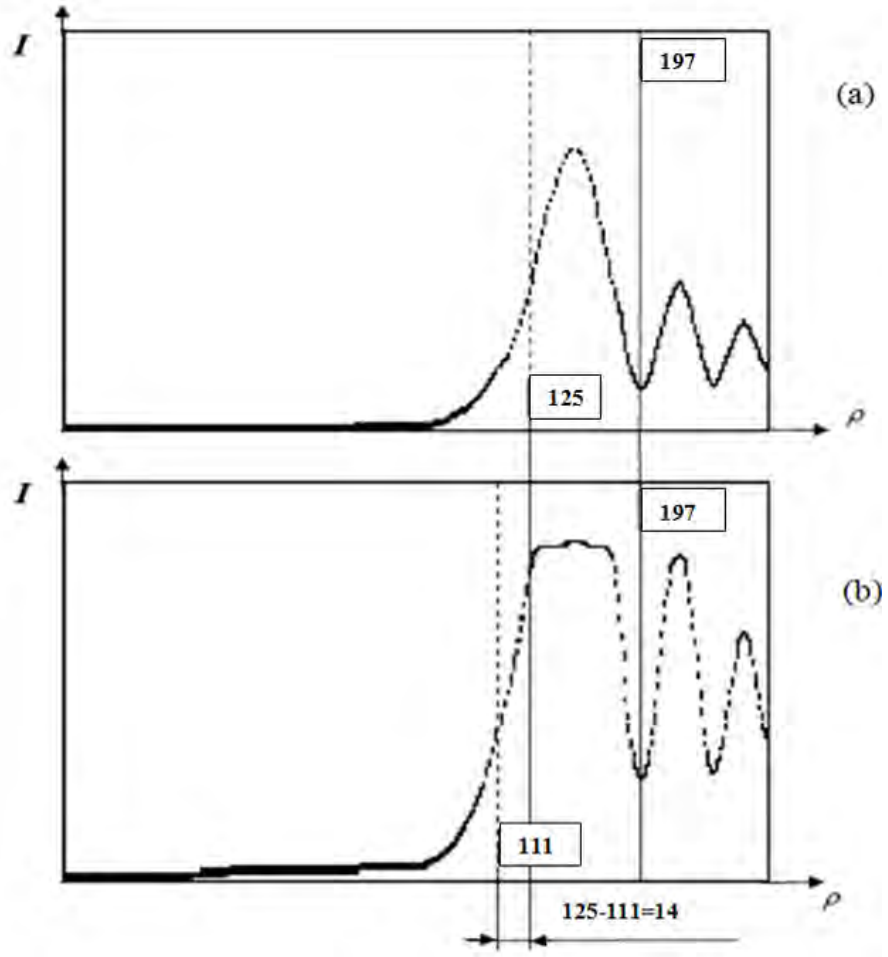

Fig. 3.17. Detection of the position of the image at two different light intensities of the laser beam projection on the linear image sensor. *I* – intensity of the laser beam; *p*-number of pixels

3.6. Conclusion

In the chapter.3, the refractometer with a new physical principle of RI measurement is described. Its basic operating principle is explained.

For mathematical modeling of the refractometers, some basic mathematical calculation formulas are derived that allow at an early design stage to define the following basic parameters

of refractometers: sensitivity, resolution, effects of the measured fluid temperature on the resolution, determine the material of construction and dimensions of the cylindrical cell, the relative distance and orientation between the following fundamental elements of the refractometer: laser, cylindrical cell and the readable optical element.

From the basic developed formulas studied is the effect of m - the number of reflections in the cylindrical cell and k - the ratio of the outer radius to the inner radius of the cylindrical cell on the sensitivity and precision of the refractometer.

By using the developed formulas the following refractometers were modeled:

- the simplest, inaccurate refractometer to demonstrate a new physical principle of refractometry;
- the refractometer (version A) with a large RI measuring range ($\delta = 5 \cdot 10^{-5}$),
- the refractometers (version B) with a small RI measuring range ($\delta = 2 \cdot 10^{-5}$),
- the particularly sensitive refractometers with a maximum RI measurement resolution ($\delta = 2 \cdot 10^{-7}$).

The mathematical modeling process of the refractometers is described in Table 3.1.

All refractometers, except the last, were manufactured and tested in order to verify the resolution of the new formulas derived. The results are shown in the chapter 4.

Table 3.1.

Initially stated and expected parameters of the refractometers

Parameters	The simplest refractometers	Refractometer A	Refractometer B	Refractometer C
λ, nm	635	635	635	635
r_1, mm	5.1	5.5	5.5	5.98
r_2, mm	4.5	4.5	4.5	4.5
n_2	1.515	1.515	1.515	2.185
L, mm	117.1	10.5	10.5	10.98
l, mm	112	5	5	5
α	-46.6°	-28.6°	-68°	+6°
Ψ	90°	90°	90°	90°
m	4	4	4	22
Δp, μm	Scale 35.6 mm	7.8	7.8	1.12
Temperature compensation	No	Yes	Yes	Yes
RI	1.3312....1.3651	1.33167...1.36454	1.33167...1.34583	1.3318...1.3324
δ, RI	10^{-3}	5.7×10^{-5}	2×10^{-5}	2×10^{-7}

Chapter 4. CYLINDRICAL CELL BASED REFRACTOMETERS FOR MEASUREMENTS OF REFRACTIVE INDEXES OF LIQUIDS

4.1. Scheme of the refractometer

Measurement algorithm and construction of cylindrical cells refractometer depends on intended use of the refractometer.

The main source of data for the design of cylindrical cells refractometer for the design planning process should be:

- Measuring ranges of the possible fluid concentrations. Based on the reference data (reference literature [47, 102], online calculators [71]) the appropriate RI measurement ranges are determined.
- Temperature ranges during the concentrations measurement process. From the reference data extension of the measurement limit RI is specified.
- Fluid pressure. If this pressure is high, it may be necessary to increase RI measurement limit, which is also possible to find in the reference data.
- Necessary measurement resolution.
- Measured liquid. Its chemical and physical properties (toxicity, chemical interaction with the cell walls and the other parts of the refractometer that come to contact with measured liquids). It is necessary to know this in order to choose the appropriate material for cell and design parts of the refractometer, which come to contact with measured liquids and sealing material.
- Measured liquid is stable or flows through the measuring part.
- Measured liquid is homogeneous or there are some insoluble particles or air bubbles in this measured liquid.
- In what form it is necessary to provide the results of measurement (display on the screen of some autonomous device or transfer data to a remote computer and display on the screen of this computer, or accumulation in the microcontroller memory with the following output on your computer).
- Prospective size and weight of the construction.
- Power supply, autonomous operation.
- Climatic conditions of operation of the refractometer.
- Special requirements for electrical safety.
- EMC requirements.

- Explosion and fire safety requirements (mines, special chemicals manufacturing).

Cell's refractometer consists of two main parts: part of optics and part of electronics.

Optical part of the cells refractometers always consists of optically transparent cylindrical cell, the laser diode, collimator located between the cylindrical cell and laser diode and linear CMOS or CCD image sensors. Cylindrical cells, collimator, laser diode and linear CMOS or CCD image sensors are rigidly mechanically connected into a single unit.

4.2. The simplest refractometers

To demonstrate the refractometer with new physical principles a simple demonstration refractometer (with a cylindrical cell) was specially made, which did not have any temperature compensation. Therefore, this model has been inaccurate. The demonstrations refractometer can operate as a simple indicator, which do not need any high precision measurements of the concentration and density of liquids.

In order to simplify the design of cells refractometers by electronic part, linear CMOS or CCD image sensors can be replaced by a conventional screen, where you can visually read RI measurements for moving the laser beam across the marked scale on the screen.

In section 3.4.1 the simplest refractometer has been mathematically modeled and designed for measuring the concentration of aqueous solutions of ethanol from 0 to 80% alc/weight within a temperature range from +15°C to +25°C), and the resolution of this refractometer should be $\delta = 2 \cdot 10^{-3}$. Therefore we can take from this section the geometrical dimensions of the cylindrical cell, the calculative distance and position of the laser, cylindrical cells and screen, as well as the physical parameters of these structural elements of the refractometer.

To imagine, how cells refractometers work, first we can consider the simplest construction of cell's refractometers. Internal construction of cell-based refractometers is shown in Fig.4.1. The appearance is shown in Fig. 4.2.

From laser pos.4 shines a laser beam passing through of lenses pos.3, and this beam falls on cylindrical cells pos.7, going through four points of reflection (Fig.4.1), and the laser beam falls on the point of the calibrated screen pos.9, pos.1. The laser is powered by a lithium battery pos.6. All cell-based refractometers are enclosed in a housing pos.8.

BS - scale for measurements of medical objects within the 1.331-1.365 range of RI values, measuring sensitivity: 0,001.

L - distance from the center of the cell to the point of pos.1.

BS and **L** correspond to analogous terms (Fig. 3.1).

The laser diode has a wavelength of 635 nm. With parameters m=4; n_2=1.515; r_1=5.1mm; r_2=4.5 mm; L=117.1mm; $\alpha = 46.6°$; ψ=90° we got size **BS**=35.6 mm. If a mathematical model and calculations are correct, then we should get the size of BS with a temperature deviation within one scale unit of RI (see the section 3.4.1). The cell is made of borosilicate glass BK (Borosilicate crown). However, the material of the cell can be any glass or even plastic. The main thing is that the material is optically transparent and homogeneous, without any inclusions in the form of bubbles, sprues. Very important is to have the constant thickness of the cell walls throughout all perimeter. It is not allowed to have a big circularity deviation of the cell walls.

The cell has a light-reflecting aluminum coating formed by vacuum deposition on vacuum coating plant in Riga.

In the simplest cell's refractometers, the laser beam travels a distance from the laser diode to the cell about 20 mm and diverges greatly; therefore collimator is designed as a lens to get the parallel beam bundles from the laser. Dimensions of the simplest cell's refractometer are 150x10x50mm, weight 70 grams.

When we had test measurements of this refractometer (measuring the concentration of aqueous solutions of ethanol from 0 to 80% alc/weight) size of BS scale was 36.5 mm. When you change the temperature range from + 15 ° C to + 25 ° C the laser beam on the screen BS shifted by no more than 1 mm over the entire range of this measurement. From Eq. (3.34), Eq. (3.35), Eq. (3.37) and Eq. (3.39) it can be seen that the thermal displacement of the length will be $\approx \pm 0.5$ mm for a variation of 20 ± 5°C degrees.

The error in determining the size of this scale (mm) is commensurable with the error of manufacture and assembly of the refractometer.

Quite a large temperature deviation of about 1 mm is due to the fact that the body base (to which all the elements of the refractometer are attached) is made of polypropylene.

Based on the above-described, we can make the following conclusion: the mathematical model and the calculations are very coincident.

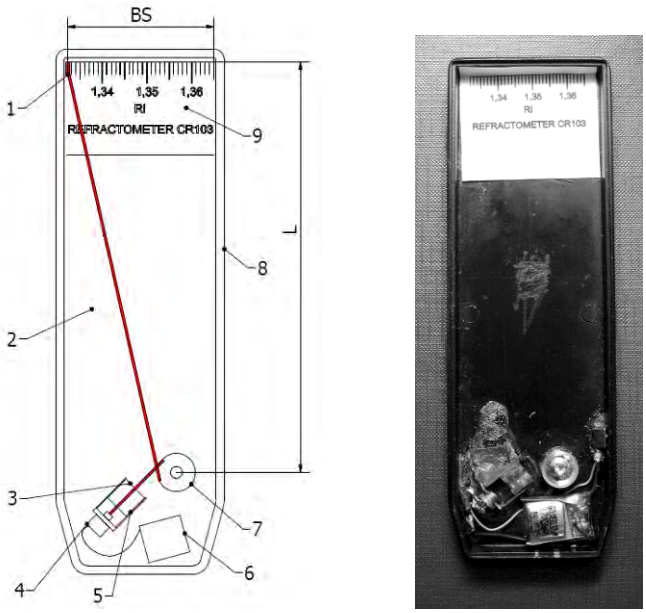

Fig. 4.1. Scheme of the optical system of the simplest refractometer and its view inside

Fig.4.2. Palm tester-type refractometer for measuring the refractive index of liquid substances. This is one of the cheapest devices of this kind. The refractive index values of liquid are indicated by the projection of the exiting beam on a scale graduated in RI units

4.3. The precision refractometers

4.3.1. Optical system

To obtain accurate measurements, it is necessary to provide a temperature control of the liquid. In addition, it is necessary to reduce the influence of thermal expansion of structural elements, and this can only be done by reducing the linear geometric dimensions of the entire block of the optical refractometer. With a decrease of the optical length of the refractometer, also reduces L – the distance from the center of the cell, to the point position 1 and the range of movement of the laser beam BS. Visual observation of the laser beam becomes impossible. In

such a case, for fixing the laser beam movement on the screen, the ideal solution is to use linear CMOS or CCD image sensors.

In section 3.4.2 was mathematically modeled and calculated the refractometer with a large RI measuring range for determining the percentage concentrations of aqueous ethanol by weight in the range from 0 to 70% alc/weight within a temperature range from +15°C to +25°C. The resolution of this refractometer should be $\delta = 5.7 \cdot 10^{-5}$. Let us label this design of the refractometer as a version A.

In section 3.4.3 was mathematically modeled and calculated the more sensitive refractometer with a small RI measuring range for determining the percentage concentrations of aqueous ethanol by weight in the range from 0 to 20% alc/weight within a temperature range from +15°C to +25°C. The resolution of this refractometer should be $\delta = 2 \cdot 10^{-5}$. Let us label this design of the refractometer as a version B.

For the purpose to maintain the experimental integrity, e.g., to use a common cylindrical cell, laser and a linear optical element, as well as to reduce the cost of the experiment, the new design of the refractometer has been developed, in which both options A and B was implemented in the single constructive device.

On Fig.4.3 shows the optical block of the precision electronic unit cells refractometer.

From a laser diode pos.4 a laser beam pos.3 passes a collimator pos.5 (which is made as a simple aperture) and enters in the cell pos.8, passes inside the cell (Fig.3.1) and after passes out of the cell pos.7, and falls on a photosensitive surface a Hamamatsu CMOS where a monochromatic linear image sensor S9226 pos.2.

Shape specifications: number of pixels 1024, pixel pitch 7.8μm, pixel height 125 μm, active area length 7.9872mm [13].

Image sensor S9226 is located on the PCB (pos.1).

Since the distance from the laser diode is less than 8 mm, it was experimentally determined that collimator device pos.5 may be formed as a simple aperture with a gap of 1 mm. The aperture is parallel to the central axis of the cell. The wavelenght of the laser diode is 635 nm, the power is 5 mW.

As we can see on Fig.4.3, we can invert PCB (pos. 1) upside down, and by changing the inclination angle of the laser α we can obtain the version A and version B.

Position of the laser, cylindrical cell, and linear optical elements are taken from section 3.4.2 and section 3.4.3.

A minimum volume of sample liquid to be measured is 0.3 ml.

Pos.9 designated SMD platinum sensor a Heraeus platinum thermal sensor SMD 0603 DIN EN60751B, 1000Ω.

All optical elements: laser diode pos.4, collimator pos.5, cell pos.8, linear optical element pos.2, electronic board pos.1 are mechanically rigidly connected by a special monolithic aluminum block pos.10. Aluminum equalized temperature levels between all the optical elements, and because of its small size, it has an insignificant thermal expansion.

Version A

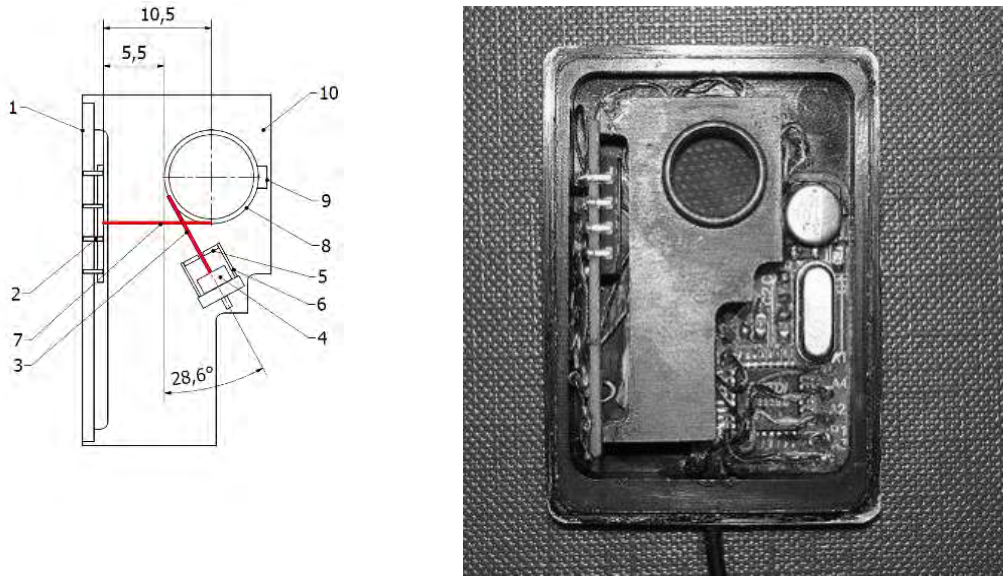

Version B

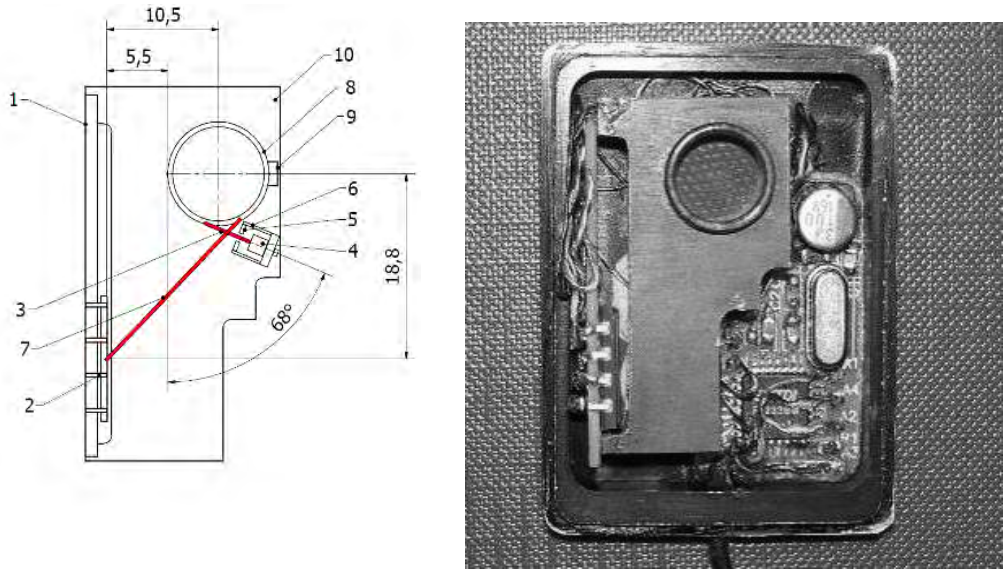

Fig.4.3 Schemes of the optical systems of precision refractometers and inside views for versions A and B

4.3.2. Electronic system

In order to test a new concept of the cell refractometers, an electronic part of the refractometer has been developed and manufactured.

The electronic circuit part consists of two parts: the board B1 and B2 board Fig.4.4. The board B1 contains a microcontroller that controls all the electronic elements of the optics module Fig.4.3. The microcontroller controls the laser and reads the data from a linear optical sensor and a platinum temperature sensor. All the data are not accumulated in the microcontroller; they are immediately transferred (after reading from a linear optical element) to a remote personal computer, where the main storage, processing, and display of the information are provided. The board B2 is acting as a connector between the microcontroller and the PC. Microcontroller sends the data through USART (The Universal Synchronous and Asynchronous serial Receiver and Transmitter) to board B2 where FT232BM chip converts USART protocol to the protocol USB (Universal Serial Bus Interface), and which are transmitted to the remote PC. Linear optical element through the board B1 is attached to the optical block and forms a single optical block. Laser and sensor are connected to the board B1 by flexible conductors. The boards B1 and B2 are also connected with each other through flexible conductors. The board is B2 separately secured insides the housing of the refractometer to the housing of the refractometer.

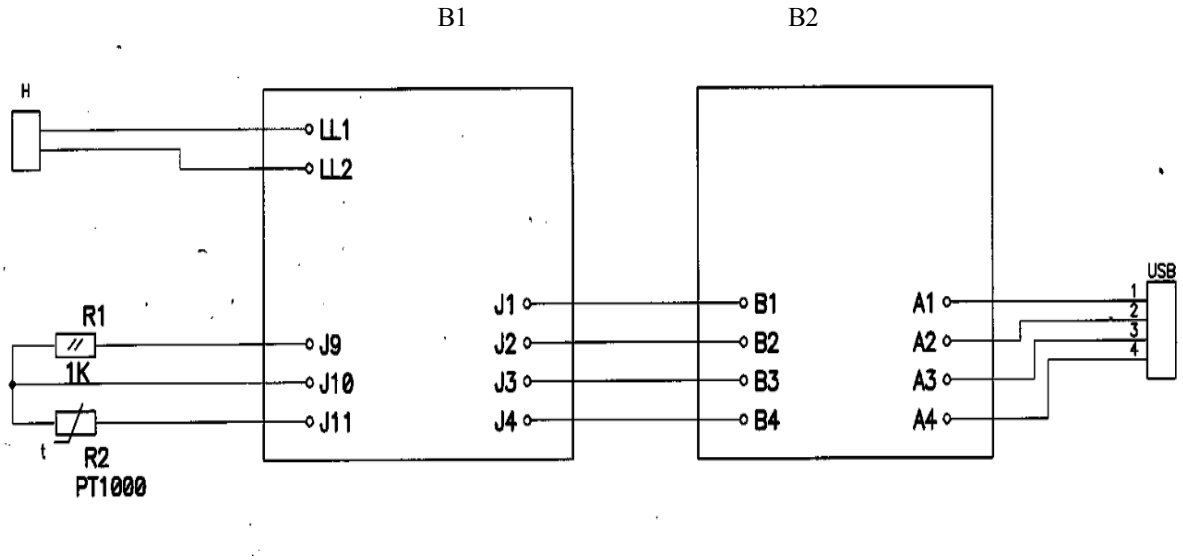

Fig. 4.4. H - the laser diode, R2 - a platinum temperature sensor, blocks B1 and B2

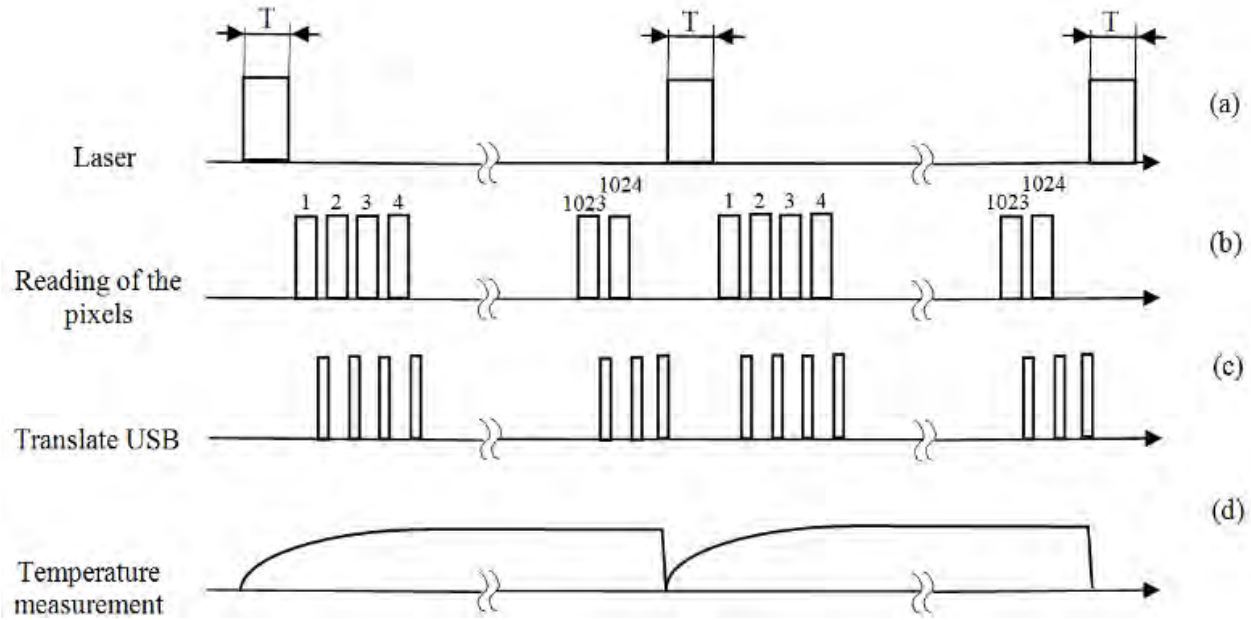

Fig.4.5. Timing diagrams the of the boards B1 and B2

On [Appendix 7] it is possible to see of components insides the optical part of the refractometer Fig.4.3. Appendix 8 shows a circuit diagram of B2 consisting USB chip to communicate with the computer. On [Appendix 9] and [Appendix 10] B1 and B2 electronic PCB are showed.

Initially, the laser provides a short impulse duration T Fig.4.5(a), and then the microcontroller starts to read all 1024 pixel from linear optical element Fig.4.5(b), immediately transferring the data to the remote USB device (computer) Fig.4.5(c).

At a certain point the thermistor measurement is provided pos. 9 Fig.4.3, See Fig.4.5(d), the temperature measurement data is also transmitted by USB device to some remote device (a computer) Fig.4.5(c).

4.3.3. Mechanical system

Fig.4.6 shows refractometer, which is equipped with a USB interface and has the following dimensions: 49 mm×35 mm×8 mm.

Structurally, the refractometer is made in universal design. Refractometer can be used as a flow-through type, i.e. built-in the rupture of a technological pipeline of some manufacturing line, as well as a portable version. In the latter case, the bottom of the cylindrical cell is closed with a rubber stopper. In the cylindrical, cell test solutions can be filled from the top. Waterproof housing of all refractometer allows not only easy to wash out all the refractometer in the water flow, but also to sink it entirely in some liquid.

Reading of the information comes via USB cable, which transmits this information to a laptop, tablet or a smartphone.

Fig.4.6 A USB-equipped device for measuring the refractive index of liquids. The device (dimensions 49 mm x 35 mm x 8 mm) is used for the experimental tests mentioned in the note

4.3.4. Algorithm of processing of measurements results

To facilitate perception of the measurement algorithm, the entire algorithm is divided into two parts (on two separate algorithms) which are presented separately in Fig.4.7 and Fig.4.8. Sometimes it is necessary in practice to minimize the measuring part of the refractometer to some size and weight limit in order to place the refractometer in some production line. Therefore, this case is described here.

When you turn on the device, in the block (A) Fig.4.7, the minimum of the laser beam intensity I = 0 is settled and the counter of the pixel numbers is reset to $p = 0$.

As shown in the timing diagram of Fig.4.7 and timing diagrams Fig.4.5 after the laser impulse, begins the reading process of the accumulated charges *U(p)* from each of the 1024 pixels of the linear optical element by using microcontroller (MCU internal ADC). In the block (A), data *U(p)* for each pixel of the sensor does not accumulate, they are immediately transmitted to the remote device through USART or USB (computers, mobile phones, tablets, or to some specialized remote units with visual indication) – the block (B).

At the same time is looking for the maximum value *U(p),* this is compared with the threshold $\boldsymbol{U}_{threshold}$ and the intensity of the laser beam I is adjusted, regulating the laser pulse duration on the sensitive surface of the sensor. This is necessary to obtain a high-quality graphics of the intensity distribution of the laser beam on the sensor pixels, when determining the number of pixel p_m of the first minimum in the chart.

In the algorithm the temperature *T* parameters from the cell with the test solution are acquired and they are immediately transmitted via USART or USB to the remote device–the block (B).

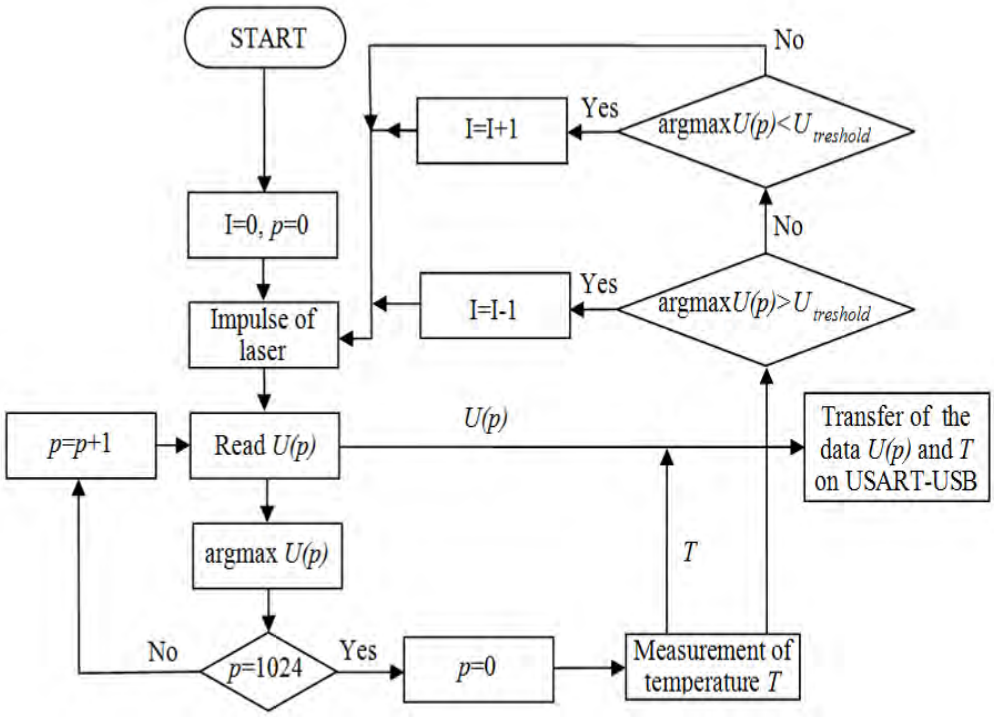

Fig. 4.7. Algorithm for solutions concentrations and RI measurements, sensor block (A)

The algorithm of the block (B) Fig.4.8. provides the procedure of work of the remote device. Here, the data *U (p)* are collected in the data array M(p). Further, from the array of M(p) the number of pixel p_m for the first minimum in the plot of the intensity distribution of the laser beam is determined. According to the number of the first minimum pixel p_m and data of the temperature *T,* by using the mathematical formulas (from Eq.(4.1) to (4.6), see section 4.4.2.1.) RI and the concentration of the test solution are detected. The calculated data are displayed on the display.

By combining two algorithm blocks (A) and (B) in one block, without remote USART or USB communication, we can obtain a compact hand-held, self-powered refractometer.

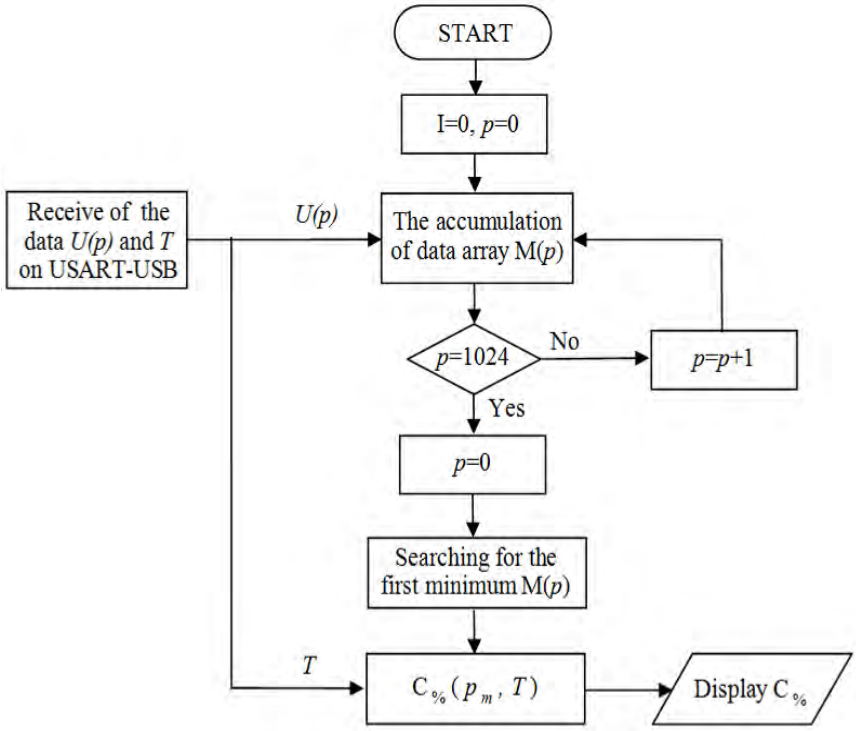

Fig.4.8. Algorithm for solutions concentrations and RI measurements, information processing and the display block (B)

On the Fig.4.6, we can see a general view of the sensor block (A). On the Fig.4.9, we can see the practical realisation of the portable autonomous block (B), equipped with a colour LCD display (to display the information).

To widen its application scope and increase convenience at use of the developed measuring device it was equipped with a number of auxiliary accessories and supplements. The measured ethanol concentration of the ethanol-water mixture is calculated and recorded in different mutually convertible units: percentage by volume (% alc/vol), weight (% alc/wt), and weight of ethanol per volume (kg/m^3) or (g/cm^3).

Furthermore, the measuring device also provides the option to see the actual measured temperature of the mixture, the measurement time (hour, minute, second) and the date (day, month, year). The data received from the sensor unit together with the results obtained from the recording and control section are optionally shown on a liquid-crystal display located in the recording section of the measuring device. The measuring unit and display are controlled by the microcontroller using five buttons located under the display. The data can also be displayed on the computer screen using a wireless *bluetooth* (*Smart Bluetooth Module*) link (Fig.4.10). The operating distance of the wireless link is up to 10 m.

Fig.4.9. View of the display block (B) (dimensions 116 mm x 78 mm x 22 mm)

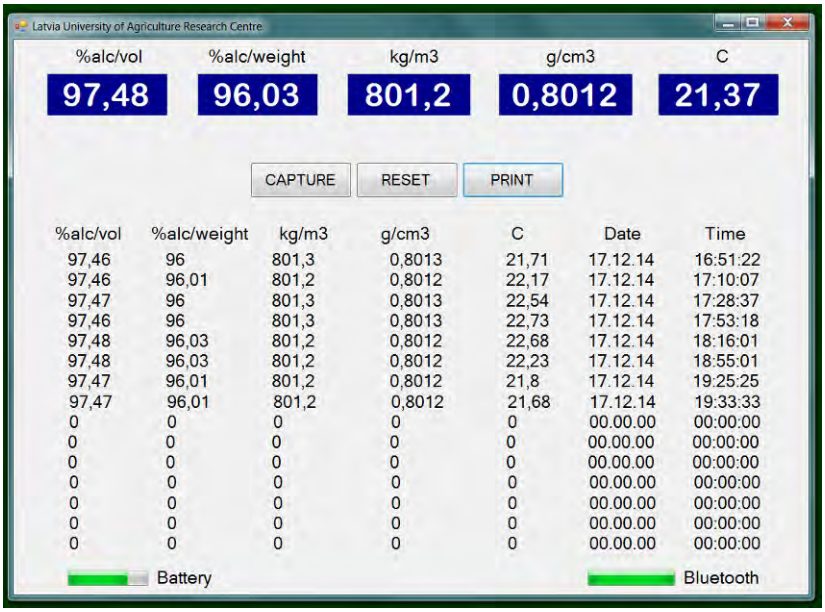

Fig.4.10. The computer screen showing the measurement data and the results obtained from the recording and control section of the measuring device

4.4. Properties of the refractometers

4.4.1. The set-up to explore properties of the refractometer

The general configuration of the equipment required for a testing process of the cells' refractometers is shown in Fig.4.11. All this equipment is universal and can be used to explore different design options of the refractometers to measure different liquids.

The equipment consists of a water bath TW2 [86] pos.1, the two-channel precision thermometer F100-A-2 pos.2; the temperature is measured simultaneously with two platinum sensors pos.3 and pos.4 with (accuracy: ±0.02°C over full range, resolution: 0.001°C, range: -200°C to +850°C, stability: <0.005°C per year, dual probe inputs) [66], peristaltic pump pos.5.

Water bath TW2 allows you to set the temperature ± 0.1ºC and maintain the desired temperature with accuracy ± 0.05 ºC. This water bath is equipped with a water pump pos.6 with adjustable speed of water supply for mixing of the liquid inside the bath at a speed of 2 to 5 liters/minute. Bath has an external output pos.7 for the external supply of the circulated inside the bath water. This external output pos.7 can be connected to an external refrigerant circuit of the refrigerator, which makes it possible to operate below indoor temperatures [86].

Inside the bath we placed a flask pos.8. This flask is filled with the bailed experimental liquid.

From the flask pos.8 an experimental liquid is pumped along the contour pos.9 by peristaltic pump pos.5 insides the contour and back into the flask pos.8. Arrows pos.10 and 11 indicate the direction of flow of this experimental liquid.

In open circuit, the following items are built in: new refractometer pos.12 and platinum sensors pos.3, pos.4.

From this refractometer (pos.12) the obtained information is transmitted to a computer (pos.14) and displayed on the screen (pos.15) via USB cable (pos.13).

The device is equipped with a *Heraeus* platinum thermal sensor SMD 1206 DIN EN60751 B, $1000\,\Omega$ at 0 ºC, measuring the temperature of the cylindrical cell and the liquid. In order to increase the temperature measurement precision of the platinum RTD, it was calibrated at two temperature reference points $t_0 = 0$ ºC and $t_{100} = 100$ ºC, and corresponding resistance values of the thermal sensor R_{0m} and R_{100m} were determined. According to the international standard DIN EN 60751, nonlinearity of the chosen platinum sensor can be expressed by the resistance–temperature interpolation equation: $R_t = R_0 \cdot (1 + At + Bt^2)$, where the sensor resistance $R_0 = 1000\,\Omega$ at t0 = 0 ºC, and the coefficients $A = 3.9083 \times 10^{-3}$ and $B = -5.775 \times 10^{-7}$. According to the algorithm and using the iterative method [57], the calculated temperature value t_c was obtained. It satisfies with a sufficient precision K both the nonlinearity of the function $R_t(t)$ obtained from the mentioned equation, and the resistance values R_{0m} and R_{100m} obtained by calibration. By choosing the precision criteria $K = 0.001$ ºC for the iteratively calculated temperature t_c, and additionally considering calculation and measurement errors

(caused by inaccuracies in resistance measurement, ice thermostat and 100 ºC thermostat, etc), the temperature measurement precision of such a platinum resistance thermometer was ensured in the range ± 0.02 ºC. For mathematical processing of the data and displaying the measurement results, *Atmel* microcontroller ATmega8 was used.

To identify the resolution to measure concentrations of solutions components, an aqueous solution of ethanol, NaCl, sucrose ($C_{12}H_{22}O_{11}$).

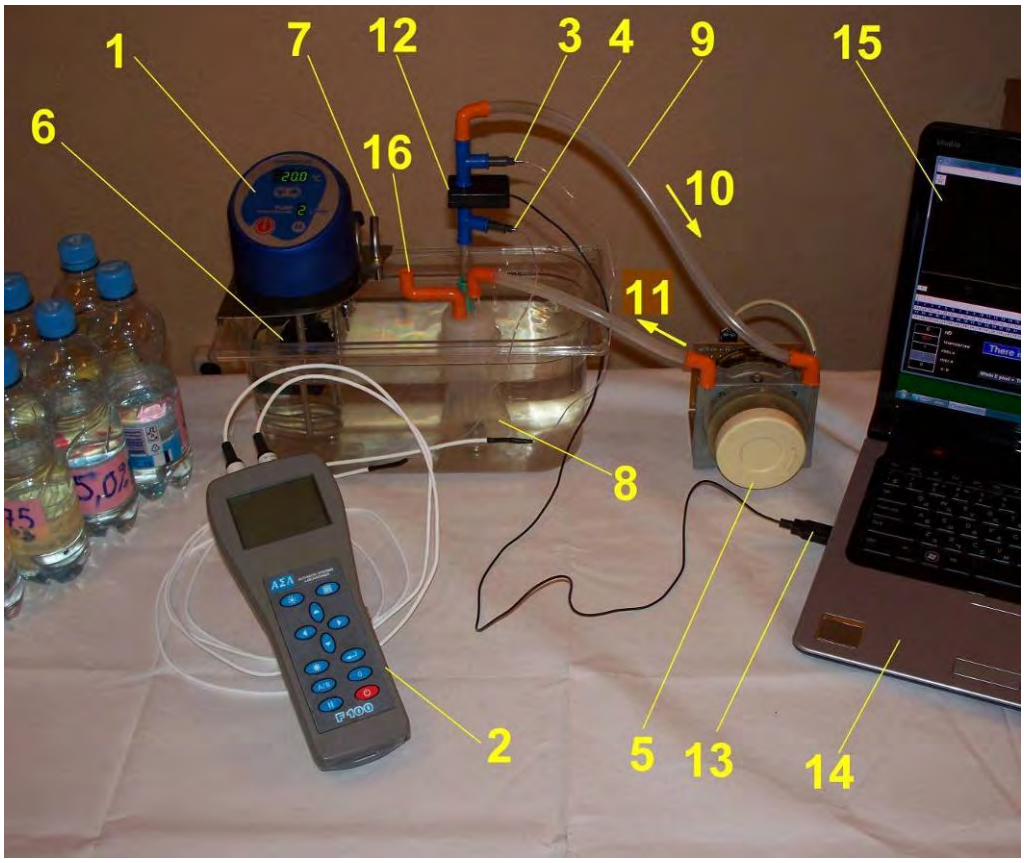

Fig.4.11 The general configuration of the equipment required for a testing process of the cell-based refractometers

4.4.2. Refractometers with a large RI measuring range

The refractometers are mathematically modeled in section 3.4.2. version A.

4.4.2.1. The calibration process of the refractometer using ethanol aqueous solution

The ethanol solutions have been prepared by precision hydrometer, at standard temperature of 20 °C . The mathematical computation of the temperature-compensated ($c_{\%TC}$)

concentration (% weight/vol.) of a given liquid sample is based upon a polynomial calibration equation (obtained as shown below). In order to illustrate the proposed computations, an example for thermo-compensated measuring device was provided.

Calculation of the thermo-compensated volume concentration of a binary liquid sample was carried as follows.

- Splitting of the measurement range of sample concentration (defined above) into smaller. The range from 0% to 70% weight/vol.
- Preparation and arranging of the measured data p_s (Table 4.1) by ascending percentages of concentration. Recording of the measured concentration of the reference sample $c_{\%R}$ value p_s set to the measured sample temperatures t_f 15°C, 20°C and 25°C.
- Using the p_s values (Table 4.1) obtained at the sample temperature of 15°C, to perform a regression analysis. Similarly, using the appropriate values measured at the sample temperature of 20°C and 25°C the following calibration equations were obtained.
- Refractometer designed as a multi-purpose device, it was necessary to provide the calibration process by taking into account the 3rd order polynomials. This is done in order to have a possibility to use the refractometer for other solutions in the future and also automatically include in the calibration process the effect of temperature influences of all constructive components of this device. When calibrating the refractometer to concentrations of alcohol the input of elements *p^2* and *p^3* in the equations were not enough and the result of this was some linear relationship, which we have used to define the resolution [102] (and see section 1.3). The device needs a new calibration for every liquid.

The volume percent ethanol concentration ($c_{\%}$) depending on the n values according to the calibration equation was approximated, to perform a regression analysis (program Origin 6.1 by Origin Lab Corporation):

$$C_{\%15} = -51.39972 + 0.36626 \cdot p - 7.53542 \cdot 10^{-4} \cdot p^2 + 6.03566 \cdot 10^{-7} \cdot p^3 \quad (t=15°C), (4.1)$$

$$C_{\%20} = -43.23919 + 0.31635 \cdot p - 6.51164 \cdot 10^{-4} \cdot p^2 + 5.39917 \cdot 10^{-7} \cdot p^3 \quad (t=20°C), (4.2)$$

$$C_{\%25} = -41.97363 + 0.32174 \cdot p - 6.8533 \cdot 10^{-4} \cdot p^2 + 5.79868 \cdot 10^{-7} \cdot p^3 \quad (t=25°C), (4.3)$$

The squared correlation coefficient of curves corresponding to Eq.(4.1), (4.2), (4.3) is R^2=0.99676, R^2=0.99839, R^2=0.99687 accordingly.

Because p – the linear optical element number can vary from 1 to 1024, its raising to the 3rd power can obtain a significant value. Therefore the third-order polynomial can not be ignored.

Table 4.1.

Measured p_s values according to the reference sample concentration $c_{\%R}$ and the measured sample temperatures t_f , by using refractometer version A

Ethanol concentration, $c_{\%R}$	Temperature, t_f	p_s
0 %	15°C	220
	20°C	208
	25°C	196
2.5 %	15°C	249
	20°C	238
	25°C	226
5 %	15°C	283
	20°C	272
	25°C	260
7.5 %	15°C	319
	20°C	308
	25°C	298
10 %	15°C	355
	20°C	345
	25°C	334
20 %	15°C	497
	20°C	487
	25°C	478
30 %	15°C	610
	20°C	601
	25°C	592
40 %	15°C	690
	20°C	682
	25°C	673
50 %	15°C	743
	20°C	734
	25°C	726
60 %	15°C	776
	20°C	768
	25°C	759
70 %	15°C	797
	20°C	789
	25°C	781

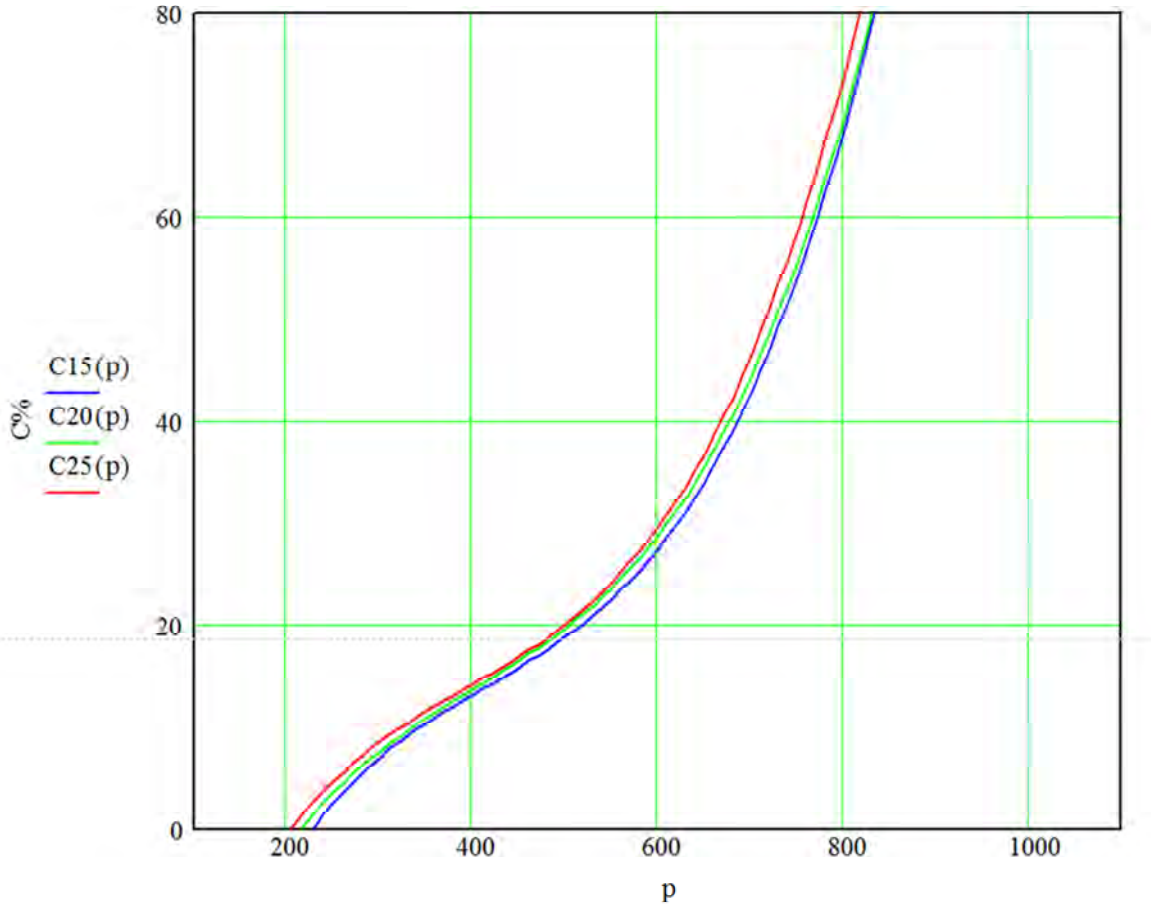

Fig. 4.12 The calibration curves of ethanol aqueous solution (for refractometer version A)

- Calculation of the thermo-compensated volume concentration $C_{\%TC}$.

For $+15°C < t_m < 20°C$:

$$C_{\%TC} = C_{\%15} + [(C_{\%15} - C_{\%20})(20 - t_m)]/\Delta t, \quad (4.5)$$

where $\Delta t = 20 - 15 = 5$.

For $+20°C < t_m < 25°C$:

$$C_{\%TC} = C_{\%20} + [(C_{\%20} - C_{\%25})(20 - t_m)]/\Delta t, \quad (4.6)$$

where $\Delta t = 25 - 20 = 5$.

Doing exemplary calculation of the thermo-compensated volume concentration $C_{\%TC}$ of a given ethanol-water mixture sample:

a) For the actual sample temperature t_m and concentration p (expressed in notional units p) measured and fixed using the developed measuring device (Fig. 4.13).

For the chosen sample, the values $t_m = 21.7°C$ and $p = 688$ are measured and recorded.

b) Using Eq.(4.2) and Eq.(4.3) and assuming p=688, the following volume percentages are obtained:

$$C_{\%25} = 42.015\,\%\text{ , and } C_{\%25} = 43.827\,\%$$

c) Substituting the above $C_{\%}$ values, for t_m=21.7°C the thermo-compensated liquid measured concentration is calculated by the Eq.(4.6), as a result, will have:

$$C_{\%TC} = 42.015 + [(42.015 - 43.827)(20 - 21.7)]/5 = 42{,}63108 = 42.631\,\%$$

The microcontroller of the sensor unit performs the calibration and recording of measured data as well as processes the data of the previous example, and records the final results.

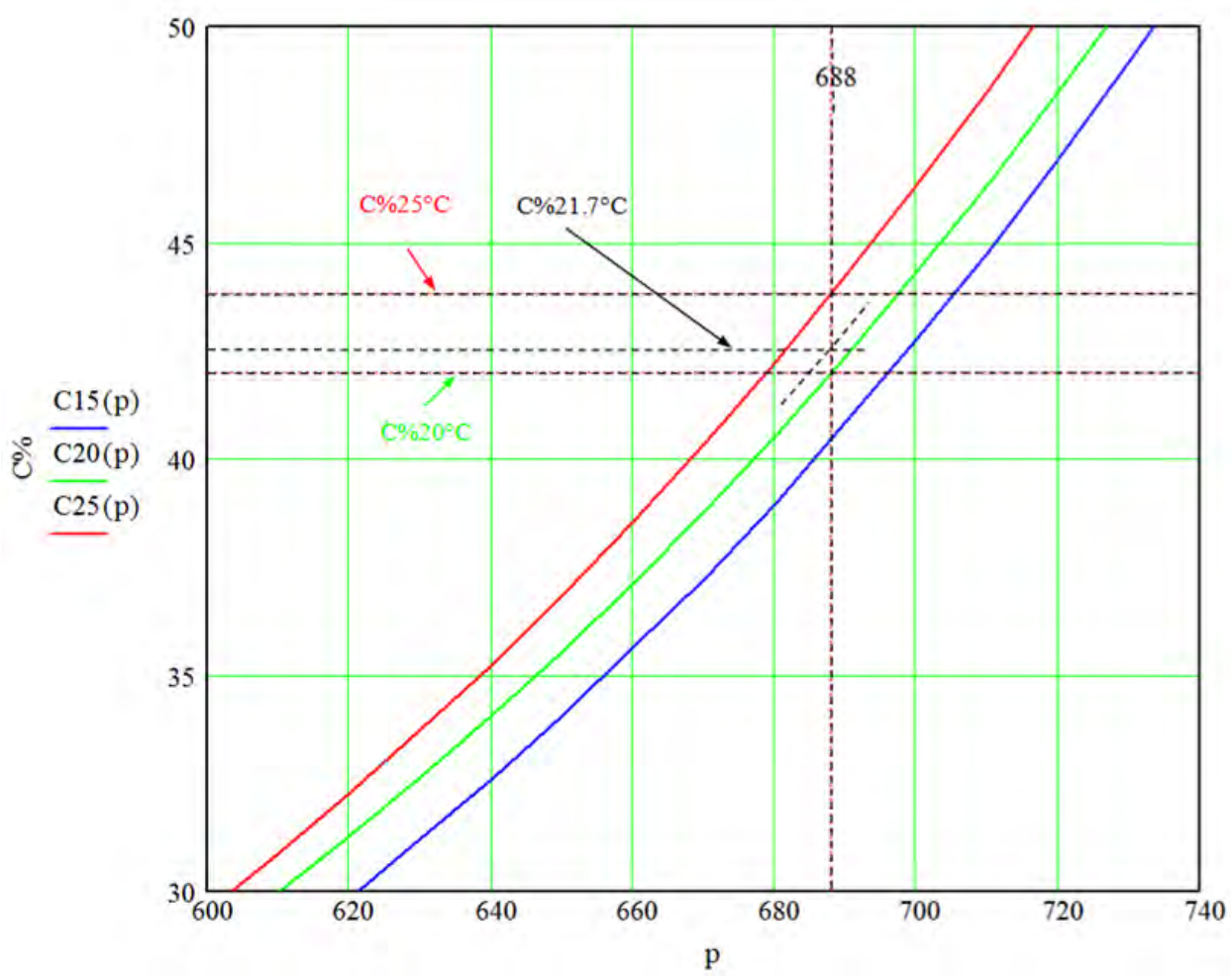

Fig. 4.13 The calculated thermo-compensated weight concentration $C_{\%}$ for a given ethanol-water mixture sample at the actual measured sample temperature t_m (p-number of pixels) (enlarged fragment Fig. 4.12)

4.4.2.2. The calibration process of the refractometer using aqueous NaCl solution

Table 4.2.

Measured p_s values arranged by ascending percentages of the reference sample concentration $c_{\%R}$ and by measured sample temperatures t_f

NaCl concentration, $c_{\%R}$	Temperature, t_f	p_s
0 %	15°C	220
	20°C	208
	25°C	196
2.5 %	15°C	314
	20°C	303
	25°C	292
5 %	15°C	401
	20°C	391
	25°C	381
10 %	15°C	562
	20°C	553
	25°C	544
15 %	15°C	710
	20°C	701
	25°C	693
20 %	15°C	850
	20°C	842
	25°C	833
25 %	15°C	986
	20°C	978
	25°C	971

$$C_{\%15} = -4.91424 + 0.01911 \cdot p + 1.57048 \cdot 10^{-5} \cdot p^2 - 4.37131 \cdot 10^{-9} \cdot p^3 \quad (t=15°C), \quad (4.8)$$

$$C_{\%20} = -4.58865 + 0.01895 \cdot p + 1.59877 \cdot 10^{-5} \cdot p^2 - 4.52725 \cdot 10^{-9} \cdot p^3 \quad (t=20°C), \quad (4.9)$$

$$C_{\%25} = -4.20749 + 0.01836 \cdot p + 1.71639 \cdot 10^{-5} \cdot p^2 - 5.23246 \cdot 10^{-9} \cdot p^3 \quad (t=25°C), \quad (4.10)$$

The squared correlation coefficient of curves in corresponding to Eq.(4.8), (4.9), (4.10) is $R^2=1$, $R^2=1$, $R^2=1$ accordingly.

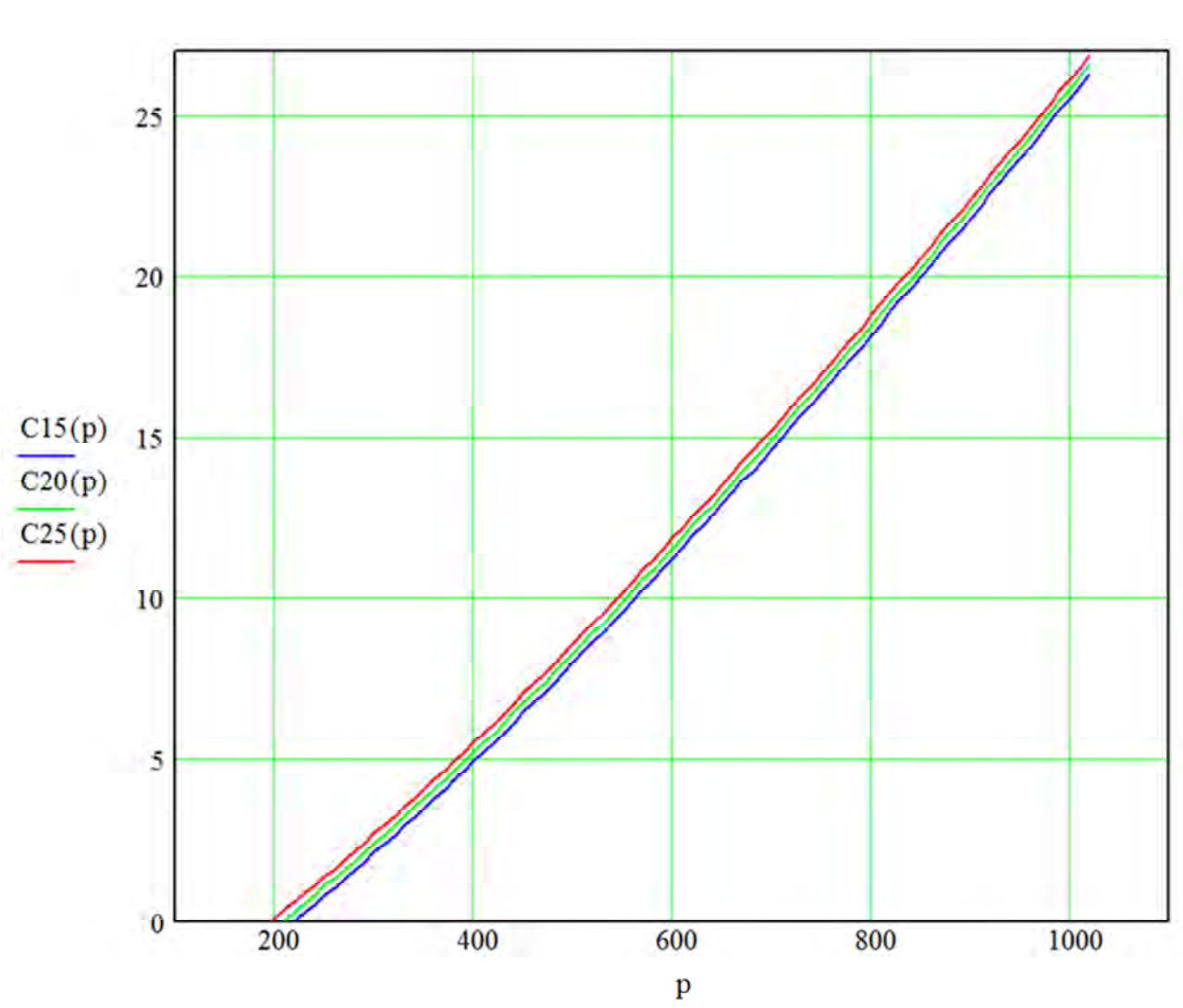

Fig. 4.14 The calibration curves of aqueous NaCl solution (refractometer version A)

4.4.2.3. The calibration process of the refractometer using aqueous sucrose solution

Table 4.3.

Measured p_s values arranged by ascending percentages of the reference sample concentration $c_{\%R}$ and by measured sample temperatures t_f

Sucrose concentration, $c_{\%R}$	Temperature, t_f	p_s
0 %	15°C	220
	20°C	208
	25°C	196
2.5 %	15°C	297
	20°C	286
	25°C	275
5 %	15°C	372
	20°C	361
	25°C	351
10 %	15°C	514
	20°C	504
	25°C	495
15 %	15°C	648
	20°C	640
	25°C	631
20 %	15°C	779
	20°C	770
	25°C	762
25 %	15°C	907
	20°C	899
	25°C	891

$$C_{\%15} = -6.34714 + 0.02617 \cdot p + 1.33357 \cdot 10^{-5} \cdot p^2 - 4.50353 \cdot 10^{-9} \cdot p^3 \quad (t=15°C), \quad (4.11)$$

$$C_{\%20} = -5.99368 + 0.02638 \cdot p + 1.27179 \cdot 10^{-5} \cdot p^2 - 4.11688 \cdot 10^{-9} \cdot p^3 \quad (t=20°C), \quad (4.12)$$

$$C_{\%25} = -5.54441 + 0.02585 \cdot p + 1.34929 \cdot 10^{-5} \cdot p^2 - 4.51737 \cdot 10^{-9} \cdot p^3 \quad (t=25°C), \quad (4.13)$$

The squared correlation coefficient of curves in corresponding to Eq.(4.11), (4.12), (4.13) is $R^2=1$, $R^2=1$, $R^2=1$ accordingly.

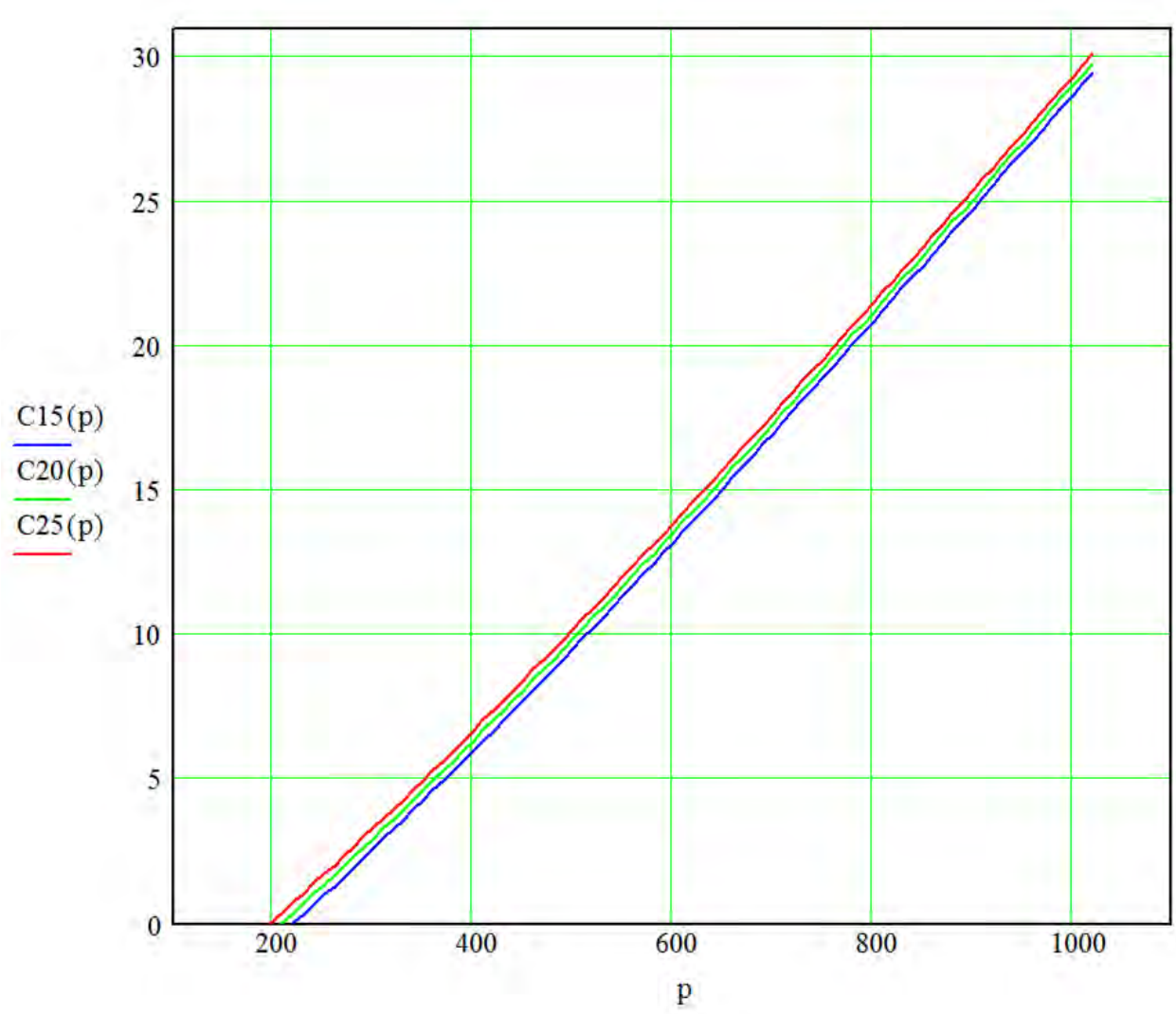

Fig. 4.15. The calibration curves of $C_{12}H_{22}O_{11}$ aqueous solution (refractometer version A)

4.4.2.4. The RI resolution check-up process of the refractometer version A

The change of the RI of distilled water for two different temperatures was determined in order to test the resolution and sensitivity of the measuring system. The measurements were calibrated based on standard data at a laser wavelength of 635 nm. Temperature of the liquid used for calibration at the moment of the measurement was fixed at a certain value with precision ±0.02°C. It was achieved by including the cell in a water bath circulator circuit, where the temperature of the flowing liquid was automatically controlled based on readings from a thermal sensor of the cell. RI values obtained from the test measurements corresponded to the standard refraction units.

Accordingly, at t_1=15C, n_3=1.33247, and at t_2=25C, n_3=1.33113 [47, 71]. Measurements show that the first minimum of the optical intensity distribution changes its position from pixel p_1 =220 at t_1=+15°C to pixel p_3=196 at t_2=+25°C (Table 4.1). In accordance with the given parameters of the optical system, the resolution of the measuring device:

$$\delta=\delta n/\delta p, \tag{4.7}$$

where $\delta n=|n_1-n_2|$is the difference in refractive indices, $\delta p=|p_1-p_2|$the difference in detected positions,

$$\delta=\frac{1.33247-1.33113}{220-196}=5.583333\cdot10^{-5}\approx5.6\cdot10^{-5}$$

Total resolution of the measurements $c_{\%R}$ from 0 to 70% weight / vol we can also define from the Table 4.1.

When we have $c_{\%R}$=0% weight/vol at t_1=+20°C, n_3=1.3318, and $c_{\%R}$=70% weight/vol at t_1=+20°C n_3 =1.364159 [47, 71]. Measurements show that the first minimum of the optical intensity distribution changes its position from pixel p_1 =220 to pixel p_{32}=789 at t_2=+20°C (Table 4.1). In accordance with the given parameters of the optical system, the resolution of the measuring device:

$$\delta=\frac{1.364-1.3318}{789-208}=5.542169\cdot10^{-5}\approx5.5\cdot10^{-5}$$

The resolution of the measurements of the data is about δ=5.6·10^{-5} measurable RI per pixel.

Resolution of the ethanol concentration per pixel is calculated from Table 4.1 as follows:

$$\delta=\frac{70\%}{789-208}=0{,}120\,\%\text{ alc/weight}$$

Resolution of the NaCl concentration per pixel is calculated from Table 4.2 as follows:

$$\delta=\frac{25\%}{978-208}=0{,}032467\approx0.032\,\%\text{ alc/weight}$$

Resolution of the sucrose concentration per pixel is calculated from Table 4.3 as follows:

$$\delta=\frac{25\%}{899-208}=0{,}03618\approx0.036\,\%\text{ alc/weight}$$

4.4.3. More accurate refractometers with a small RI measuring range

The refractometers are mathematically modeled in section 3.4.3. version B.

4.4.3.1. The calibration process of the refractometer using ethanol aqueous solution

Table 4.4.

Measured p_s values according to the reference sample concentration $c_{\%R}$ and the measured sample temperatures t_f, by using refractometer B

Ethanol concentration, $c_{\%R}$	Temperature, t_f	p_s
0 %	15°C	230
	20°C	197
	25°C	164
5 %	15°C	397
	20°C	368
	25°C	339
10 %	15°C	578
	20°C	552
	25°C	526
15 %	15°C	747
	20°C	724
	25°C	701
20 %	15°C	895
	20°C	874
	25°C	854

$$C_{\%15} = -8.44003 + 0.04251 \cdot p - 2.97694 \cdot 10^{-5} \cdot p^2 + 1.98727 \cdot 10^{-8} \cdot p^3 \quad (t=15°C), \quad (4.14)$$

$$C_{\%20} = -6.87204 + 0.03931 \cdot p - 2.60827 \cdot 10^{-5} \cdot p^2 + 1.86354 \cdot 10^{-8} \cdot p^3 \quad (t=20°C), \quad (4.15)$$

$$C_{\%25} = -5.4247 + 0.03624 \cdot p - 2.19761 \cdot 10^{-5} \cdot p^2 + 1.68678 \cdot 10^{-8} \cdot p^3 \quad (t=25°C), \quad (4.16)$$

The squared correlation coefficient of curves in corresponding to Eq.(4.14), (4.15), (4.16) is $R^2=1$, $R^2=1$, $R^2=0.99995$ accordingly. See Fig.4.16.

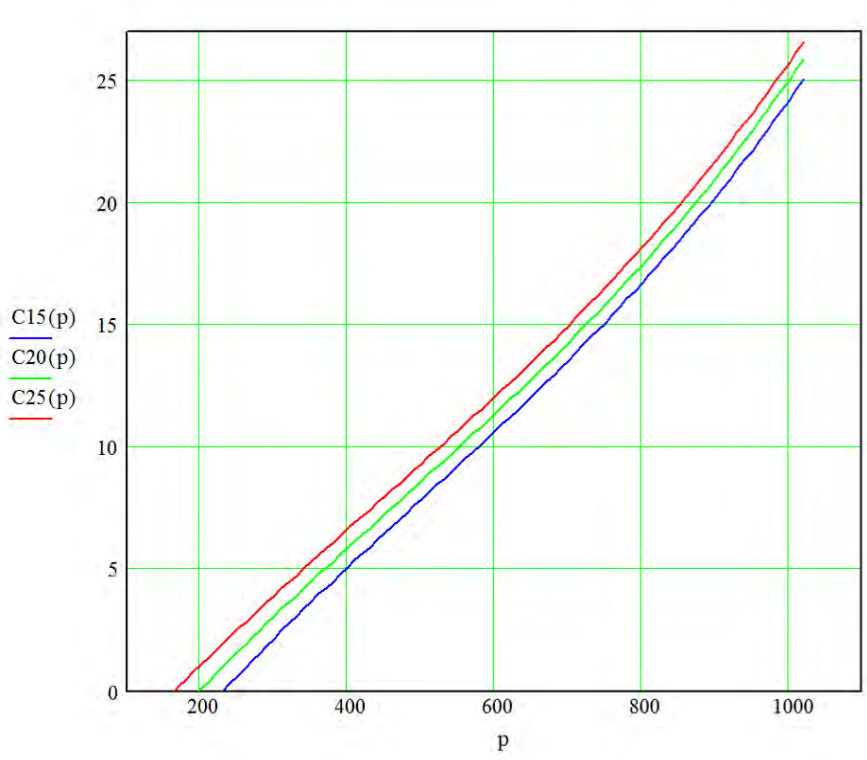

Fig. 4.16. The calibration curves of ethanol aqueous solution (refractometer version B)

4.4.3.2. The calibration process of the refractometer using aqueous NaCl solution

Table 4.5.

Measured p_s values arranged by ascending percentages of the reference sample concentration $c_{\%R}$ and by measured sample temperatures t_f

NaCl concentration, $c_{\%R}$	Temperature, t_f	p_s
0 %	15°C	230
	20°C	197
	25°C	164
2.5 %	15°C	475
	20°C	448
	25°C	420
5 %	15°C	684
	20°C	661
	25°C	636
7.5 %	15°C	865
	20°C	845
	25°C	824
9 %	15°C	963
	20°C	944
	25°C	924

$$C_{\%15} = -2.02338 + 0.00826 \cdot p + 2.01372 \cdot 10^{-6} \cdot p^2 + 1.34207 \cdot 10^{-9} \cdot p^3 \quad (t=15°C), \quad (4.17)$$

$$C_{\%20} = -1.70886 + 0.00823 \cdot p + 1.97187 \cdot 10^{-6} \cdot p^2 + 1.404 \cdot 10^{-9} \cdot p^3 \quad (t=20°C), \quad (4.18)$$

$$C_{\%25} = -1.40878 + 0.00821 \cdot p + 2.06495 \cdot 10^{-6} \cdot p^2 + 1.33701 \cdot 10^{-9} \cdot p^3 \quad (t=25°C), \quad (4.19)$$

The squared correlation coefficient of curves in corresponding to Eq.(4.17), (4.18), (4.19) is $R^2=1$, $R^2=1$, $R^2=1$ accordingly. Fig.4.17

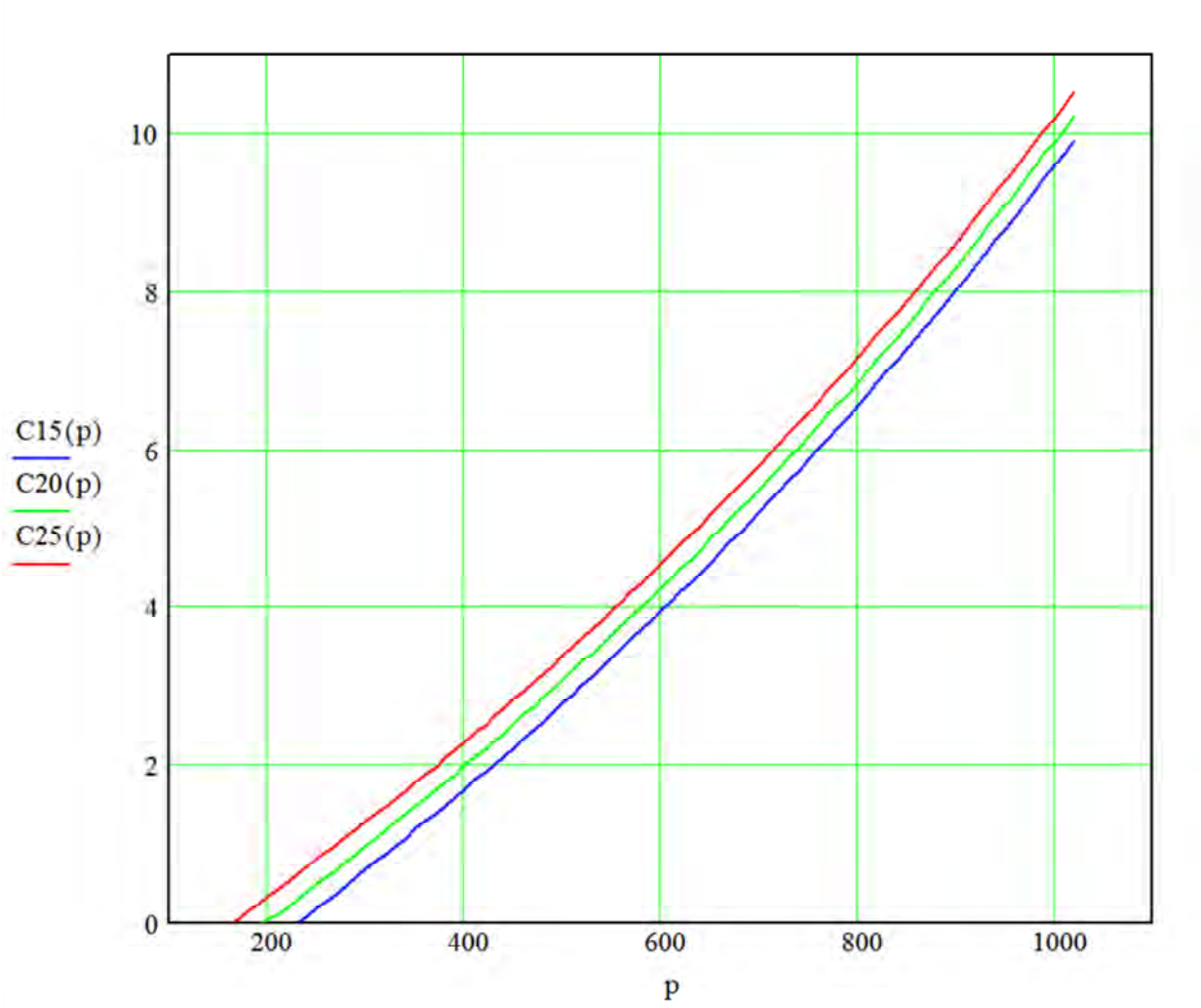

Fig. 4.17. The calibration curves of aqueous NaCl solution (refractometer version B)

4.4.3.3. The calibration process of the refractometer using aqueous sucrose solution

Table 4.6.

Measured p_s values arranged by ascending percentages of the reference sample concentration $c_{\%R}$ and by measured sample temperatures t_f

Sucrose concentration, $c_{\%R}$	Temperature, t_f	p_s
0 %	15°C	230
	20°C	197
	25°C	164
2.5 %	15°C	434
	20°C	406
	25°C	377
5 %	15°C	616
	20°C	592
	25°C	566
7.5 %	15°C	781
	20°C	758
	25°C	736
10 %	15°C	929
	20°C	910
	25°C	890

$$C_{\%15} = -2.02338 + 0.00826 \cdot p + 2.01372 \cdot 10^{-6} \cdot p^2 + 1.34207 \cdot 10^{-9} \cdot p^3 \quad (t=15°C), \quad (4.20)$$

$$C_{\%20} = -1.70886 + 0.00823 \cdot p + 1.97187 \cdot 10^{-6} \cdot p^2 + 1.404 \cdot 10^{-9} \cdot p^3 \quad (t=20°C), \quad (4.21)$$

$$C_{\%25} = -1.40878 + 0.00821 \cdot p + 2.06495 \cdot 10^{-6} \cdot p^2 + 1.33701 \cdot 10^{-9} \cdot p^3 \quad (t=25°C), \quad (4.22)$$

The squared correlation coefficient of curves in corresponding to Eq.(4.20), (4.21), (4.22) is $R^2=1$, $R^2=1$, $R^2=1$ accordingly. See Fig.4.18.

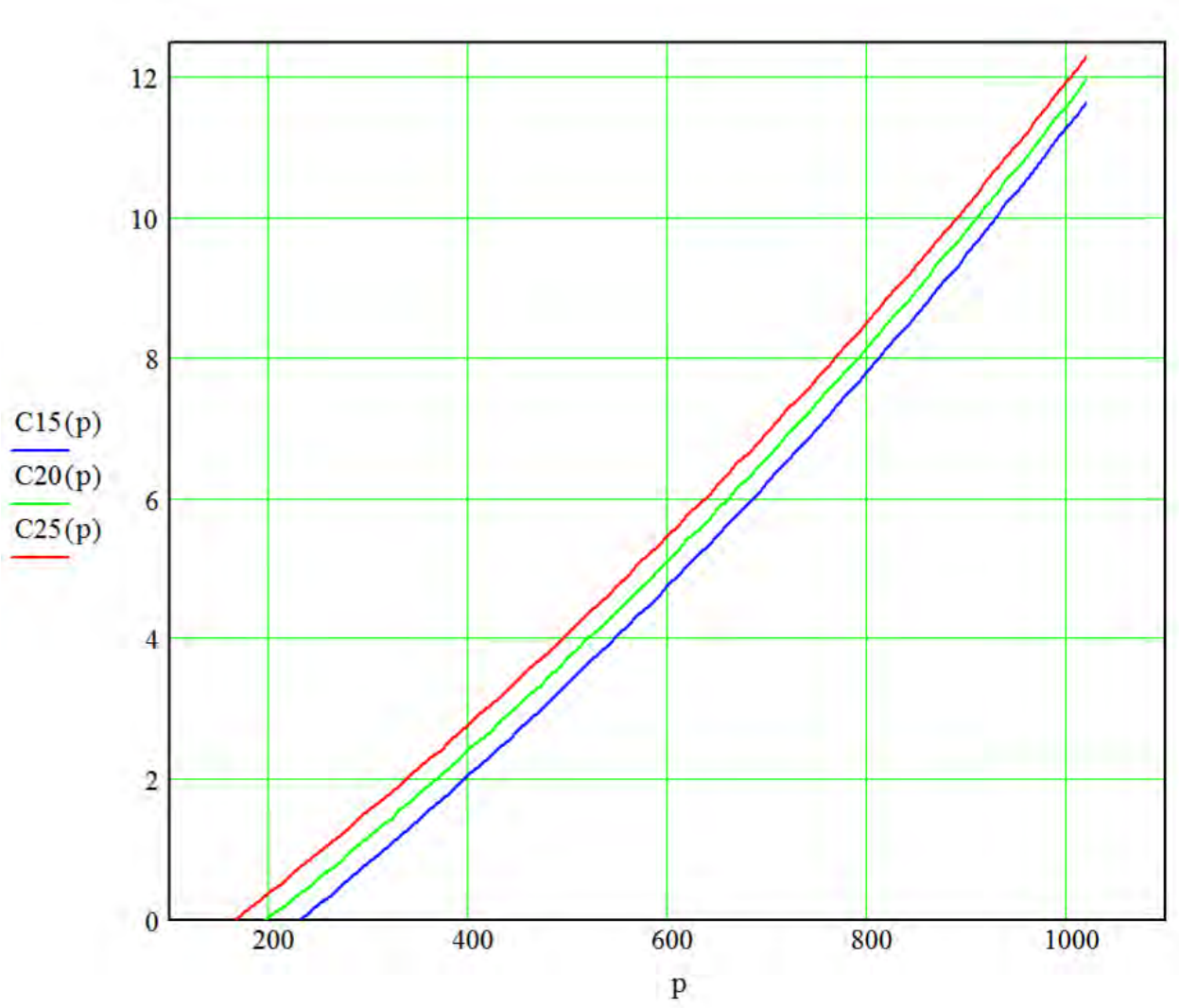

Fig. 4.18. The calibration curves of $C_{12}H_{22}O_{11}$ aqueous solution (refractometer version B)

4.4.3.4. The RI resolution check-up process of the refractometer version B

Accordingly, at t_1=15C, n_3=1.33247, and at t_2=25C, n_3=1.33113 [47, 71]. Measurements show that the first minimum of the optical intensity distribution changes its position from pixel p_1 =230 at t_1=+15°C to pixel p_3=164 at t_2=+25°C (Table 4.4). In accordance with the given parameters of the optical system, the resolution of the measuring device:

$$\delta = \frac{1.33247 - 1.33113}{230 - 164} = 2.0303 \cdot 10^{-5} \approx 2 \cdot 10^{-2} \qquad (4.24)$$

Total resolution of the measurements $c_{\%R}$ from 0 to 20% weight/vol we can define from the Table4.4.

When we have $c_{\%R}$=0% weight/vol at t_1=+20°C, n_3=1.3318, and $c_{\%R}$=20% weight/vol at t_1=+20°C n_3 =1.3457 [47, 71]. Measurements show that the first minimum of the optical intensity distribution changes its position from pixel p_1 =220 to pixel p_{32}=789 at t_2=+20°C. (Table 4.4). In accordance with the given parameters of the optical system, the resolution of the measuring device:

$$\delta=\frac{1.3457-1.3318}{874-197}=2.05318^{-5}\approx 2\cdot 10^{-5} \tag{4.25}$$

The resolution of the measurements of the data is about δ=2·10^{-5} measurable RI per pixel.

Resolution of the ethanol concentration per pixel is calculated from Table 4.4 as follows:

$$\delta=\frac{20\%}{874-197}=0.02954\approx 0.03\,\%\ \text{alc/weight}$$

Resolution of the NaCl concentration per pixel is calculated from Table 4.5 as follows:

$$\delta=\frac{9\%}{944-197}=0.012048\approx 0.012\,\%\ \text{alc/weight}$$

Resolution of the sucrose concentration per pixel is calculated from Table 4.6 as follows:

$$\delta=\frac{10\%}{910-197}=0.014025\approx 0.014\,\%\ \text{alc/weight}$$

4.4.4 Stability of the position of the first minimum for the waveform light intensity distribution over the image sensor

To prove the high stability of the reference points reading of the first minimum of the light intensity (falling on the linear optical element) distribution as compared with the conventional method of reading at a leading edge, an experiment was made.

To prove the high stability of the reference points reading of the first minimum of the light intensity (falling on the linear optical element) distribution as compared to the conventional method of reading at a leading edge, an experiment was made. Change of flatness (decrease of slope peaks) is shown in the graph of the distribution of light falling on the linear optical element. It is not necessary to change the composition and temperature of the test liquid, varied by changing the light intensity of the laser beam.

The slope of the graph of the light distribution becomes similar to the one observed in the liquid when the big light distribution caused by multiple alternating passage of the laser beam

through the cell wall and the test liquid, due to the appearance of colloidal particles and air bubbles.

The intensity of light can also be changed due to the instability of the luminous flux of the laser (because of its warm-up).

In order to test the precision and stability of the measuring system, two images were detected on the linear measuring sensor at two different light intensities of the beam exiting the cylindrical cell. Distilled water in the cylindrical cell was maintained at a temperature of +20.00ºC $\pm$ 0.02ºC.

The refractometer option with a small RI measuring range has been used (see Table 3.1., version B, Fig.4.3).

The images shown in Fig. 3.17(*a*) at the nominal light intensity I_1 of the exiting beam (in relative units), while demonstrates the distribution of the optical intensity of the incident beam over the area of the linear image sensor.

The position of the image is detected using the position of the first minimum of the waveform light intensity distribution over the image sensor, which in this case corresponds to the pixel number 197 marked by the solid vertical line shown in Fig. 3.17(*a*). The dashed line marks position 125 residing on the steepest part of the light intensity distribution at the boundary between illuminated and dark transition regions, and corresponds to another method of image detection [31, 75].

Fig. 3.17(*b*) illustrates the case when the laser intensity was increased 2.5 times and shows the light intensity distribution over the linear sensor. It follows from Fig. 3.17(*a*) and (*b*) that such a change of measuring conditions has no effect on the image position marked by the pixel number 197. The conventional method of image detection [31, 75] under the same conditions leads to the image position shift by 125-111=14 pixels. Considering the resolution of the device mentioned above and used in the measurement $\delta \approx 2 \cdot 10^{-5}$ experimentally determined with no mathematical processing and averaging (see Eq.(4.24), (4.25)), a deviation of $\delta \times 14$ pixels leads to a measurement error of $2.8 \cdot 10^{-4}$ measurable RI.

Results of the experimental tests lead to the conclusion that the developed measuring device and the applied detection method of the image position ensure an accurate detection of the image position, and therefore also high resolution and stability of RI measurements. Furthermore, the developed approach is practically unaffected by either varying intensity or instability of the light source, or by inclusions of air or other admixtures in the liquid being examined.

4.5. Conclusion

In the chapter 4 are described the experimental data from studies of a new refractometer with a new physical principle of RI measurement. Measurements were carried out based on a new methodology for determining the reference point in the distribution of the light intensity, readable on the linear optical elements.

The chapter 4 describes the process of the technological measuring stand to study a new refractometer.

The following new refractometers were modeled:

- the simplest, inaccurate refractometer to demonstrate a new physical principle of refractometry;
- the refractometer with a large RI measuring range ($\delta = 5 \cdot 10^{-5}$) version A and with a small RI measuring range ($\delta = 2 \cdot 10^{-5}$) version B:

Table 4.7.

Initially stated and expected parameters of the refractometers

Parameters	Refractometer A	Refractometer B
RI	1.33167..1.36454	1.33167..1.34583
Ethanol, $\delta_{simulation}$, RI	5.7×10^{-5}	2×10^{-5}
Ethanol, δ_{real}, RI	5.6×10^{-5}	2×10^{-5}
Ethanol, % weight/vol	0-70	0-20
$\delta_{ethanol}$, % weight/vol.	0.12	0.03
NaCl, % weight/vol	0-25	0-9
δ_{NaCl},% weight/vol	0.032	0.012
Sucrose, % weight/vol	0-25	0-10
$\delta_{sucrose}$,% weight/vol	0.036	0.014

All refractometers have been tested in order to verify the correctness of the newly developed mathematical formulas (see chapter 3).

The tests showed the faithfulness of the all newly derived mathematical formulas for the mathematical simulation.

RESUME

1. The basic operating principles for CCR were developed, where an optical beam refraction and multiple reflections in a cylindrical cell are used; thereby increasing the RI measurement resolution by one power and achieving MR = 10^{-5}.

2. The mathematical model has been developed and analyzed, which takes into account the temperature effect on the detection of resolution, the possibility to achieve the resolution up to 10^{-7} has been demonstrated. It has been shown; that the multiple light beam passage through cylindrical cell with test liquid increases the RI measurement resolution in line with the number of the passage cycles.

3. The RI measurement algorithm and measurement method have been developed, where a minimum place of the detectable beam interference pattern has been used, that allows to achieve the RI measurement resolution $2 \cdot 10^{-5}$. The calibration and verification of CCR prototypes for ethanol, NaCl and sucrose aqueous solutions have been provided. The RI measurements (with the resolution of $2 \cdot 10^{-5}$) for all the above mentioned solutions have been achieved. The applicability of CCR to identify concentrations of ethanol, NaCl and sucrose were tested. The corresponding resolutions of the following weight/vol. were achieved: 0.03%; 0.012%; 0.014%.

4. CCR prototypes have been designed and developed (including optical, electronic, computing and mechanical systems) to verify practical applications-possibilities of the refractometers.

5. CCR were implemented for practical use at 8 research and industrial institutions (3 in Latvia, 2 in Germany, 3 in USA).

ACKNOWLEDGEMENT

The present research was supported in the framework of:

- ESF project Nr. 2009/0144/1DP/1.1.2.1.2/09/IPIA/VIAA/005.
- ERAF project "Innovative bio-ethanol dehydration technology and design parameters of the measuring device" 2010/0281/2DP/2.1.1.1.0/10/APIA/VIAA/003.
- Project "Methanol fuel cell sensor adaptation and other control and measurement systems" TOP 06-14.

I am very grateful to Prof. Yuri Dekhtyar and Prof. Peteris Shipkovs, who helped me to complete this work.

Especially I would like to say thanks to Dr. habil. phys. Mr. Oskars Vilitis, who is my friend and teacher and a scientific companion in many research projects and publications, and who provided a lot of valuable comments during the writing process of this dissertation.

I would like to thank my wife Vita for her help with my scientific tests and data collection.

I am very grateful to the Biomedical Engineering and Nanotechnology Institute research team for their help and valuable advices during my studies and during the preparation and writing of this work.

I very much would like to say thanks to Mr. V.Kozlovs who at the very beginning stage of this work introduced me in this field of science and putted in touch with great specialists, and together with these people it was possible for me to continue my research.

I would like to thank Mr. Ivan Mironov, president of ELMI Ltd, for his great support during of long years in my research work.

REFERENCES

1. *Abbe refractometer DR-A1. User Manual.*
2. *Aminabhavi T.M.: Use of mixing rules in the analysis of data for binary liquid mixtures. J. Chem. Eng. 1984, - 29, -pp.54–55.*
3. *Angelis M., Nicola S., Ferraro P., Finizio A., Pierattini G. Liquid refractometer based on interferometric fringe projection. Opt Comm 2000, -175, -pp.315–321.*
4. *AR200 Automatic Digital Refractometer. User Manual.*
5. *Barer R., Ross K.F.A., Tkaczyk S. Refractometry of living cells // Nature. - 1953. - Vol. 171. – 4356. - p. 720-724.*
6. *Bashkatov A. N. and E. A. Genina E. A. Water refractive index in dependence on temperature and wavelength: a simple approximation, Proc. SPIE, 2003, -vol.5068, -pp.393–395.*
7. *Bergman T. L., Munoz D. R., Incropera F. P., Viskanta R., Measurement of Salinity Distributions in Salt-Stratified, Double-Diffusive Systems by Optical Deflectometry, Rev. Sci Instrum., 1986, -vol.57 -pp.2538-2542.*
8. *Bergman T.L., Incropera F.P., Stevenson W. H., Miniature Fiber-Optic Refractometer for Measurement of Salinity in Double-Diffusive Thermohaline Systems, Rev. Sci. Instrum., 1985, -vol.56, -pp.291- 296.*
9. *Bornhop D.J., Dovichi N.J. (1986) Anal. Chem., 1986, -58 -pp.504–505.*
10. *Caesar Saloma and Jesus Muñoz, "Refractive-index measurement at high spatial resolution by source doubling," Opt. Lett., 1994, -19, -pp.1088-1090.*
11. *Chiu M.-H., Lee J.-Y., Su D.-C. Refractive-index measurement based onthe effects of total internal reflection and the uses of heterodyne interferometry //Appl. Opt.- 1997. -36. -p.2936-2939.*
12. *Ciddor P.E., Refractive index of air: new equations for the visible and near infrared, Appl.Opt., 1996, -35, -pp.1566–1573.*
13. *CMOS linear image sensor S9226. Hamamatsu User Manual.*
14. *Colin E. Webb, Julian D. C. Jones, Handbook of Laser Technology and Applications, Taylor & Francis. 2004,- pp.1738–1740.*
15. *Djurisic A. and Stanic B. Modeling the temperature dependence of the index of refraction of liquid water in the visible and the near-ultraviolet ranges by a genetic algorithm, Appl. Opt.,1999, -38(1), -pp11–17.*
16. *Dobbins H.M. and Peck E.R. Change of refractive index of water as a function of temperature, J. Opt. Soc. Soc. Am., 1973,- 63(3), -pp.318–320.*
17. *Durán-Ramírez V.M., Martínez-Ríos A., Muñoz-Maciel J. Peña-Lecona F.G., Casillas-Rodríguez F.J., Selvas-Aguilar R., Mora-González M. Method for measuring the refractive index of liquids using a cylindrical cell, Optical Engineering, 2013, -52(7), -art. no. 074101.*
18. *Gillen G.D., Guha S., Use of Michelson and Fabry-Perot interferometry for independent determination of the refractive index and physical thickness of wafers, Appl. Opt. 2005, -44, -pp. 344–347.*
19. *Gladstone J.H., Dale J.: On the influence of temperature on the refraction of light. Philos. Trans. R. Soc. London, 1858, -148, -pp.887–902.*
20. *Goldberg H.E. Refractometer // US Patent Nr. US 3,625,620.,-1970.*
21. *Grange B.W., Stevenson W.H, Viskanta R. Refractive index of liquid solutions at low temperatures: an accurate measurement. Appl Opt., 1976, -15, -pp.858–859.*
22. *Harvey A. H., Gallagher J. S. and Levelt Sengers J. M. H. Revised formulation for the refractive index of water and steam as a function of wavelength, temperature and density // J. Phys. Chem. Ref. -1998, - 27, -p.773.*

23. *Hattori H. et al., Liquid refractometry by the rainbow method, Appl. Opt., 1998, -37(19), -pp.4123–4129.*
24. *Hattori H. et al., Using minimum deviation of a secondary rainbow and its application to water analysis in a high-precision, refractive-index comparator for liquids," Appl. Opt., 1997, - 36(22), -pp.5552–5556.*
25. *Heller W.: The determination of refractive indices of colloidal particles by means of a new mixture rule or from measurements of light scattering. Phys. Rev., 1945, -68, -pp.5–10.*
26. *Herraez J.V., Belda R. Refractive Indices, Densities and Excess Molar Volumes of Monoalcohols + Water, J. Solution Chem, 2006, -35, -pp.1315–1328.*
27. *Herraez J.V., Belda R.: Viscous synergy of pure mixtures in water and its relation to concentration. J. Solution Chem., 2004., -33, -pp.117–129.*
28. *Huang P. S, Ni J, Angle measurement based on the internal-reflection effect and the use ofright-angle prisms // Appl, Opt, 1995, - 34, - pp. 4976-4981.*
29. *Huang P. S., Kiyono S., Kamada 0. Angle measurement based on the internal-reflection effect: a new method // Appl, Opt, 1992, -31.- pp.6047-6055.*
30. *Ikeda K. Ultrasonic Measurement of Concentration in Solutions by a Phase-Locked*
31. *Instruction Manual for In-line Refractometer PR-03, -2000, -p.123*
32. *Jarvis P. R., Meeten G. H. Critical-angle measurement of refractive index of absorbing materials: an experimental study //J. Phys. -1986. -19. - p. 296-298.*
33. *Jenkins DD. Refractive indices of solutions. PhysEduc, 1982, -17, -pp.82–83.*
34. *Jensen William B. (University of Cincinnati. Oesper Collections in the History of Chemistry; University of Cincinnati, 2014.*
35. *Jose V. Herr´aez · R. Belda Refractive Indices, Densities and Excess Molar Volumes of Monoalcohols + Water J. Solution Chem., 2006 -35, -pp.1315–1328.*
36. *Kahre J.,* Method for refractometer measuring using mathematical modelling //*US Patents: No 5.617.201.*
37. *Kahre J., Prismatic device for use with process refractometers// US Patents: No 5, 309.288.*
38. *Kamrat E., Measuring window for a process refractometer // US Patents: No 4,571,075.*
39. *Konishi T., Naka S., Ito A., Saito K., Transient two-dimensional fuel-concentration measurement technique, Appl. Opt., 1997, -36, -pp.8815-8819.*
40. *Kozlov V., Merkulov D., Vilitis O., New method for measuring refractive index of liquids Proc. SPIE 4318, Smart Optical Inorganic Structures and Devices, 89 (March 8, 2001), -pp.89-92.*
41. *K-PATENTS, Refractometer PR-03, brochure.*
42. *Krishna V., Fan C. H. and Longtin J. P. Real-time precision concentration measurement for flowing liquid solutions // Rev.Sci. Instrum. -2000, http://dx.doi.org/10.1063/1.1288236.*
43. *Kumar V.N., Rao D.N. Using interference in frequency domain for precise determination of thicnkness and refractive indices of dispersive materials. Opt Soc Am 1995, -12, -pp.1559–1563.*
44. *Laser Components. AlGaInP Visible Laser Diode ADL-63054TL. Datasheet.*
45. *Lawall J., Interferometry for Accurate Displacement Metrology, Opt. Photon. News 2004, -15, -pp.40-45.*
46. *Leung A.F., J. J. Vandiver J.J., Automatic refractometer, Opt. Eng., 2003, -42(4), -pp. 1128-1131.*
47. *Lide R., (ed.) CRC Handbook of Chemistry and Physics // Internet Version 2005, <http://www.hbcpnetbase.com>, CRC Press, Boca Raton, FL, 2005.*

48. *Logofatu P. C., Apostol D., Damian V. Optimum angles for determining the optical constants from reflectivity measurements, Meas. Sci. Technol. 1996. - 7, - p.52-71.*
49. *Longtin J. P. and Fan C. H. Precision laser-based concentration and refractive index measurement of liquids// Microscale Thermophys. Eng. -1998, -pp.261–272.*
50. *Loop Method, Jap. J. Appl. Phys., 1997, -vol. 36, -pp.3180-3183.*
51. *Luneburg R.K., Mathematical Theory of Optics., Bercley: Univ. Of California Press, 1964. -456 p.*
52. *Mahmood bin Mat Yunus W., Bin Abdul Rahman A. Refractive index of solutions at high concentrations. Appl Opt. 1988, -27, -pp.3341–3343.*
53. *Mark II Abbe (Misco) or TMR 33-36 High Accuracy Refractometer, Index Instruments // Meas. Sci. Technol. 1996. - 6. - pp.328-354.*
54. *Meeten G.H., Refractive index errors in the critical-angle and Brewster-angle methods applied to absorbing and heterogeneous of biotissue by total internal reflection, Appl. Opt. 1996. - 35, - p.1793-1795.*
55. *Meeten G.H., North A.N., Refractive index measurement of turbid colloidal fluids by transmission near the critical angle, Meas. Sci. Technol., 1991, -2, -pp.441–447.*
56. *Meeten G.H., North A.N., Refractive index measurement of absorbing and turbid fluids by reflection near the critical angle, Meas. Sci. Technol., 1996, - 6, - pp.214-221.*
57. *Moiseeva N. P. 2001 Methods of constructing an individual calibration characteristic for working platinum resistance thermometers Meas. Tech., -2001, -vol. 44, -pp.502–505.*
58. *Moreels E., De Greef C., Finsy R. Laser light refractometer. Appl Opt., 1984, -23, -pp.3010–3013.*
59. *Mussil V. et al., A proximate method for determining the refractive indices of liquids, Instrum. Exp. Tech., 2011, -54(3), -pp.397–399.*
60. *Naoki Sadayori and Yuji Hotta Polycarbodiimide having high index of refraction and production method thereof // US patent № 0158021 A1 (2004).*
61. *Narayanan V. A., Narayanan R. Laser-based liquid prism sucrosemeter - a precision optical method to find sugar concentration. // J. Chem. Educ., 1997, -74 (2), -p.221.*
62. *Nemoto S. Measurement of the refractive index of liquid using laser beam displacement, Appl. Opt., 1992, -31(31), -pp.6690–6694.*
63. *Noll E. D. Measuring the index of refraction of liquids with a laser, Phys. Teach., 1973, -11(5), -pp.307-308.*
64. *Ovchinnikov Y.B., Pfau T. Revivals and oscillations of the Momentum of light in a planar multimode Waveguide, Physical Review Letters, 2001, -87, -No12, -pp.12390-1 – 123901-4.*
65. *Plucinski J., High resolution optical refractometer for dispersion measurement in UV-NIR range, Eur. Phys. J. Special Topics.- 2008, - 154, -p.159-163.*
66. *Precision thermometer F100-A-2. AUTOMATIC SYSTEMS LABORATORIES User Manual.*
67. *Preston-Thomas H., The International Temperature Scale of 1990 (ITS-90), Metrologia, 1990, - 7, - p 107.*
68. *Process refractometer for concentration measurement PR-03-M; K-Patents, INC; 6 p.*
69. *Psaltis D., Quake S.R. and Yang C. Developing optofluidic technology through the fusion of microfluidics and optics, Nature (London), 2006, - 200442, -pp.381–386.*
70. *Rashed Roshdi, A pioneer in anaclastics: Ibn Sahl on burning mirrors and lenses, 1990, -81(3), -pp.464–491.*
71. *Refractive index database. Optical constants of 1000+ materials./Internets.- http://www.refractiveindex.info/*
72. *Refractometer Models by Rudolph Research Analytical./Internets.- http://www.rudolphresearch.com/*

73. *Refractometer – Model J457. User Manual.*
74. *Rheims J., Koser J., Wriedt T., Refractive index measurements in the near-IR using an Abbe refractometer ., Meas. Sci. Tech. -1997. -8. -p.601-605.*
75. *Salo H. Refractometer // US Patent No 6,067,151., -2000.*
76. *Samedov F. Laser-based optical facility for determination of refractive index of liquids // Optics and Laser Technology., -2006,- 38, - pp.28–36.*
77. *Samsung 13 MP CMOS Image Sensor S5K3L2, 2012.*
78. *Sarov Y.E., Kostic I., Minov S., Mitkov S., Minchev G., Uher L., Automatic laser refractometer, Proc. SPIE 5226, Laser Physics and Applications, 194 (November 6, 2003), -pp.194-199.*
79. *Sella Andrea, Abbé's refractometer, Chemistry World, 2008, -p.67.*
80. *Sorensen H. S., Pranov H., Larsen N. B., Bornhop D. J. and Andersen P. E. 2003 Absolute refractive index determination by microinterferometric backscatter detection // Anal. Chem., -2003, -75(8), -pp.1946–1953.*
81. *Stone, J., Measurements of the Absorption of Light in Low-Loss Liquids,J. Opt. Soc. Am., 1972, -**62**, -pp.327–333.*
82. *Stone J.A., Decker J.E., Gill P., Juncar P., Lewis A., Rovera G.D., Viliesid M., Advice from the CCL on the use of unstabilized lasers as standards of wavelength: the helium-neon laser at 633 nm, Metrologia, 2009, -46(1), -pp.11–18.*
83. *Syngle J. L. Geometrical Optics. An Introduction to Hamilton's Method.- L.: Cambridge Univ. Press, 1954. -p.524.*
84. *Synovec R. E. Refractive index effects in cylindrical detector cell designs for microbore high-performance liquid chromatography// Anal. Chem.*-1987, *-59(24), -pp.2877–2884.*
85. *Synowicki R.A., Tiwald Thomas E., Method of determining bulk refractive indicies of fluids from thin films thereof // US Patent No 6,738,139., -2004.*
86. *Thermostat TW2. ELMI User Manual.*
87. *Tuchin V.V. Laser and fiber optics in biomedicine // Laser Physics. 1993. -Vol.3. -pp. 767-820.*
88. *Tuchin V.V. Lasers light scattering in biomedical diagnostics and therapy // J. Laser Appl. – 1993. - Vol. 5. - 2,3. - p.43-60.*
89. *Vilitis O., Merkulovs D., Optical cell for measuring refractive index and concentration of liquids, Latvian Journal of Physics and Technical Sciences, Riga, 2004, -4, -p.58–66.*
90. *Vilitis O., Merkulovs D., Refraktometra gaismas staru kūļa optiskā attēla detektēšanas paņēmiens, Patents LV13598, International Publication Date 20.09.2007.*
91. *Wilson T.A., Read W.F., Low Cost, Interferometric Differential Refractometer, Am. J. Phys. 1993, -vol.61,- pp.1046-1048.*
92. *Welford W.T. Optics, Oxford University Press, Oxford, UK, 1988.*
93. *Wolf K.B. (1995), Geometry and dynamics in refracting systems, European Journal of Physics., 1995., -16, -pp.14–20.*
94. *Барановский В.Ф., Горелкин С.М., Городенцева В.А. Физико -химические методы анализа: М.: Высшая школа, 1972.*
95. *Борен К., Хафмен Д. Поглощение и рассеяние света малыми частицами. М.: Мир, 1986. - 656 с.*
96. *Бретшнайдер С. Свойства газов и жидкостей. - М.: Химия, 1966. -536с.*
97. *Буланов В.М., Максимова И.Л., Татаринцев С.Н., Шубочкин Л.П. Спектральные характеристики дисперсных систем с учетом многократного рассеяния в приближении малых углов // Оптика и спектроскопия. 1993. - Т. 74. - 4. - с. 710-716.*
98. *Викторов М.М. Методы вычисления физико-химических величин и прикладные расчеты. - Л.: Химия, 1977. -360 с.*

99. *Горшков А.И., Ошуркова О.В., Константинов В.Б. Повышение чувствительности рефракционного метода регистрации на границе в капиллярных методах разделения // Журн. техн. физ. -2001, -71(5), -с.119–122.*
100. *Дрейпер Н., Смит Г. Прикладной регрессионный анализ. Множественная регрессия, М.: Диалектика, 2007. - с.912.*
101. *Ермакова С.М., Математическая теория планирования эксперимента, М.: Наука, 1983. - 392с.*
102. *Иоффе Б.В. Рефрактометрические методы химии. - Ленинград: Химия, 1983, - 352с.*
103. *Кассандрова О.Н., Лебедев В.В. Обработка результатов наблюдений. - М.: Наука, 1970. -104 с.*
104. *Ньютон И. - Оптика, Пер. акад. С.И. Вавилова, ГИЗ, Ленинград, 1927, -с.211-216.*
105. *Перепадов Е.А., Таблицы для определения содержания этилового спирта в водоспиртовых растворах. М.: Наука, 1979. -240 с.*
106. *Петровского Г.Т. (ред.) Бесцветное оптическое стекло СССР. Каталог. М.: Дом оптики, 1990. -131с.*
107. *Радченко Станислав Григорьевич, Методология регрессионного анализа, К.: Корнийчук, 2011. - с.376.*
108. *Рид Р., Праусниц Дж., Шервуд Т. Свойства газов и жидкостей. - Л: Химия, 1982. - 592с.*
109. *Сизиков В. С. Математические методы обработки результатов измерений: Учебник для вузов. СПб: Политехника, 2001. -2001с.*
110. *Таблицы физических величин. / Под ред. акад. И.К. Кикоина. - М.: Атомиздат, 1976. - 1008 с.*
111. *Тиходеев П.М. Световые измерения в светотехнике. - М.: Госэнергоиздат, 1962, - 464с.*
112. *Тихонов А.Н., Самарский А.А. Уравнения математической физики. - М.: Наука, 1977. - 736с.*
113. *Чернакал В. Л. Рефрактометр и рефрактометрические методы исследования в работах М.В. Ломоносова, Усп.физ.наук, 1950, т.42, с.41.*
114. *Чернов С.М., Жилик К.К., Рабзонов П.Г. Определение показателя преломления жидкостей и газов в капиллярах // Журн. приклад. спектр. -1982, -37, -455–459.*
115. *Шишловский А.А., Прикладная физическая оптика,. Физмат ГИЗ, 1970, -с.822.*
116. *Якушенков Ю.Г., Проектирование оптико-электронных приборов М.: Логос, 2000.*

APPENDIXES

Appendix 1.

Approbation statement for the project "Methanol fuel cell sensor adaptation and other control and measurement systems"

FIZIKĀLĀS ENERĢĒTIKAS INSTITŪTS
INSTITUTE of PHYSICAL ENERGETICS

Aizkraukles iela 21 * LV 1006 * Rīga * Latvija * Reģ. Nr. 90002128912
TĀLRUNIS: (+371) 67552011 * FAKSS: (+371) 67550839 * E-pasts: fei@edi.lv * http://www.innovation.lv/fei

Rīgas Tehniskās universitātes
promocijas padomei

Augstas precizitātes
cilindriskas šūnas refraktometra

APROBĀCIJAS AKTS

Dmitrijs Merkulovs ir piedalījies vairākos Fizikālās enerģētikas institūta pētnieciskajos projektos, kuru izstrādē tika izmantoti viņa pētījumi. D. Merkulovs piedalījās portatīva augstas precizitātes cilindriskas šūnas refraktometra ar mērīšanas izšķirtspēju 10^{-5} RI konstruēšanā un izstrādē, kas tika aprobēts degvielas elementu etanola un metanola koncentrāciju mērījumiem.

Šī konstrukcija ir Rīgas Tehniskās universitātes Biomedicīnas inženierzinātnes un Nanotehnoloģiju institūta doktoranta Dmitrija Merkulova promocijas darba rezultāts. Latvijā etanolu izmanto kā benzīna piedevu 5% līdz 10% apmērā no kopējā degvielas daudzuma. Refraktometrs tika kalibrēts no 0% līdz 40%, ar precizitāti 0,01%. Aprobētā ierīce praktiski pierādīja atzīstamas ekspluatācijas īpašības. Izstrādātās un izgatavotās mērierīces parametri nodrošina augstu mērīšanas precizitāti, un tā var tikt rekomendēta plaša mēroga pielietošanai.

D.Merkulova pētījumi atspoguļoti viņa promocijas darbā un sekmīgi tiek izmantoti Fizikālās enerģētikas institūta pētnieciskajos projektos.

Fizikālās enerģētikas institūta direktors
Akadēmiķis Juris Ekmanis

2014. gada 12.augustā

Appendix 2.

Approbation statement for the project "Innovative bio-ethanol dehydration technology and design parameters of the measuring device"

LATVIJAS LAUKSAIMNIECĪBAS UNIVERSITĀTES AĢENTŪRA
LAUKSAIMNIECĪBAS TEHNIKAS ZINĀTNISKAIS INSTITŪTS

Reģ. Nr. 90001836622, Institūta ielā 1, Ulbroka, Stopiņu novads, LV 2130, tālr. 67910879, fakss 67910873,
e-pasts uzc@apollo.lv, www.llu-ltzi.lv

19.08.2014 reģ. Nr. 01-30

AUGSTAS PRECIZITĀTES CILINDRISKAS ŠŪNAS REFRAKTOMETRA APROBĀCIJAS AKTS

Latvijas Lauksaimniecības universitātes aģentūras Lauksaimniecības tehnikas zinātniskajā institūtā etanola dehidratācijas procesa kontrolei tika aprobēts portatīvais augstas precizitātes cilindriskas šūnas refraktometrs ar mērījumu izšķirtspēju 10^{-5} RI.

Refraktometra konstrukcija tika izstrādāta Rīgas Tehniskās universitātes Biomedicīnas inženierzinātnes un Nanotehnoloģiju institūta doktoranta Dmitrija Merkulova promocijas darba ietvaros.

Aprobējamā ierīce (augstas precizitātes cilindriskas šūnas refraktometrs) tika izmantota etanola koncentrāciju mērījumiem no 85% līdz 99,98% ar precizitāti 0,02% etanola dehidratācijas procesa laikā.

Veiktās aprobācijas laikā, tika konstatēts, ka refraktometrs nodrošina ļoti stabilus un precīzus mērījumu rezultātus, kā arī teicamas ekspluatācijas īpašības (ekspluatācijas drošums un stabilitāte).

Vadošais pētnieks, Dr.sc.ing. Ādolfs Ruciņš

Direktors, Dr.sc.ing. Semjons Ivanovs

Appendix 3.

Approbation statement. ELMI Ltd (Riga, Latvia) has commenced the manufacturing process for commercial use and market research of refractometers.

elmi Ltd.
laboratory equipment

AUGSTAS PRECIZITĀTES CILINDRISKAS ŠŪNAS REFRAKTOMETRA
APROBĀCIJAS AKTS

SIA ELMI veica portatīvā augstas precizitātes cilindriskas šūnas refraktometra ar mērījumu izšķirtspēju 10^{-5} RI testēšanu un aprobāciju.

Refraktometra konstrukcija tika izstrādāta Rīgas Tehniskās universitātes Biomedicīnas inženierzinātnes un Nanotehnoloģiju institūta doktoranta Dmitrija Merkulova promocijas darba ietvaros.

Aprobējamā ierīce (augstas precizitātes cilindriskas šūnas refraktometrs) tika izmantota etanola koncentrāciju mērījumiem no 0 līdz 60 % un 85% līdz 99,98% ar precizitāti 0,02% etanola.

Veiktās aprobācijas laikā tika konstatēts, ka refraktometrs nodrošina ļoti stabilus un precīzus mērījumu rezultātus, kā arī ieicamas ekspluatācijas īpašības (ekspluatācijas drošums un stabilitāte).

Ar labiem panākumiem ierīce tika prezentēta izstādē BIOTECHNICA 2013 no 08.10.2013. – 10.10.2013., Vācijā, Hanoverā.

Ierīce rekomendēta sērijveida ražošanai.

Paraksts: Ivans Mironovs, prezidents, SIA ELMI 02.12.2014.

SABIEDRĪBA AR IEROBEŽOTU ATBILDĪBU SIA FIRMA ELMI

Registration address:	Office address:	Phones:	Fax:	Firm: ELMI
D.Brantkalna 3 – 38 Riga, LV-1082 Latvia	Warehouse: Aizkraukles 21-136, Riga, LV-1006, Latvia,	(+371) 29438725 67558743	(+371) 67551934	D.Brantkalna 3 – 38 Riga, LV-1082 Latvia VAT.. # LV 40003005832 AS Swedbank , SWIFT HABALV22, IBAN LV28HABA0551023604851

Corespondent Bank:
Deutsche Bank, Frankfurt
Swift code: DEUTDEFF

Appendix 4.

Approbation statement of the high precision cylindrical cell's refractometer for commercial use and market research from the company REVITEQ (USA)

REVITEQ scientific

5115 Douglas Fir St. Unit G,
Calabasas, CA 91302
877-847-8090 877-310-9156
info@reviteq.com

Reviteq LLC Tax ID# 45-2044601

APPROBATION STATEMENT OF THE HIGH PRECISION CYLINDRICAL CELL'S REFRACTOMETER

Reviteq Scientific LLC provided the testing and validation process of the Compact device of high sensitivity for measurement of the refractive indices for both stationary and flowing liquids - HIGH PRECISION CYLINDRICAL CELL'S REFRACTOMETER with the measurement accuracy of 10–5 RI.

The construction of the refractometer is designed at the Institute of Engineering Sciences and Nanotechnology at the Riga Technical University as a doctoral thesis of postdoctoral student Dmitrijs Merkulovs.

The tested device has been used for measuring the ethanol concentrations from 0 to 70% and from 85% to 99.98% with an accuracy of 0.02%, and measurement of NaCl concentration from 0 to 20% with an accuracy of 0.015%.

During testing process has been established that the refractometer provides a very stable and accurate measurements, and excellent operation properties (stability and safety of operation).

Portable high precision cylindrical cell's refractometer has been shown at the Pittsburgh Conference (Pittcon) in Chicago, IL, USA on March 2 2014 and at the American Association for Clinical Chemistry (AACC) in Chicago, IL, USA on July 27 2014, where a great interest aroused.

The device is recommended for production ASAP.

President
Alex Reviakin

11/20/2014

Appendix 5.

Seminar in RTU Biomedical Engineering and Nanotechnology Institute

RĪGAS TEHNISKĀ UNIVERSITĀTE

Biomedicīnas inženierzinātņu un nanotehnoloģiju institūts

Ezermala 6k, Rīga LV-1014, Latvija Tālr./fakss: 371-7089383, e-mail: bini@rtu.lv

I Z R A K S T S
no
BIOMEDICĪNAS INŠENIERZINĀTŅU UN NANOTEHNOLOĢIJU INSTITŪTA
2015. gada 22. janvāra zinātniskā semināra PROTOKOLA Nr. 3

Piedalījās:
BINI padomes locekļi:
G. Sagalovičs, J. Dehtjars, A. Balodis, A. Kataševs, V.Zemīte, V. Vendiņa, M. Romanova, I. Kozaks, M.Šneiders

Dienas kārtībā:

1. Par doktorantes D. Merkulova promocijas darba priekšaizstāvēšanu

Par promocijas darba : rezultātiem ziņoja doktorants D. Merkulovs **"CILINDRISKAS ŠŪNAS REFRAKTOMETRS UN TĀ PIELIETOŠANAS METODOLOĢIJA"**

2. Diskusija

Prof. A. Balodis norādīja uz to, ka jāizlabo dažas darbā nepamanītās kļūdas, ieteica iespējamo risinājumu.

Nolēma:
1. veikt darba papildinājumus un korekcijas;
2. rekomendēt virzīt darbu aizstāvēšanai RTU promocijas padomē **„RTU P-16"**, „Mēraparātu un metroloģijas apakšnozarē"

BINI zinātniskā semināra vadītājs A. Kataševs

Appendix 6.

Seminar in Latvian National Mechanics Committee (LNMK)

and RTU Institute of Mechanics (MI)

Latvijas Nacionālās Mehānikas Komitejas (LNMK)
un
RTU Mehānikas institūta (MI)
***semināra sēdes* (protokola Nr. 3. no 17.02.2015.)**
izraksts

Piedalījās:
prof. J. Vība, prof. . Pavelko, prof. V. Gonca, asoc.prof. V. Beresņēvičs, inž. V. Jakušēvičs, prof. S. Cifanskis, doc. J. Kalinka, prof. A. Krasņikovs, prof. M. Zakrževskis, prof. J. Auziņš, prof. A. Januševskis, doc. T. Novohatska.
Darba kārtība:

1. **Dmitrija Merkulova**, doktora studiju programmas "Inženiertehnika, mehānika un mašīnbūve (RMDM8)" **doktoranta promocijas darba** "CILINDRISKAS ŠŪNAS REFRAKTOMETRS UN TĀ PIELIETOŠANAS METODOLOĢIJA" ziņojums.

Protokola Nr.	Datums	Atbild par referātu	Lektors, tēma	Atzīmes
1	2	3	4	5
3.	17.02. 15.	1. J. Dehtjars 2. V. Beresņēvičs	Darbības MEKLĒJUMS CYLINDRICAL CELL BASED REFRACTOMETER AND ITS APPLICATIONS METHODOLOGY (DISERTĀCIJA) Par 2017. gada konferenci Rīgā, plānojama iespējamais pieteikums.	LNMK*)

1&

Klausījās. Dmitrija Merkulova ziņojumu par izstrādāto promocijas darbu. Darbs saistīts ar cilindriskas formas refraktometra jauna paņēmiena (patentēta) teorētisku un praktisku izpēti. Darbs nopublicēts vairākos zinātniskos rakstos un atbilst pašreizējām prasībām no kvalitātes viedokļa.
Jautājums uzdeva: J. Auziņš, M. Zakrževskis, J. Vība, V. Pavelko.
Uzstājās: M. Zakrževskis, J. Dehtjars, J. Vība. Visi izteica viedokli, ka darbs pēc satura un publikāciju kopas atbilst promocijas darba prasībām un ir rekomendējams tālākai caurskatīšanai VZZK.
Nolēma: Dmitrija Merkulova, promocijas darbs "CILINDRISKAS ŠŪNAS REFRAKTOMETRS UN TĀ PIELIETOŠANAS METODOLOĢIJA" atbilst doktora studiju programmas "Inženiertehnika, mehānika un mašīnbūve (RMDM8)" saturam un var tikt rekomendēts inženierzinātņu doktora grāda aizstāvēšanai.

RIGAS TEHNISKĀ UNIVERSITĀTE RTU MEHĀNIKAS INSTITŪTS

Semināra vadītājs: Dr.habil.sc.ing., prof., Jānis Vība

(Vārds, uzvārds, paraksts)

Protokolēja: Dr.habil.sc.ing., prof., Jurijs Dehtjars

(Vārds, uzvārds, paraksts)

Appendix 7.

Schematic diagram of the block B1, consisting of a linear optical sensor and microcontroller

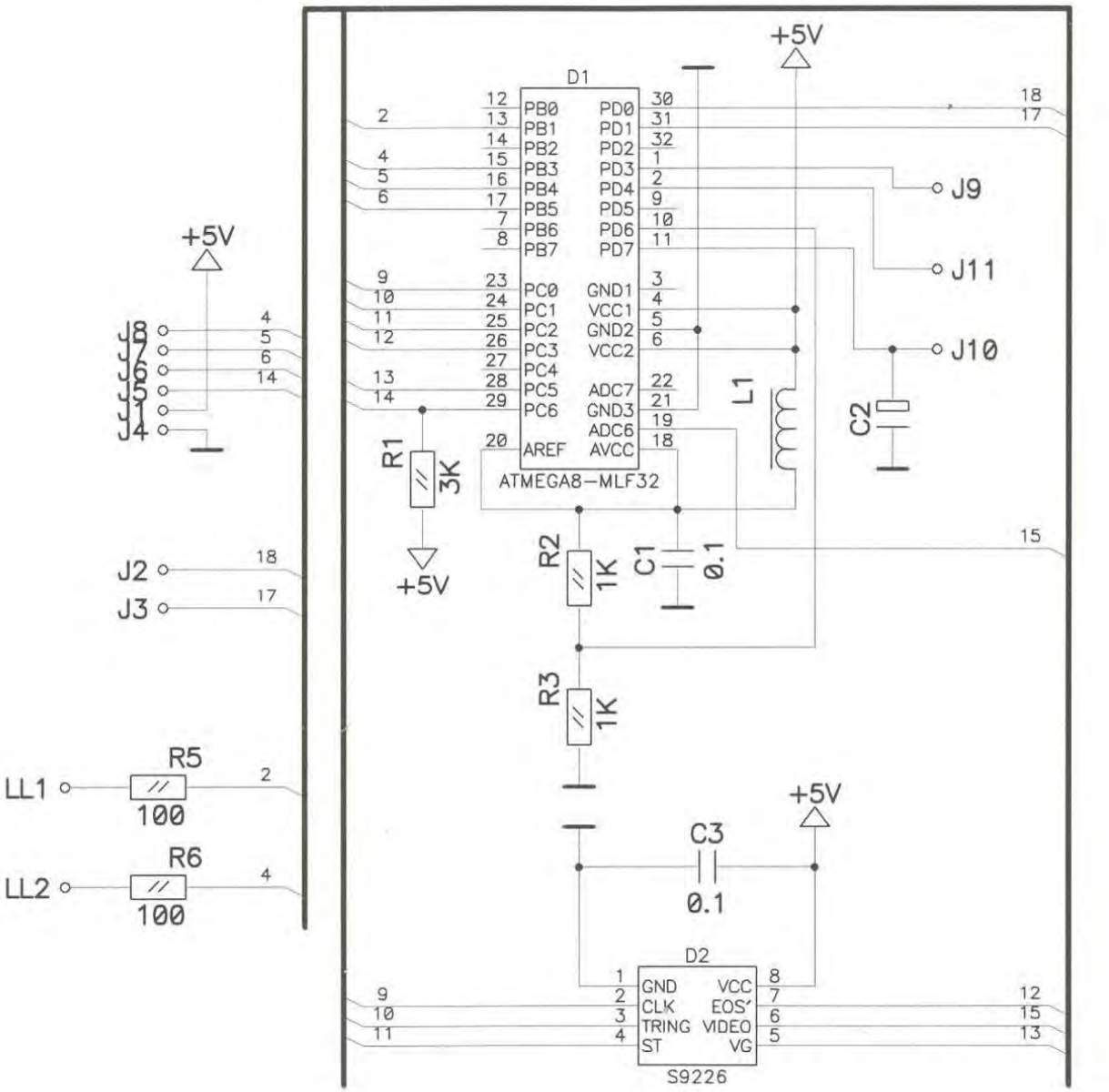

Appendix 8.

Circuit diagram of B2 consisting USB chip to communicate with the computer

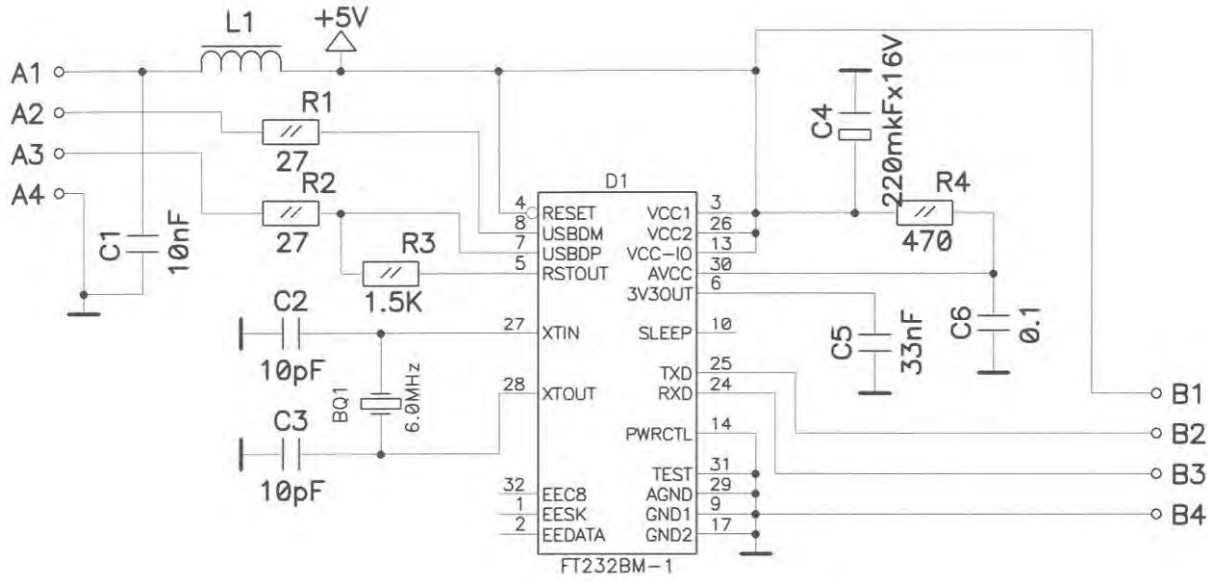

Appendix 9.

B1 electronic board

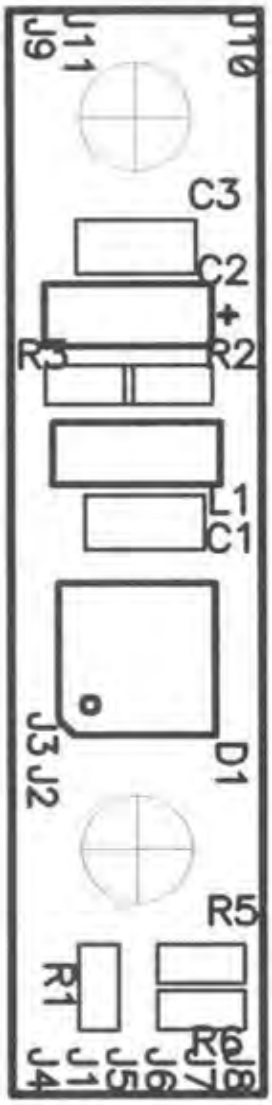

Appendix 10.

B2 electronic board